BETA AND GAMMA RAY STUDIES

OF ^{144}Ce AND ^{207}Bi

A thesis submitted by

RAMESH KUMAR MISHRA

M.Sc. (Pat.), M.Sc.(Lond.)

for the degree of

Doctor of Philosophy in

the University of London

August, 1970

Bedford College

University of London

DEDICATED TO

MY REVERED PARENTS

ACKNOWLEDGEMENTS

I am most grateful to Professor H. O. W. Richardson for his constant and kind supervision throughout the work. I am grateful to Dr. D. K. Butt of Birkbeck College for his valuable suggestions. I thank Dr. P. Rice-Evans and Mr. R. N. Thomas for their interest, Dr. Divora Michelson for her suggestions in the source preparation for β-ray spectroscopy, Dr. N. W. Behnee for permitting me to get the avalanche discriminator circuit from his Ph.D. thesis. The technical assistance provided by Messrs. F. A. Grimes, A. K. Betts, W. Baldock and A. King is gratefully acknowledged. I also thank Magadh University, Bihar (India) for granting me study leave, Bedford College for providing me with research facilities, Paterson, Belby and Amy Lady Tate Scholarships, the British Council for the overseas grant from hardship fund, Edwina Mountbatten Fund for giving me a grant to meet the cost of thesis, and Miss Franklin for typing my thesis.

ABSTRACT

The work described in this thesis has been carried out independently by the author under the supervision of Professor H. O. W. Richardson. A brief introduction on the scope of $\beta^- - \gamma$ ray spectroscopy is given in Chapter I. Chapter II deals with the modification of the detecting systems of the prolate spheroidal field β-ray spectrometer (large spectrometer) and the medium size magnetic lens spectrometer (small spectrometer). The "venetian blind" E M I photomultipliers previously used in both the spectrometers have been replaced by 56 AVP photomultipliers and fast electronics using avalanche discriminator circuits. The NE 102 phosphors were replaced by the fast NE 104 scintillators. A further improvement in the large spectrometer was made by replacing the conical phosphor and a straight light guide by an equiangular spiral light guide.
Chapter IV describes the preparation of β-sources. An improved technique using the electrospraying method has been applied in the preparation of Th B and ^{144}Ce sources. The $e^- - e^-$ coincidence measurements of ^{144}Ce using the two spectrometers have been described in Chapter VI.
But the most important and original contribution of this thesis is the $e^- - \gamma$ coincidence measurements of ^{144}Ce using the large spectrometer and a Ge(Li) X-ray detector in conjunction. The $e^- - \gamma$ coincidence measurements have been described in Chapter VI. Very possibly a magnetic spectrometer and a Ge(Li) X-ray detector have been used for the first

/time

timein these $e^- - \gamma$ coincidence measurements on ^{144}Ce. The single γ-ray spectra of ^{144}Ce measured with the 5 cc Ge(Li) detector and with X-ray detector are also described in this chapter. The use of a Ge(Li) X-ray detector in the $e^- - \gamma$ coincidence measurements of ^{144}Ce has made it possible to solve the ambiguities in the literature concerning some low energy transitions and in the placing of the upper excited level in ^{144}Pr. The results can be taken as the most reliable ones obtained so far. Our results agree best with Geiger et al (1960,61).

Chapter VII describes some NaI (Tl)/Ge(Li) $\gamma - \gamma$ coincidence measurements of ^{207}Bi and it is possible that these are the first measurements on ^{207}Bi with this type of equipment.

C O N T E N T S

C H A P T E R I

C H A P T E R I I

CHAPTER III

CHAPTER IV

Preparation of β-sources

C H A P T E R V

C H A P T E R V I

/(b)

CHAPTER VII

/(c)

List of Figures & Tables

<u>CHAPTER IV</u>

<u>CHAPTER V</u>

<u>CHAPTER VI</u>

CHAPTER VII

C H A P T E R I

Introduction on the scope of β-γ ray spectroscopy

The discovery of radioactivity by Bequerel (1896) has been the source of much information on nuclear and atomic structure. Though the discovery of radioactive rays occurred long before, nuclear spectroscopy started actually after 1911. Chadwick (1914) discovered the continuous distribution of electrons which form the main portion of the β-spectrum and they alone could be identified as disintegration electrons, whereas Von Bayer, Hahn and Meitner (1911,12) discovered the presence of definite energy lines in the β-spectrum known as conversion lines. The analysis of internal conversion in β-ray spectra of the natural radioactive elements was made for the first time by Von bayer and Hahn (1910) using a non focusing magnetic spectrometer. Chadwick (1914) used in his experiment an improved form of magnetic spectrometer with a particle counter. In the course of development in experimental techniques, $\beta^- - e^-$, $e^- - e^-$, $\beta^- - \gamma$, $\gamma - e^-$, and $\gamma - \gamma$ coincidence experiments have been carried out by many workers in the study of decay schemes of isotopes. The present work is concerned with studies of the cascade nature of γ - rays in the decay of ^{144}Ce and ^{207}Bi isotopes, by observing conversion electron spectra, γ-ray spectra and making $e^- - e^-$, $e^- - \gamma$ and $\gamma - \gamma$ coincidence measurements. A prolate spheroidal field β-ray spectrometer and a magnetic lens spectrometer were used in $e^- - e^-$ coincidence experiments whereas a Ge(Li) X-ray detector was used in

/conjunction

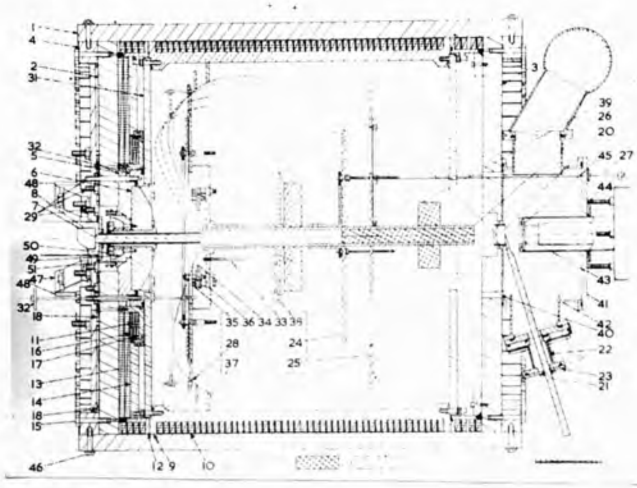

FIG. 1.1. DETAIL DRAWING OF THE LARGE SPECTROMETER

(Evans et al. 1958).

conjunction with the large spectrometer in $e^{-} - \gamma$ coincidence measurements. The $\gamma - \gamma$ coincidence measurements on ^{207}Bi were carried out with a 5 cc. Ge(Li) detector and a NaI(Tl) counter. An improved technique of electrospraying method has been applied in the preparation of the thin uniform β sources.

The Prolate spheroidal field β-ray spectrometer

The focusing properties of prolate spheroidal magnetic field were investigated theoretically by Richardson H.O.W. (1949), His computational analysis shows that the rays with emission angle of nearly 80° possess two focal rings, one of them near the equatorial region and the other close to the axis. The particle focusing properties of the prolate spheroidal field β-ray spectrometer was further studied by Michelson and Richardson (1963). A description of the spectrometer appears in the paper by Evans et al (1958). Some further modifications have been described by Michelson, D. (1961), and its automation by French, S. (1966). A detailed drawing of the unmodified large spectrometer (Evans et al, 1958) is shown in Fig. 1.1.

The Small Spectrometer

It is a medium size magnetic lens spectrometer. The source and the detector are placed 28" apart outside the magnetic field which make it suitable for coincidence measurements. A non-uniform magnetic field is produced by passing current through the coils. The slit opening is varied by a rotating screw which operates a gear and chain drive. Michelson (1961) described the baffle system and gave detailed diagram of the spectrometers arranged for $e^- - e^-$ coincidence measurements.

CHAPTER II

Modification of the detecting system of spectrometers

In the previous detecting systems of the spectrometers, EMI 9514B photomultiplier, NE 102 plastic scintillator were used by Freeman (1960) and Evans (1958) in their β-γ coincidence experiment and by Michelson, D.(1961) and French, S. (1966) in their $\beta^- - \beta^-$ coincidence experiment. It was decided to improve the timing resolution of the coincidence system by using a fast photomultiplier, a fast scintillator and fast discriminator for both the spectrometers. This chapter describes the modifications in the detecting system of the large and the small spectrometers.

The large spectrometers

The previous detecting system of the large spectrometer was replaced by a new light guide, NE 104 plastic scintillator, 56 AVP photomultiplier and avalanche discriminator. In place of MgO, a special type of reflector NE 560 has been used. The Nuclear Enterprise maker claims that NE 560 has efficiency nearly 15% over the packed MgO. Two types of light guide were tested, one was a straight light guide as used before and the other was an equiangular spiral light guide. From comparative studies of their pulse height spectra, the equiangular spiral light guide was found to have a better performance than the straight one. Descriptions of the NE 104, NE 560, machining and polishing of the light guides and the phosphors are given below.

NE 104: It has a very short decay time ($\sim$1.9 ns), shortest of any commercially available plastic scintillator

/having

having light output approximately 65% relative to anthracene. The wavelength of maximum emission is 4050 Au.

(b) NE 560:- The NE 560 is a special kind of reflector which adheres to the plastic phosphor and is resistant to mechanical shock. It consists of a special grade of Titanium-dioxide selected for its higher reflectivity.

(c) Machining and polishing of phosphor and light guide

While machining the phosphor on lathe it is essential to take care of minimum surface-heating and minimum tension in order to avoid the appearance of cracking after finishing. Therefore the phosphor is lightly clamped using a suitable soft material to spread the pressure over a large area. Hacksaw with soapy water was used for cutting the phosphor. While drilling in the lathe, soapy water was used as a coolant. The scintillator was turned on a regular metal cutting lathe, preventing vibrations by controlling the speeds. Turning lines were removed by hand rubbing at right angles and using 500 grade silicone carbide waterproof polishing paper with soapy water. Final polishing was done with I.C.I. perspex polish No.1 followed by No.2A on a fine grade cotton-wool. Similar procedures were adopted in cutting and polishing the light guide. In order to get rid of any greasy substance, both the light guide and the phosphor were washed in a soapy water and then in running tap water. They were dried with cotton-wool.

(d) Ring type conical phosphor

The reason for using a special type of conical shape of phosphor was to improve the light collection efficiency. This shape was used previously by Evans (1958) and Freeman

/(1960).

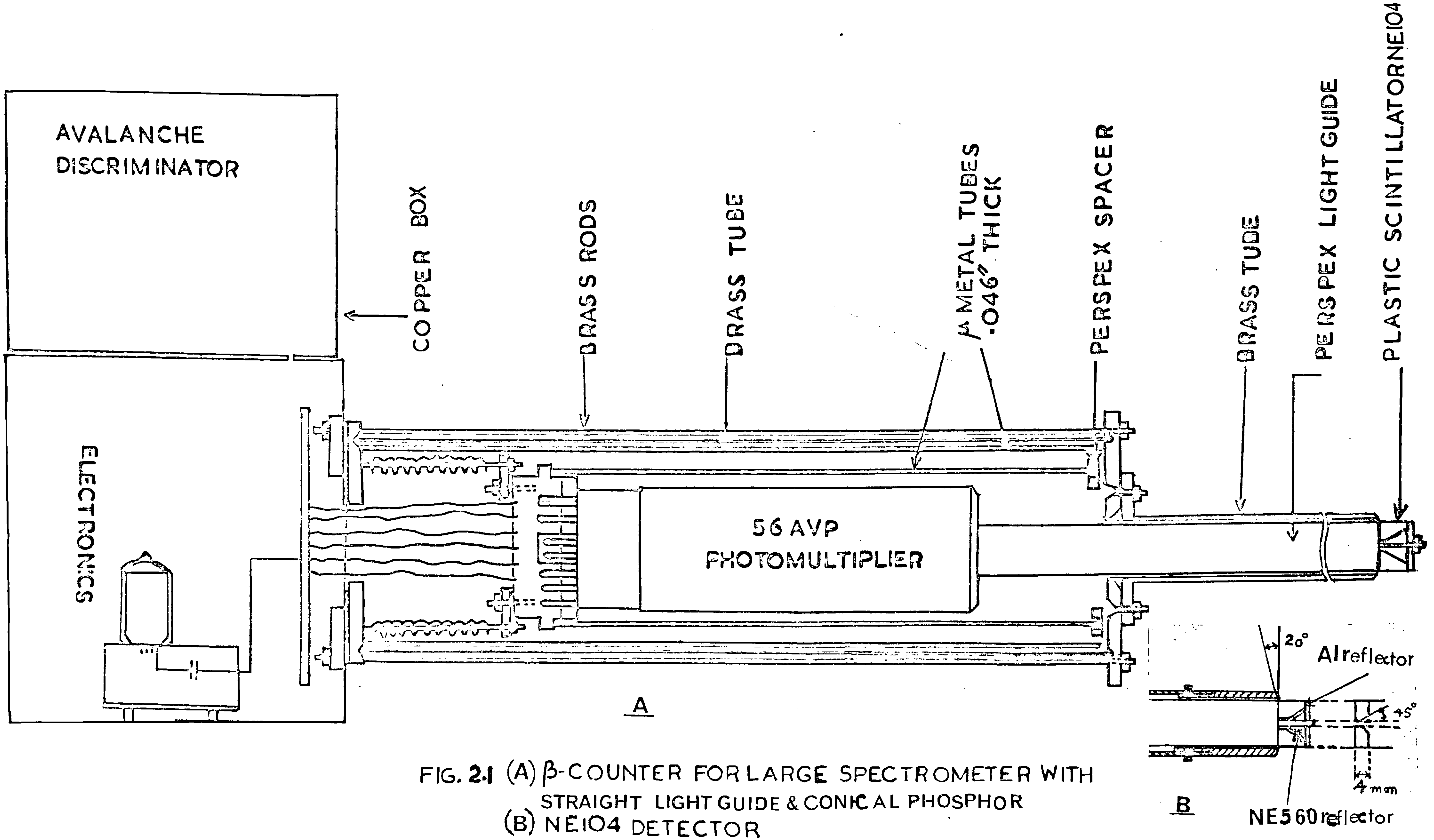

FIG. 2.1 (A) β-COUNTER FOR LARGE SPECTROMETER WITH STRAIGHT LIGHT GUIDE & CONICAL PHOSPHOR
(B) NE104 DETECTOR

$\frac{1}{2}$ SCALE

(1960). They used a packed MgO powder as a reflecting substance while in present experiment coatings of NE 560 paste were used to get light reflections. The pastewas at first diluted with distilled water in the ratio 1:10 and then stirred well with a wooden stick. A thin layer was deposited on inside the cone of the phosphor, a second coating was made when the former was dried. Eight such coatings were sufficient for a good reflection. The light guide with conical shaped phosphor is shown in Fig. 2.1B The phosphor is screwed on to a 3/4" perspex light guide and an optical contact is achieved with a silicone fluid. The light guide passes through a brass tube and is optically coupled on to the 56 AVP photomultiplier. The photomultiplier is mounted on a spring base. An O-ring vacuum seal is used between the light guide and the brass flange. The photomultiplier base stands on a black thick rubber flange compressed against another brass flange. This is done in order to achieve light-tightness of the photomultiplier can. The details of the β-counter with straight light guide and 56 AVP photomultiplier are shown in Fig. 2.1A The photocathode of 56 AVP photomultiplier is the most magnetically sensitive region for the electrons, therefore the photomultiplier as well as a portion (2") of the light guide were surrounded by two coaxial μ-metal tubes. The purpose of using μ-metal is to shield the photomultiplier from magnetic fields of the surroundings.

The 56 AVP photomultiplier circuit is shown in Fig.2.3.

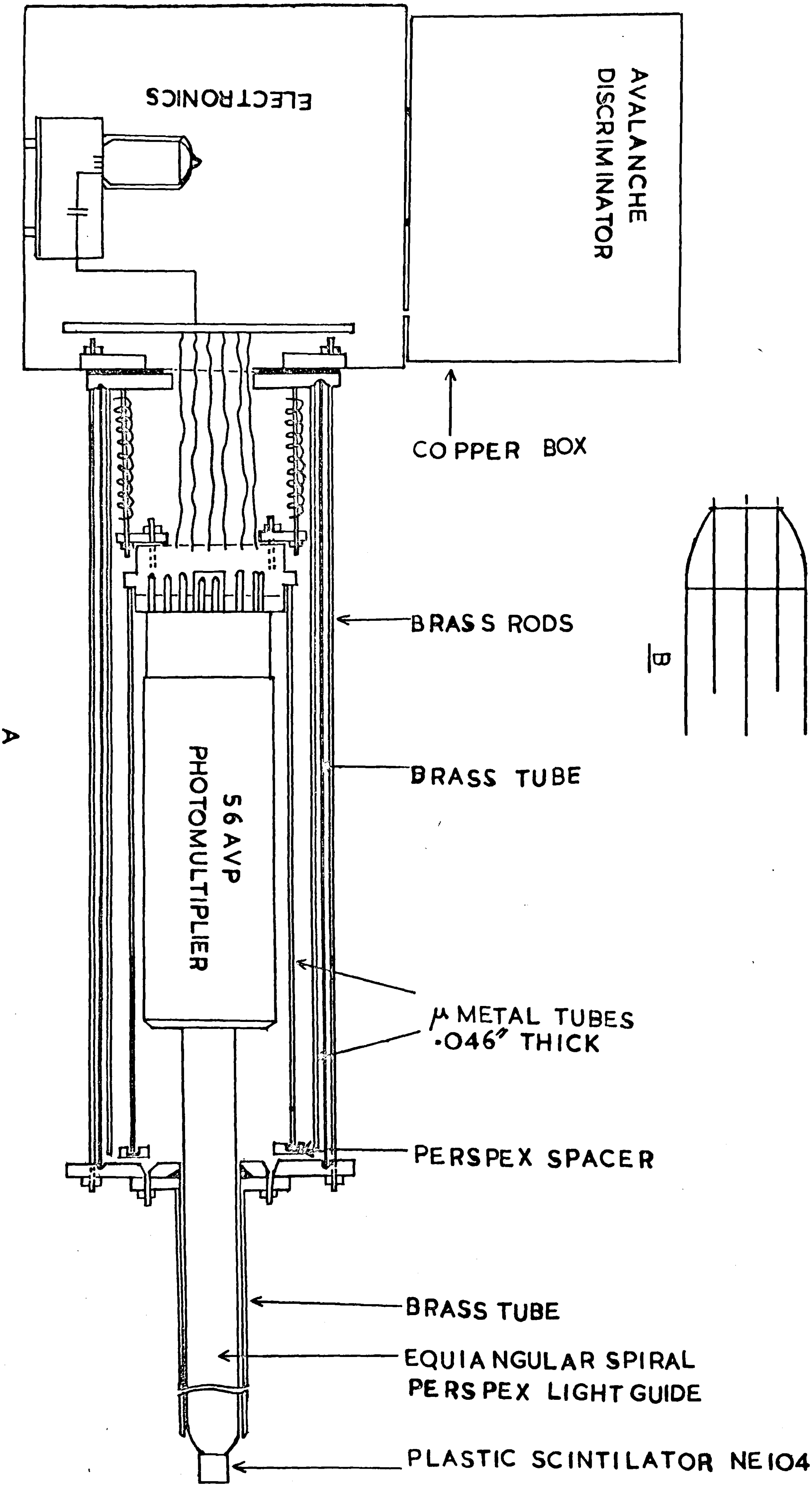

FIG. 2.2 (A) β-COUNTER FOR LARGE SPECTROMETER WITH EQUIANGULAR SPIRAL LIGHT GUIDE (SCALE $\frac{1}{2}$)
(B) A DETAIL DIAGRAM OF THE HEAD OF THE LIGHT GUIDE.

(e) Equiangular spiral light guide

Various methods have been adopted by different workers to improve light collection efficiency. Gerholm (1955) in his $e^- - e^-$ coincidence experiment used a lucite light guide machined to a certain profile in order to get a maximum light collection. An efficiency of nearly 60% was reported by him for the total guide of length 22.5 cm. Tove, P.A. et al (1956) used two different kinds of light guide (1) a simple logrithmic spiral with an input diameter of 14 mm and 21 mm long and (2) the other based on Gerholm light guide. Both these were reported to have collected all the light coming across the input surface.

Following an exponential decrease in transmitted light, they found a transmission of 45% of light over a path length of 1 meter guide pipe (plexiglass).

An equiangular spiral light guide 12 3/8" long and 4/5" in diameter made of perspex (μ = 1.49), designed by H.O.W. Richardson has been used in the large spectrometer throughout the experiment. The head of the light guide is shaped in order to get total reflections from the surface. The idea is to get a maximum light collection efficiency combined with a minimum diameter to the light guide. The advantage of using the minimum diameter of the light guide is to get the light concentrations on to the most sensitive part of the photocathode and also the transit time variations of the photoelectron path lengths become smaller. A detailed diagram of the equiangular spiral light guide is given in Fig. 2.2B. The NE 104 phosphor (1 cm x 1 cm) is cemented on the spiral head of the light

/guide

guide with a special optical cement NE 580. Care was taken to keep the phosphor at the centre of the head and remove all air bubbles from the interspace, if any.

2. <u>56 AVP Photomultiplier</u>

Nuclear particle detection requires usually a good energy resolution as well as a high detection efficiency. A high time-resolution is essential in fast coincidence experiments and in life-time measurements which require a fast scintillator, a fast photomultiplier and a fast discriminator. The 56 AVP photomultipliers were used in both the spectrometers. They are very fast photomultipliers, having anode rise time 2 ns, low dark current and a high gain. Their characteristics with voltage divider A as given by Phillips are listed below:-

Supply voltage for gain 10^8

Average	2.2 kV
Maximum	2.5 kV

Dark current at gain 10^8 (measured at 25°c)

Average	0.5 μA
Maximum	5.0 μA

Anode Pulse rise time at 2.5 kV = 2 ns

Transit time difference between the centre of the photocathode and the edge at 2.5 kV is 0.5 ns.

Bellettini et al (1963) have studied in detail the effect on the gain and linearity of 56 AVP of variations in inter-dynode voltages. Hyman et al (1964) have given the

/technique

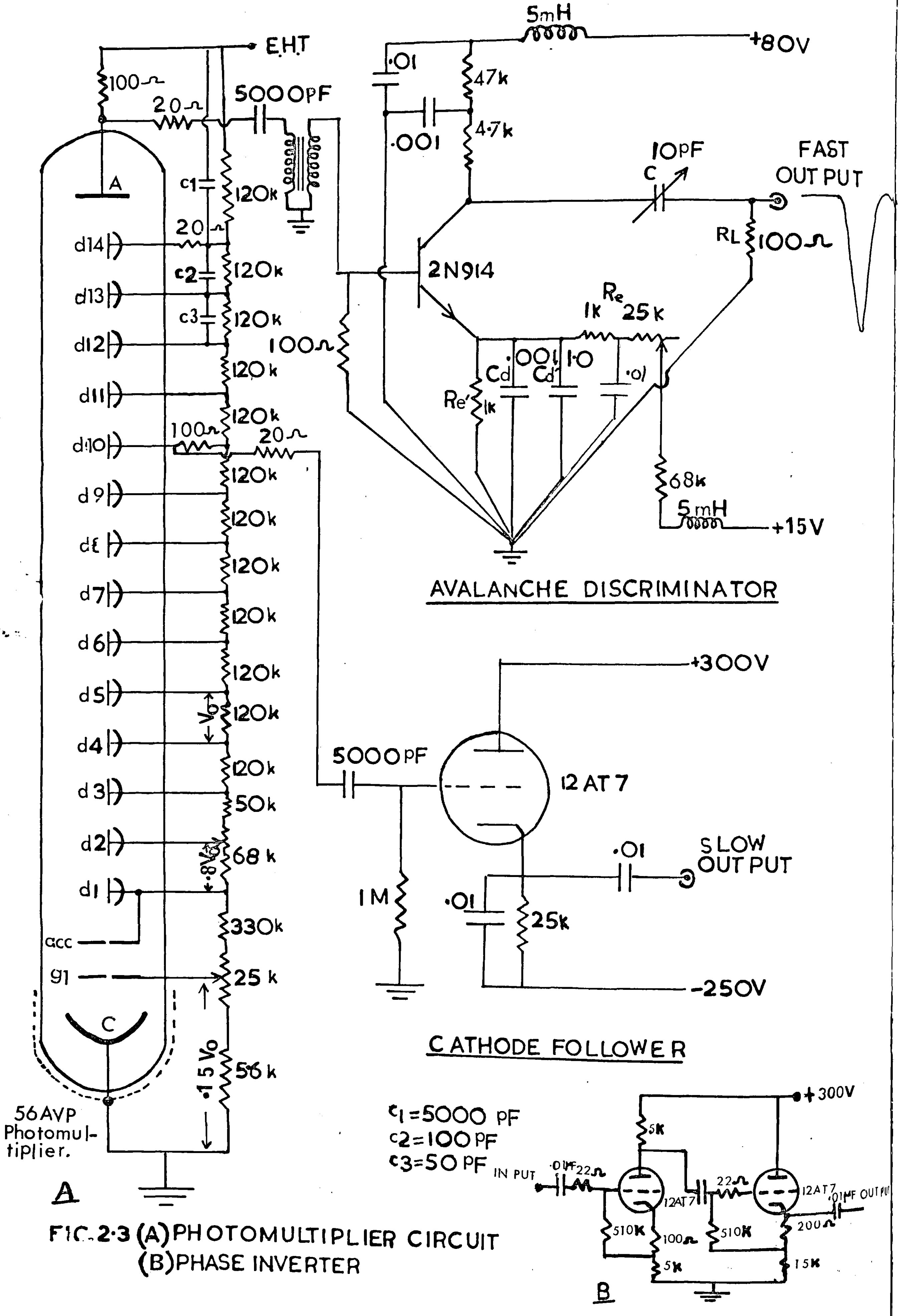

FIG. 2·3 (A) PHOTOMULTIPLIER CIRCUIT
(B) PHASE INVERTER

technique of optimising the pulse shape and linearity of the 56 AVP. Theyused a small 50Ω Subminax co-axial connector on the anode and unused pin and found the full width at half maximum (F.W.H.M) of anode pulse as 2 ns for infinitely short light pulses. In our present photomultiplier circuit, [FIG2.3A] 20Ω damping resistors were used in the anode and the last dynode in order to avoid ringing. A 100Ω anode load resistor was used which matched with the transmission line (impedance 100Ω).

The theoretical calculations of Wahab and Kane (1962) indicate that the major time spread originates in the region between the scintillator and the first dynode. The recommended circuit No.A by Phillips was modified to suit the requirements. The current flowing through the potential divider chain was nearly 1.25 mA. The voltage between the cathode and the first dynode is three times that of the voltage per stage in order to get a better collection efficiency. The focusing variable voltages $Vd_3 - d_2$, $Vd_1 - d_2$ and $Vg_1 - k$ are those recommended by Phillips. They act as a fine and coarse control respectively. These controls are adjusted for a maximum anode output. Energy signals are taken from the 10th dynode with 100Ω load resistor. As mentioned previously, the anode load is also kept 100Ω in order to match the transmission cable and damping resistors of 20Ω were used in the anode and 14th dynode in order to avoid ringing. The F.W.H.M. of the anode output pulse is $\sim$8 ns (Fig.2.4a)
The anode pulses are similar to those found by Hyman et al.(1964)

/In

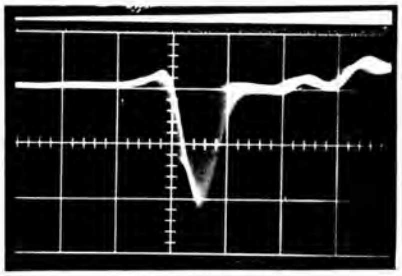

1v cm^{-1}

10 ns cm^{-1}

(a)

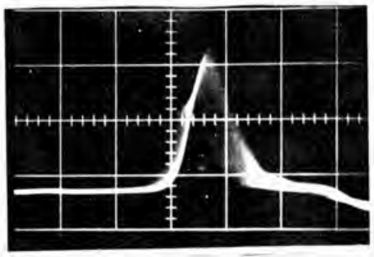

1v cm^{-1}

10 ns cm^{-1}

(b)

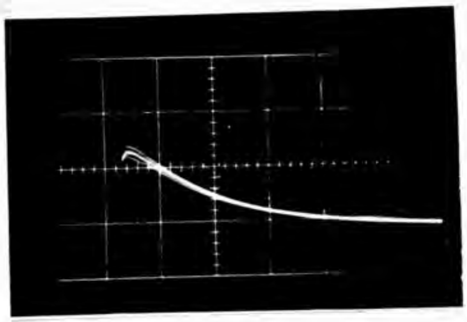

5v cm^{-1}

10 ns cm^{-1}

(c)

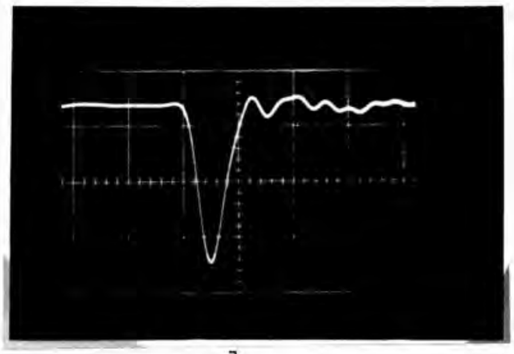

1v cm^{-1}

10 ns cm^{-1}

(d)

FIG. 2.4. OUTPUT PULSE FROM:-

(a) Anode

(b) 14th dynode

(c) 10th dynode

(d) Avalanche discriminator

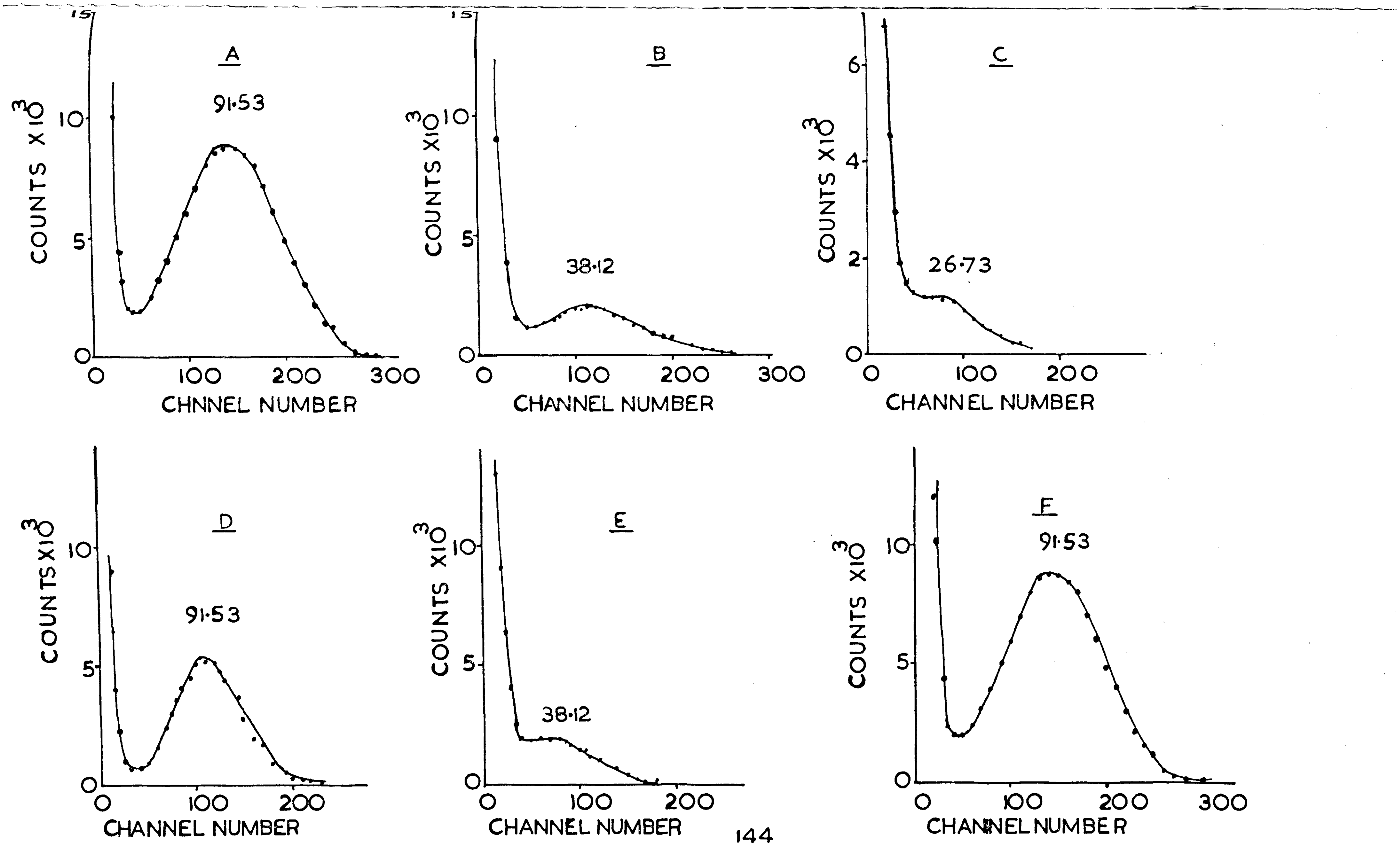

FIG. 2·5 PULSE HEIGHT SPECTRA OF COVERSION LINES OF ^{144}Ce MEASURED WITH THE LARGE SPECTROMETER (A,B,C) WITH EQUIANGULAR SPIRAL LIGHT GUIDE (D, E) WITH STRAIGHT LIGHT GUIDE. (Lines energies are given in keV) (F) PULSE HEIGHT SPECTRUM OF 91 keV LINE MEASURED WITH THE SMALL SPECTROMETER.

In order to avoid electric-field disturbances in the electron-optical system, the external conductive coating M (pin No. 18) is connected to the cathode potential which is earthed. The last stages of the tube are decoupled by means of capacitors in order to avoid serious voltage drop across the dynodes. The reason for using a 100 Ω anode load resistor is that the tube is capable of producing a very high peak current nearly 1A and therefore the output time constant must be very small. The voltage divider circuit with avalanche discriminator and cathode follower is shown in Fig. 2.3. Fig. 2.2A shows the equiangular spiral light guide with NE 104 plastic scintillator and 56 AVP photomultiplier for the large spectrometer.

3. Comparative studies of the straight and equiangular light guides.

The comparative studies of these two light guides were done by studying the pulse-height spectra of some of the conversion lines of ^{144}Ce with the large spectrometer. The detector with each light guide in turn was set on the maximum β-ray counting by plotting the axial distribution of β-rays intensity near the detector (Chapter III, Sec.2). Pulses from the 10th dynode were fed through cathode follower and phase inverter into the I.D.L. wide band amplifier, the output of which was displayed over the Intertechnique 400 multichannel analyser. The pulse height spectra taken with the two light guides under the same conditions are shown in Fig. 2.5,A,B,C,D,E,F. The signal to noise ratios in each case are listed in table 2.1. On comparing the signal to noise

/ratio

ratio, the performance of the equiangular light guide was found superior to that of the straight light guide. Hence the equiangular light guide was retained in the large-spectrometer throughout the experiment.

Table 2.1

	Straight light guide		Equiangular light guide		
Energy in kev	91	38.12	91	38.12	26.73
signal: noise	9:1	7:1	13:1	8:1	6.6:1

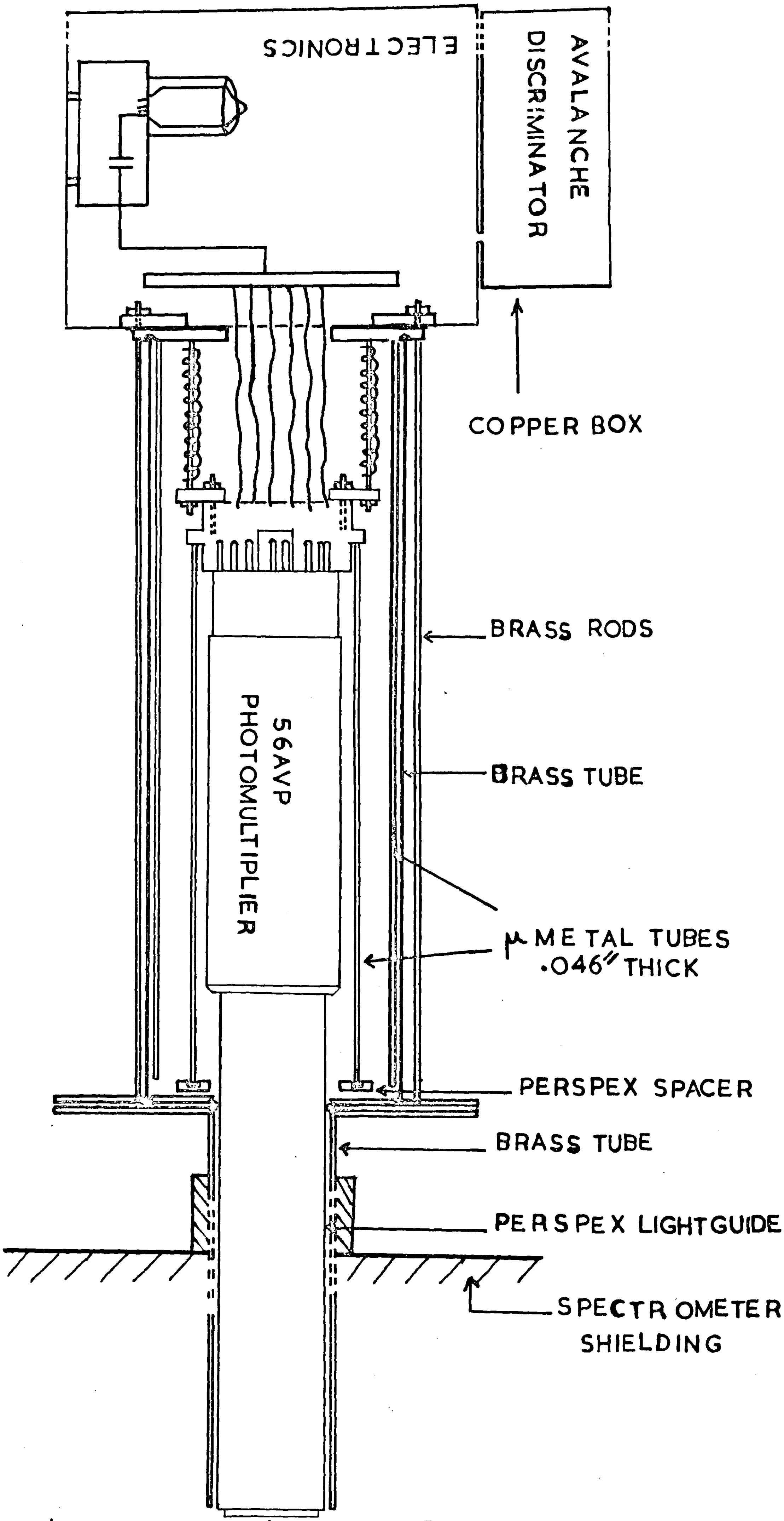

FIG2·6 ARRANGEMENT OF β–COUNTER FOR SMALL SPECTROMETER

$\frac{1}{2}$ SCALE

4. Modification of the detection system of the small spectrometer

The detector of the small spectrometer was modified by inserting a new phosphor NE104, a new light guide, and using a 56 AVP photomultiplier (Fig. 2.6). The phosphor NE 104 ($1\frac{1}{2}$" diameter and 1/8" thick) was cemented with NE 580 cement on to a polished surface of the perspex light guide (diameter 1 3/4", length 8 5/16"). The photomultiplier and a portion of the light guide (3") were surrounded by two coaxial μ-metal tubes. The photomultiplier circuit is the same as in the case of large spectrometer. The energy signal is taken from the 10th dynode. An increase in the pulse voltage of the 91 keV conversion line of ^{144}Ce over that taken with the large spectromer suggests the greater optical transmission of detector in the small spectrometer. The signal to noise ratio for the 91 keV line in the large spectrometer was 13:1 whereas in the small spectrometer it was 15:1 (Fig.2.5F).

5. Cathode follower and phase inverter

The circuit diagrams for cathode follower and phase inverter are shown in Fig. 2.3. They are the same as used by Freeman (1960).

CHAPTER III

1. Electronics for e^- - e^- coincidence experiment

(a) Avalanche discriminator:

Standardisation of fast pulses of different energies is desirable where timing selection and fast coincidence is required. Avalanche transistors are readily used in fast-discriminator circuits, as they produce a very fast and big pulse at a very low current. Freeman (1960) Evans (1958) and Michelson (1961) used 6 AM6 valve limiters in their fast coincidence channels, whereas French, S. (1966) used ASZ23 avalanche transistors in discriminator and in adder circuits. Bennee, N.W. (1968) prefers Fairchild Silicon 2N914 transistor in life time measurement experiments because of its superior rise time, large signal output and better reliability. The 2N914 avalanche transistor has been used in fast discriminator circuits throughout e^- - e^-, e^- - γ and γ - γ coincidence experiments. The avalanche discriminator circuit (Fig. 2.3) is based on the design by Bennee with some adjustment.

The base is grounded to earth by 100-Ω resistor. Bias is applied on to emitter through resistors Re, Re' and de-coupling capacitors Cd - cd'. Output is taken from the collector via a variable capacitor C. The amplitude and time constant were adjusted to desired values by varying the value of C and keeping load resistor RL constant. The value of load resistor RL was kept 100-Ω in order to match

/the

impedance of transmission line. The use of inductance of 5 mH in the power supply line and the bias line is to protect power supply and other units against the reflected avalanche pulses. The anode output is inverted by a transformer and a positive trigger pulse is applied on to the base of the transistor 2N914. Ringing in the output pulse is reduced by making the connection leads as short as possible. The avalanche output pulse is shown in Fig.2.4d.

The whole circuit is kept in a copper box, grounded to earth. The connecting lead from anode to the base of transistor is made as short as possible. The bias on the emitter is adjusted to cut off the noise level. The circuit can trigger input down to 0.1 volt.They produce very fast standard output pulse of F.W.H.M8ns.

(b) Fast coincidence unit

A Harwell 2035C type fast coincidence unit was used throughout the coincidence experiments. This is a transistorised multichannel coincidence unit having 4-coincidence input channels and 2 anticoincidence input channels. The minimum coincidence resolving time as claimed by the manufacturer is 2ns. The output pulse from the avalanche discriminator satisfies the input requirements of the coincidence unit. Three P & T sockets are associated with each channel, two of them are internally connected in parallel - one is called INPUT and the other is called TERMINATE. The "TERMINATE" is terminated with a 100-Ω termination plug. The third socket marked as "Clipping

/line

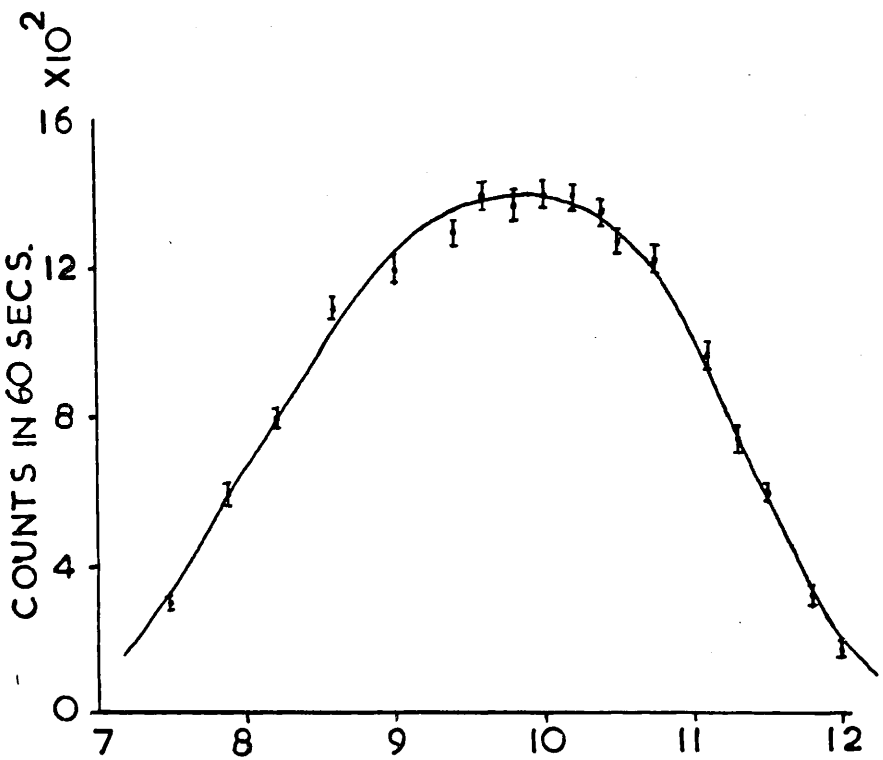

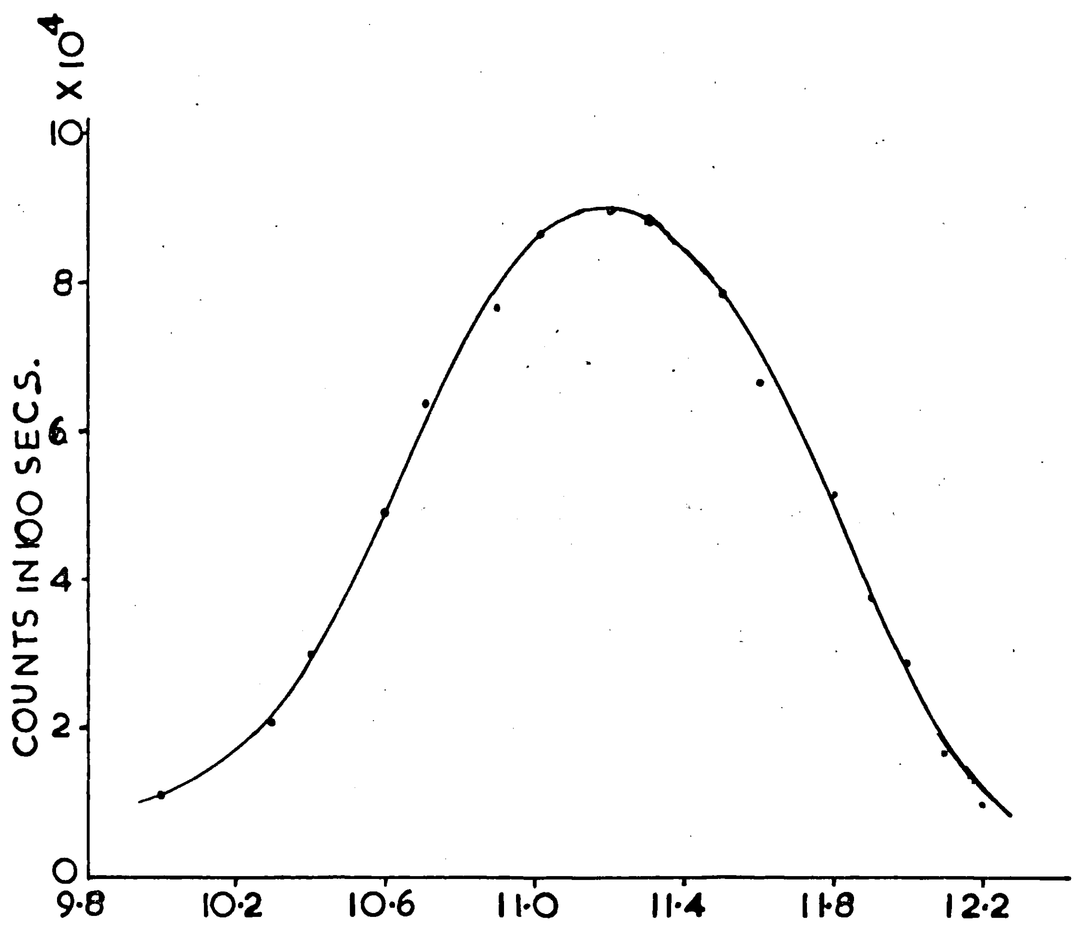

FIG.3·1 AXIAL DISTRIBUTION OF THE BEAM INTENSITY NEAR THE DETECTOR OF THE LARGE SPECTROMETER FOCUSED ON THE
(A) CONTINUOUS β RAY OF ThB SOURCE WITH OLD DETECTOR
(B) 91 keV CONVERION LINE OF ^{144}Ce WITH EQUIANGULAR SPIRAL LIGHT GUIDE, NE104 PHOSPHOR AND 56AVP PHOTOMULTIPLIER.

line" is terminated with an extra length of coaxial cable which determines the coincidence resolving time. The particular channel is switched off when the coaxial cable is taken out. The unit provides two types of standard out pulses (see Manual AE55 (R) 11078), one a fast narrow negative pulse and the other a slow pulse of -7V amplitude and F W H M = 0.5 μs. The slow output is used to derive the Harwell type 2019B fast scaler.

(c) Slow coincidence unit

The slow coincidence unit used in γ - γ coincidence experiment was a Harwell 2013 type. The unit consists of two channels, one a coincidence and the other an anti-coincidence. It is provided with input amplitude discriminator controls (Disc "A" and Disc "B"), delay range switch "A" and "B" and a resolving time range selector. The two discriminator controls provide a continuously variable threshold level of +1.5 V to 11.5 volt. It rejects the negative going pulse provided the overshoot does not exceed 1.5 volt. It also accepts a negative going pulse up to 1.5 volt and rejects the positive going overshoot not exceeding 1.5 volt. Standard negative output pulse is produced at the three sockets (i) scaler A (ii) scaler B and (iii) coincident or anti-coincident output.

2. Adjustment of the large spectrometer

The axial distributions of β-ray intensity near the end of the phosphor were plotted (Fig. 3.1) when the large spectrometer's current was focused on the peak of 91 kev

/conversion

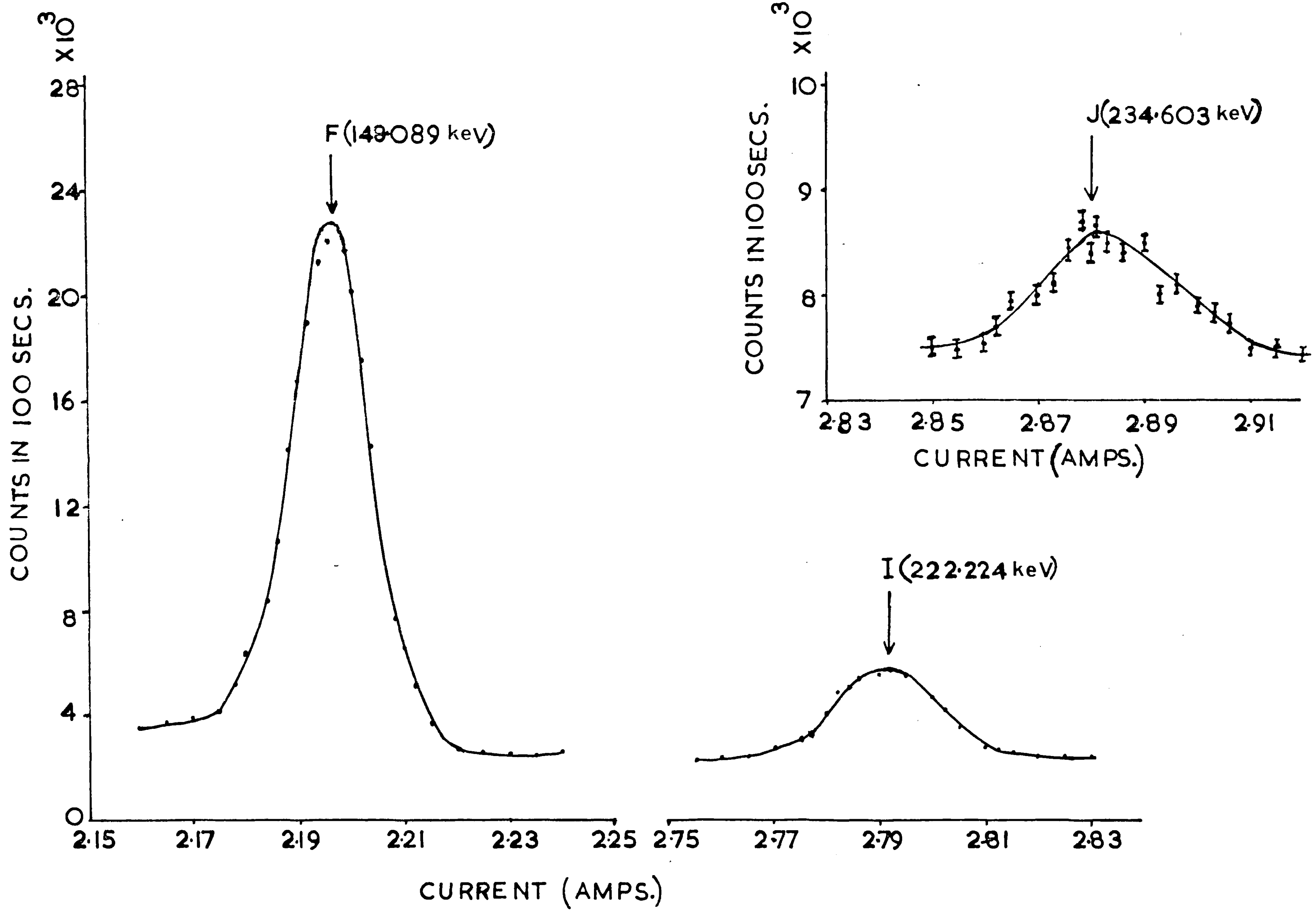

FIG.3.2 CONVERSION LINES OF Th(B+C+C'') MEASURED WITH THE LARGE SPECTROMETER

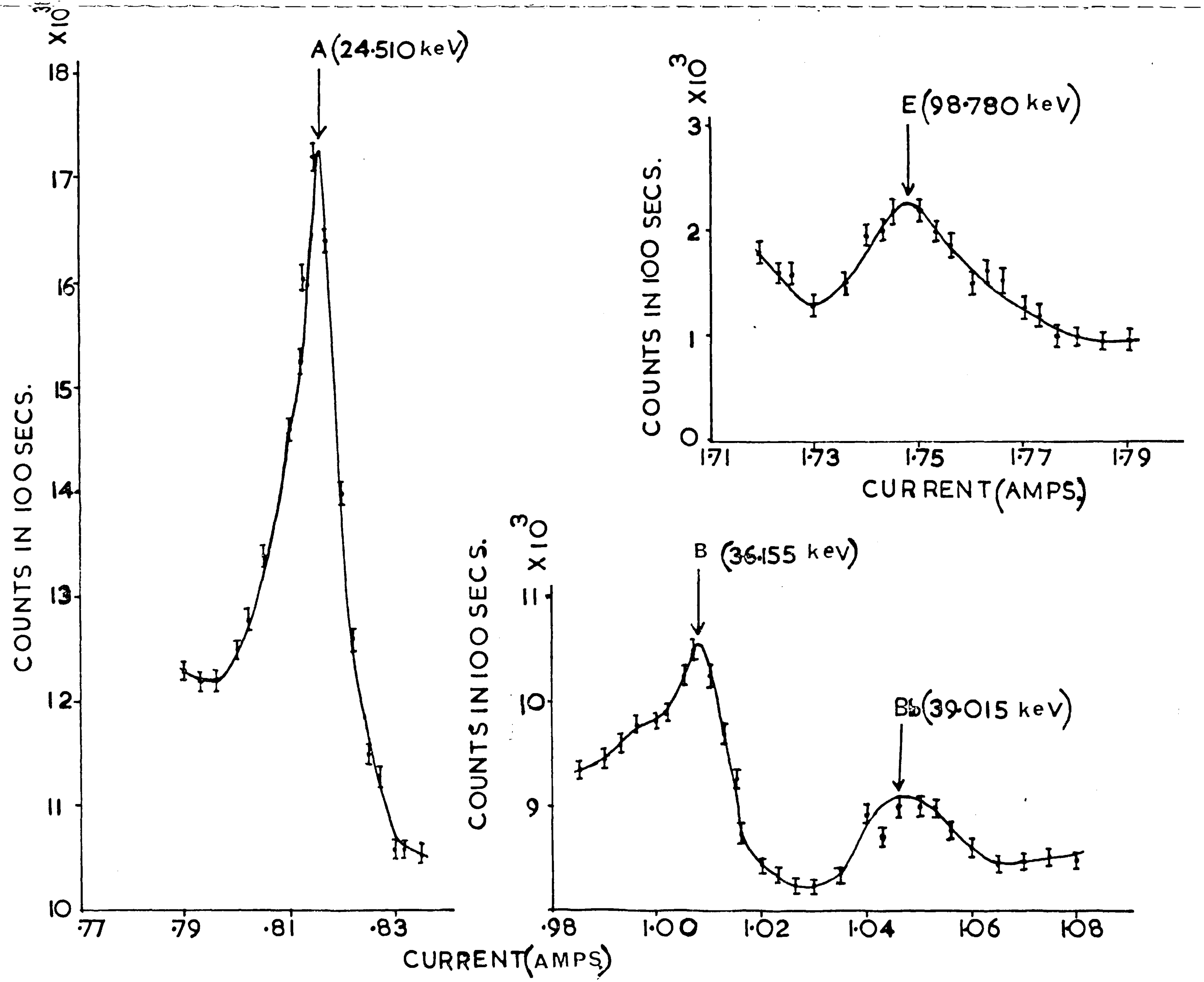

FIG. 3·3 CONVERSION LINES OF Th(B+C+C'') MEASURED WITH LARGE SPECTROMETER

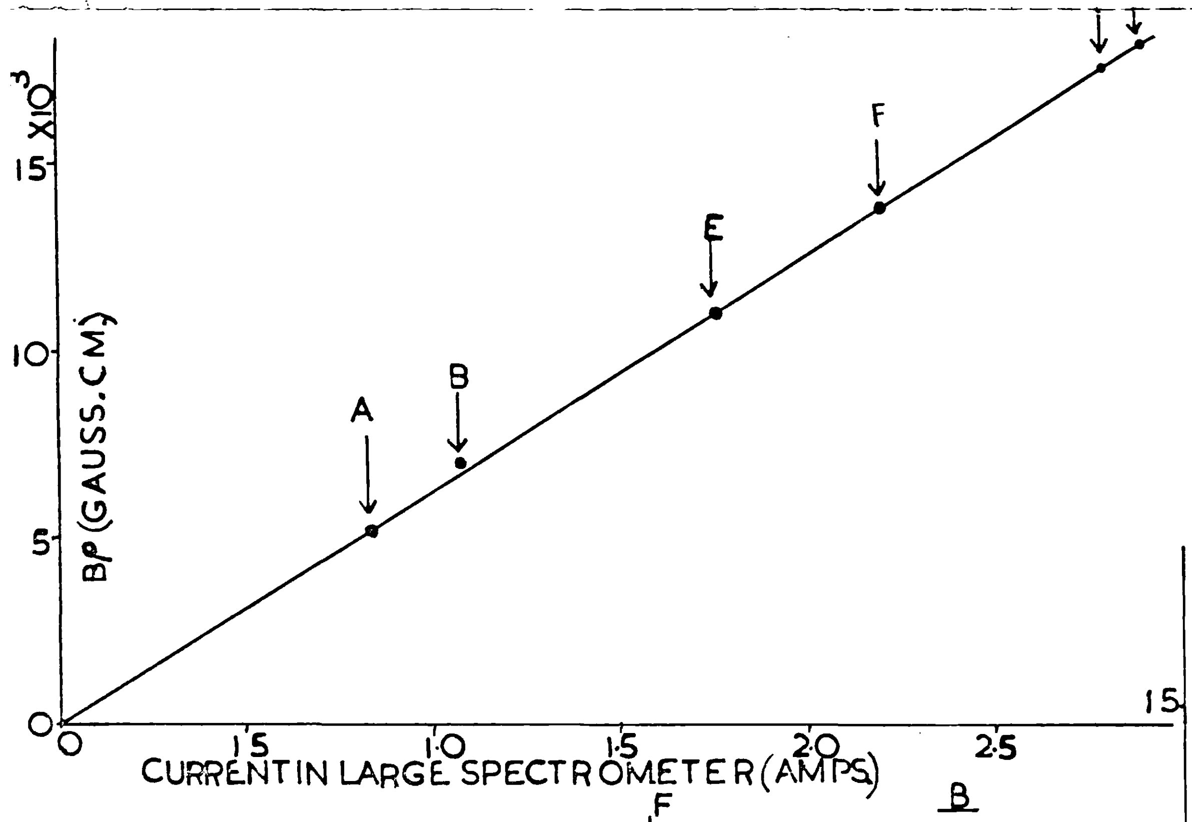

Line	Energy in keV	Bρ (gauss.cm)
A	24·510	534·21
B	36·155	652·43
E	98·780	1109·85
F	148·089	1388·49
I	222·22	1753·95
J	234·603	1811·09

Conversion lines of Th(B+C+C″)

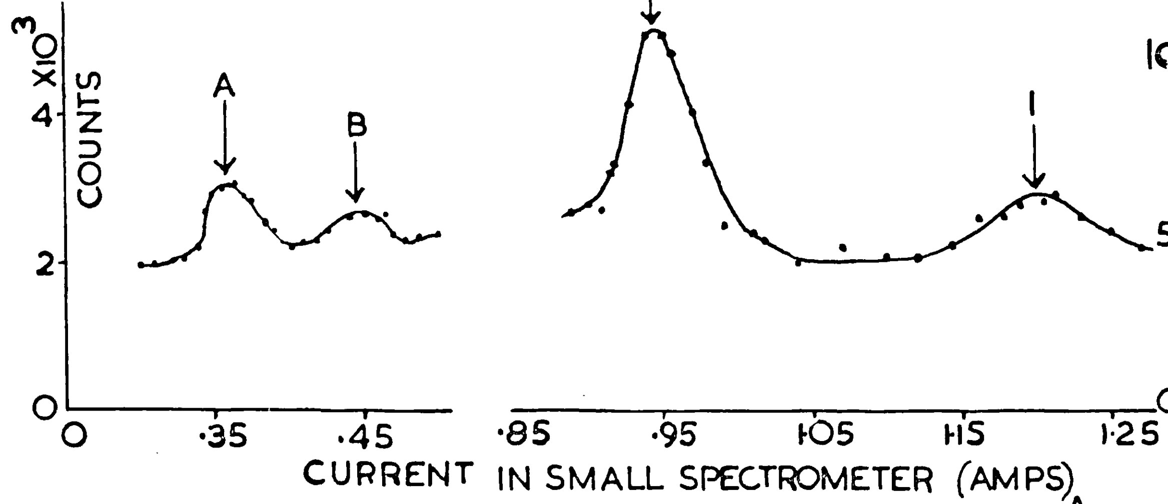

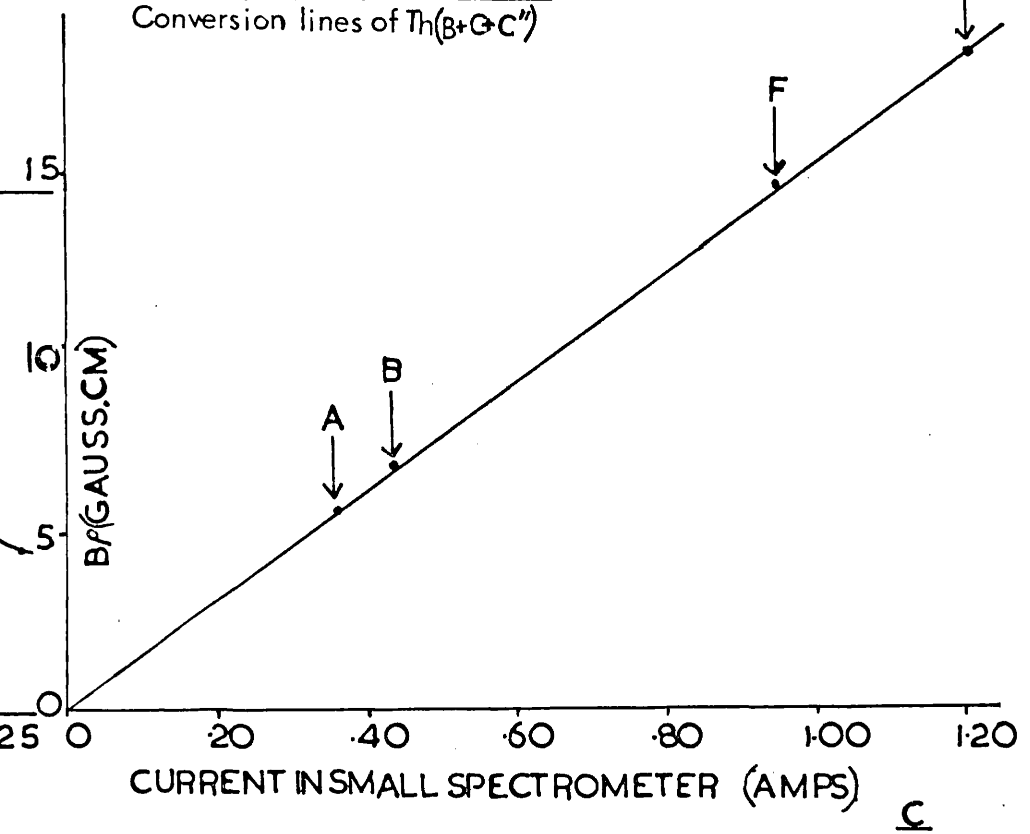

FIG. 3·4 (A) CONVERSION LINES OF Th(B+C+C″) MEASURED WITH THE SMALL SPECTROMETER
CALIBRATION OF (B) LARGE SPECTROMETER (C) SMALL SPECTROMETER WITH Th(B+C+C″) SOURCE

conversion line of ^{144}Ce and 148 keV conversion line of ThB. The axial position of the detector was set for the maximum counting rate of β-particles.

3. Conversion lines of ThB and calibration of spectrometers.

Both the large and small spectrometers were calibrated with conversion lines of a Th.B source. The slit opening of the large spectrometer was kept narrow and transmission 4% of 4π. Conversion line spectra of Th.B source are shown in Fig. 3.2 & 3.3. Resolution for Th B - F line with 5 mm deposit on a metallic screw head was 0.8%.

The Th.B conversion line spectra taken with small spectrometer with wide slit opening are shown in the Fig. 3.4A. and the resolution for Th.B F line was 5%.

4. Test of the spectrometers using pulse height analysis

Pulse height spectra of different conversion lines taken on both the spectrometers are shown in Fig. 2.5. The transmission of the large spectrometer was found 1.6 times that of the small spectrometer.

6. Measurement of the transmission of large-spectrometer

The transmission is expressed as the ratio of counting rate at the peak of Th.B - F line to the total F line intensity. The Bendix Ericsson type 1320D α counter was masked with a lead to represent 1 cm^2 aperture and the source was placed at a distance of 2.4 cms from the counter. The solid angle dΩ subtended at the source by the aperture was calculated and the α-particles emitted in the solid angle by the daughter nuclei (Th C' + c') were counted after allowing a sufficient time (~ 21 hrs.) to elapse so that the Th (C + C') lie in equilibrium with its parent Th.B. Thus the total α-particles collected in solid angle of 4π was measured. The disintegration rate was calculated by multiplying the decay constant

$$\left(\frac{\lambda_{ThC} - \lambda_{ThB}}{ThC} \right)$$ by α counting rate Nα

which is equal to $N\alpha \left(\frac{\lambda_{ThC} - \lambda_{ThB}}{\lambda_{ThC}} \right)$

$$= 0.9\alpha \qquad (1)$$

The F line intensity per disintegration is ~ 0.3 (Martin and Richardson) (2)

From (1) and (2) the F line intensity was determined. The counting rate of Th.B - F line was corrected for decay. The transmission thus measured was 44% of 4π and resolution 0.8%

7. <u>Magnet power supplies for large and small spectrometers.</u>

Current in the large spectrometer was supplied by the Newport Instrument type C225. Fifteen large capacity accumulators were used to supply magnetising current in small spectrometer. Details of resistors are given by French, S. (1966). Currents in both large and small spectrometers were measured with Tinsley potentiometer, type 4363A across a standard resistor.

CHAPTER IV

Preparation of β - sources

1. Introduction

In the study of low energy β-particles it is essential to keep the thickness of the source and backing as thin as possible. Usually two important points have to be taken into consideration; firstly to reduce the absorption of β-rays in the sample, and secondly to avoid back scattering from the backing. The back scattering causes increase in low energy electrons whereas the thick source reduces the β-ray energy. These two effects produce distortion in the β-spectrum.

2. Preparation of thin films

While preparing the thin film, the following considerations have to be taken into account: the film should have uniform thickness, good tensile strength, good lasting properties, low composite atomic number in order to avoid back scattering, and high resistance to chemical reagents. Aluminium film as thin as 130 μ gm/cm^2 could be obtained but it is thicker than plastic film. Some authors have used films of nylon and formvar. Pate and Yaffe (1962) suggests a better organic material VYNS resin which consists of polyvinylchloride acetate copolymer. This resin was chosen for preparing the thin film. A mixture of one part of resin in 9 parts of cyclohexanone by weight was prepared. A wooden scale was placed at one end of the sink filled with water. A few drops of VYNS solution were pipetted along between the scale and the wall of the sink. The wooden

/scale

scale was released and the solution was allowed to expand over the entire area of the sink. The films were then lifted by a wire frame. Uniformity and thickness of the film depends on the speed with which the barrier is moved and on the quantity of solution. The film was fixed on an aluminium ring for experiments.

(a) <u>Deposition of Aluminium layer on the thin film</u>

Rendering the film conducting is essential otherwise it will distort the electric field by acting as an insulator. If the film were not conducting, it may build up a charge due to emission of charged particles from the radioactive deposit on the thin film and thereby changing the velocity of the electrons. A shift in the β-spectrum of ^{144}Ce for the 38.12 keV line was found towards the low energy by as much as 16 keV when insufficient quantity of Al was deposited on the VYNS resin film. The film can be painted with aquadag, but because of its large size grains, a thin layer can not be expected. The strong dependence of back scattering on the atomic number necessitates the backing to be made of low atomic number. Organic compounds and aluminium are, therefore, most suitable for backing purposes. The Edward coating unit (type 12E 115) has been used for depositing an aluminium layer on the thin film. A few small pieces of aluminium were hung on the tungsten wire of diameter 0.5 mm across the filament terminals. The Al-ring supporting the film was placed on a mica sheet having a circular hole, at a distance of 16 cms above the filament coil, in order to protect the film from overheating. A current

/of

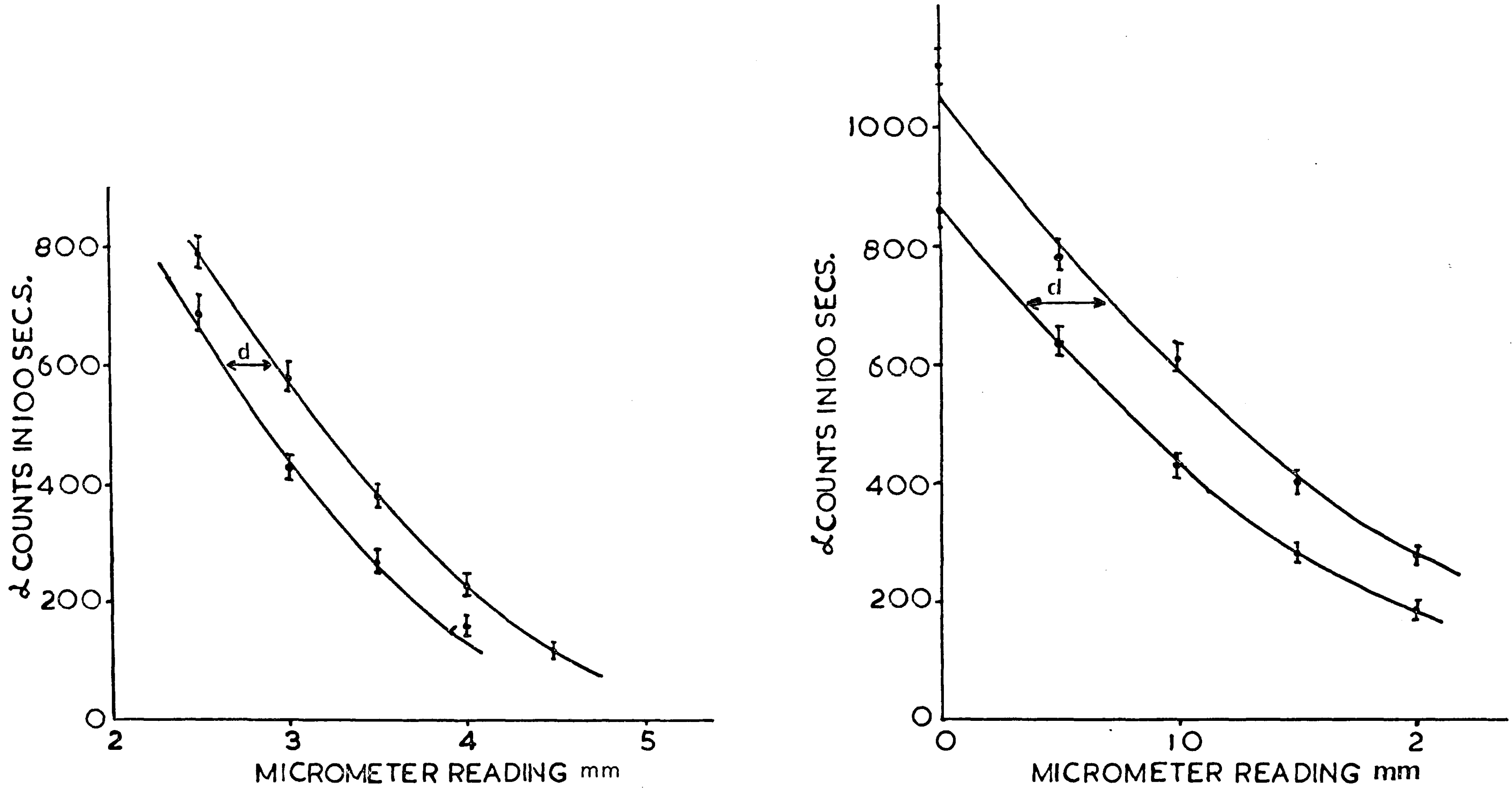

FIG. 4·1 VARIATION OF THE COUNTING RATES OF THE α PARTCLES WHEN THE DISTANCE BETWEEN THE SOURCE & THE COUNTER IS CHANGED.

of 13 Ampere was passed through the filament coil for about two minutes, while the pressure inside the chamber was 10^{-9} mm Hg. A rough estimation of thickness of aluminium deposit could be made by observing the change in colour of the film.

(b) Measurement of film thickness

There are mainly three methods of measuring film thickness:-

(i) Gravimetric (ii) optical and (iii) absorption of α-radiation. The absorption of α-particle technique was described by French, S. (1966) while measuring film thickness. The same technique has been applied in this work. ^{241}Am isotope was used as an α-source. The α-counting rate for different distances between the source and counter was recorded when the film was interposed and also when it was not there. The results were plotted in Fig. 4.1.

The thickness in μgm/cm^2 was calculated by multiplying the air equivalent a by the density of air. The minimum film thickness used in the experiment has been 25/μgm/cm^2.

3. Source preparation

As mentioned in the previous section of this chapter, the preparation of thin uniform sources on thin backing is essential in studies of low energy β-rays. Several methods, e.g. evaporation of a solution under an infra red lamp, vacuum evaporation, electroplating and electrospraying methods have been suggested by Yaffe (1962). Evaporation of solution under an infra red lamp produces a non-uniform deposit. The material concentrates in large crystals and

/forms

forms a ring shaped deposit at the periphery of the drop. Uniformity can be achieved by adding insulin, colloidal silica or cupric ferro cyanide to the drop before evaporation but they add to the source thickness. Electroplating technique produces a uniform thin source but is limited to certain materials. The electrospraying method has been found more successful in preparing β- source. The advantage of this technique is that the loss of solute is small and thin substrates do not become overheated.

4. Electrospraying method.

The electrospraying method was first proposed by Carswell and Milsted (1957). In this technique the material to be sprayed is dissolved in an organic liquid and then kept in a glass tube drawn to a capillary at one end. The anode connected to a high voltage supply is immersed into the liquid. The foil on which the liquid is to be sprayed is connected to the cathode. On applying a suitable voltage the liquid is forced out of the tube and dispersed in fine droplets over the film. Brunix and Rudstam (1961) used this technique and investigated a number of variables. Verdingh and Lauer (1963,64,67) prefer hypodermic needle connected to the glass container which allowed a constant flow rate. Michelson and Richardson (1962) used a straight glass capillary for making β- sources. The disadvantage of using a straight capillary tube is that a constant flow rate of liquid cannot be maintained. Recently Michelson (1968) has found a pyrex capillary bent twice at right angle more suitable in the preparation of thin source.

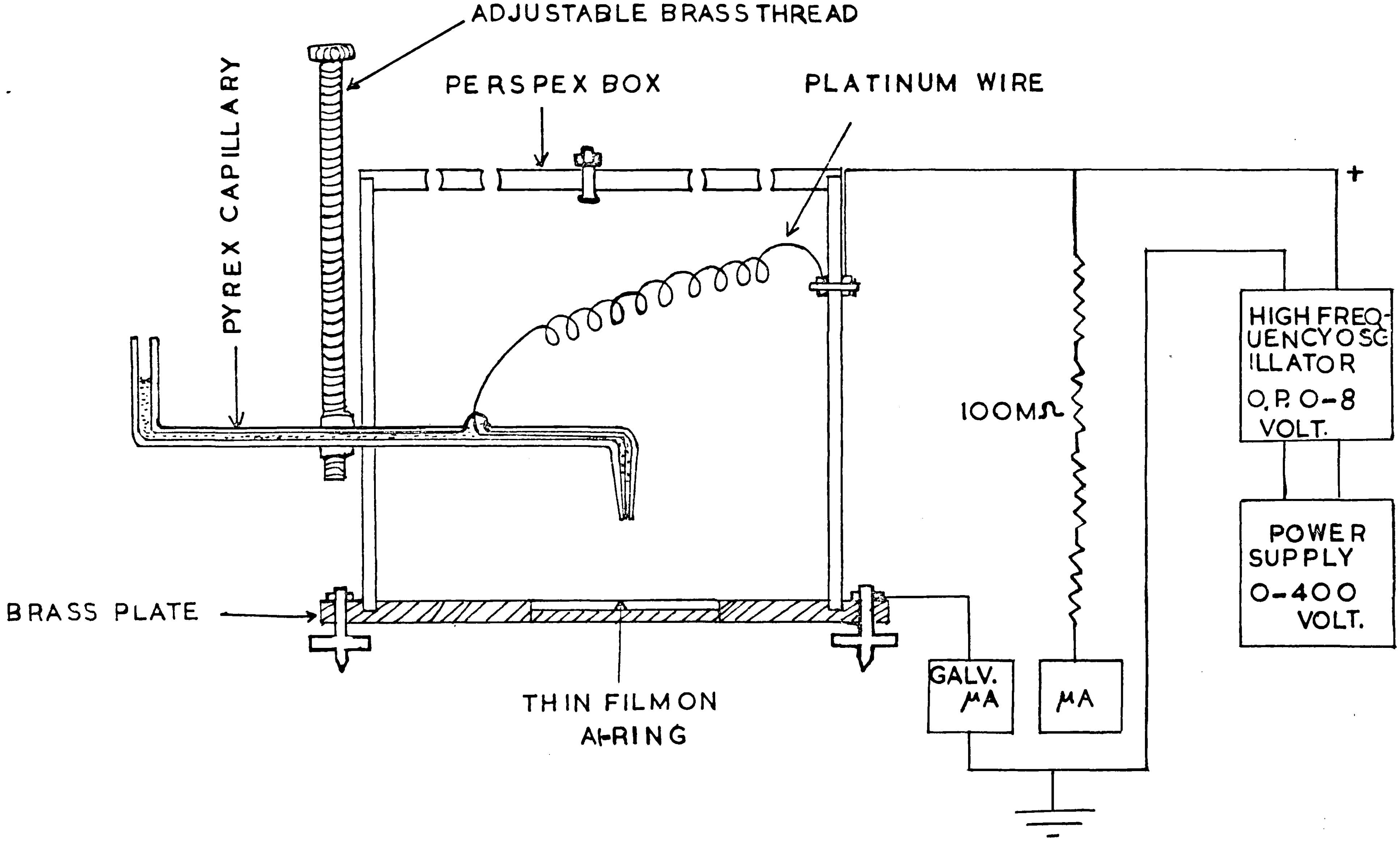

FIG. 4·2 DIAGRAM OF THE APPARATUS FOR PREPARING THIN AND UNIFORM SOURCE BY ELECTROSPRAYING METHOD.

(a) Experimental arrangement

The experimental arrangement is shown in Fig.4.2. The apparatus consists of a circular brass plate covered with plastic in order to protect the metallic surface from contamination. The walls and top of the box are made of perspex. The lid is provided with a few holes for ventilation. The whole system stands on levelling screws. A capillary jet of pyrex tube of 0.4 mm I.D. was drawn in an oxygen flame while rotating the tube in a hand-drill and letting it fall vertically under gravity (Michelson and Richardson 1962). The horizontal position of the tube keeps the hydrostatic pressure constant which is not possible with a vertical tube. The diameter of hole at the end of the capillary was 0.230 mm whereas that of the central wire was 0.229 mm. The end of the wire was kept nearly 1 mm above the tip of the tube. A central wire of Pt.-Ir alloy was preferred as it is not attacked by acid nor does it undergo corrosion. The tube can be moved up and down by adjusting the brass thread. The horizontal position can be adjusted by sliding the tube through the hole. The discharge phenomena and formation of drop at the tip can be seen through a microscope placed in front of the box and using a lamp at the back.

5. Spraying conditions

(a) Choice of capillary and central wire

The critical size of capillary and that of the electrode is an important factor for a good spray. A number of capillaries of different diameters were tried and a suitable combination of capillary and wire was chosen for the

/experiment.

experiment. A quick test, as suggested by Brunix and Hudstam was carried out by filling the capillary with liquid and inserting the central wire near the tip of the capillary. The combination for which the liquid dropped out were rejected and that with which no liquid dropped out was selected.

(b) Cleanliness of the capillary

The wire and the capillary were degreased first in chromic acid and then washed with distilled water Care was taken not to leave air bubbles inside the tube as they cause drops to fall on the target.

(c) Choice of organic solvent

For a good spray, the solvent should have (i) low surface tension to check the formation of big srops (i) high vapoure pressure to accelerate the process of evaporation :

With a mixture of alcohol and water (50:50) no spray could be obtained. A mixture of alcohol and water (66:34) was, however, found suitable for a good spray.

6. Preparation of Th B sources.

Th B - sources were deposited on the platinum spiral. The active deposit from pt.wire was dissolved into a few drops of $\frac{N}{10}$ Hcl acid and then dried under an infra red lamp. It was redissolved in a mixture of distilled water and alcohol (34:66). Nearly 50 per cent of active deposit was taken out of the pt. wire. The radioactive solution was then taken into the capillary and sprayed on a thin

/conducting

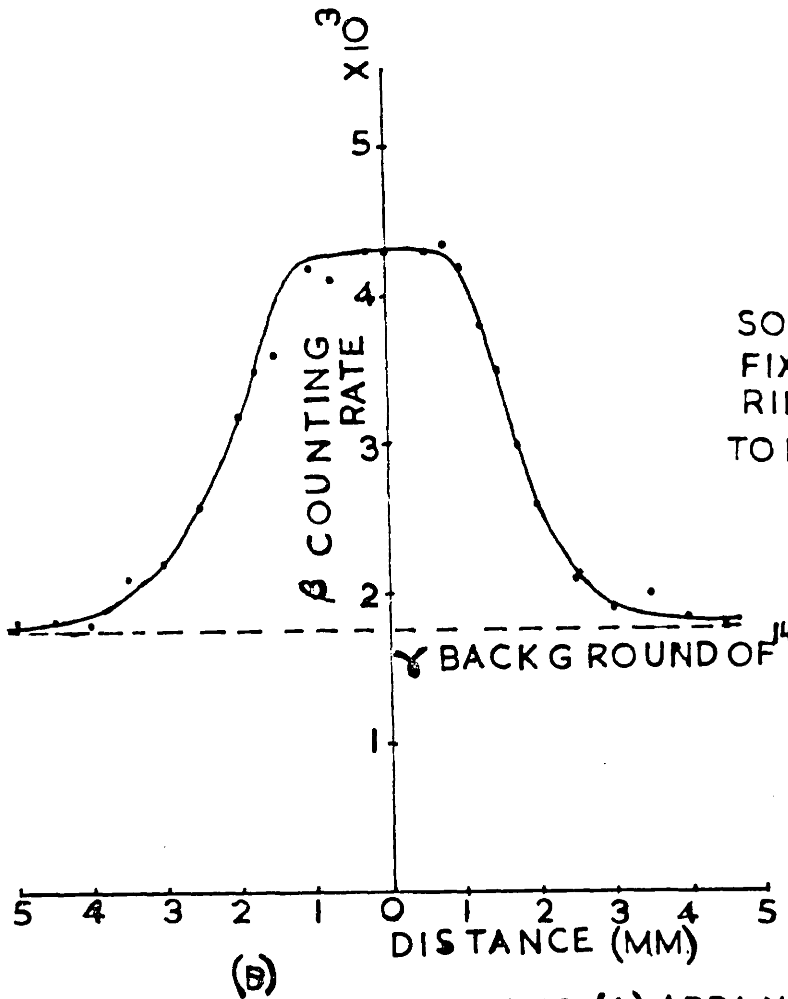

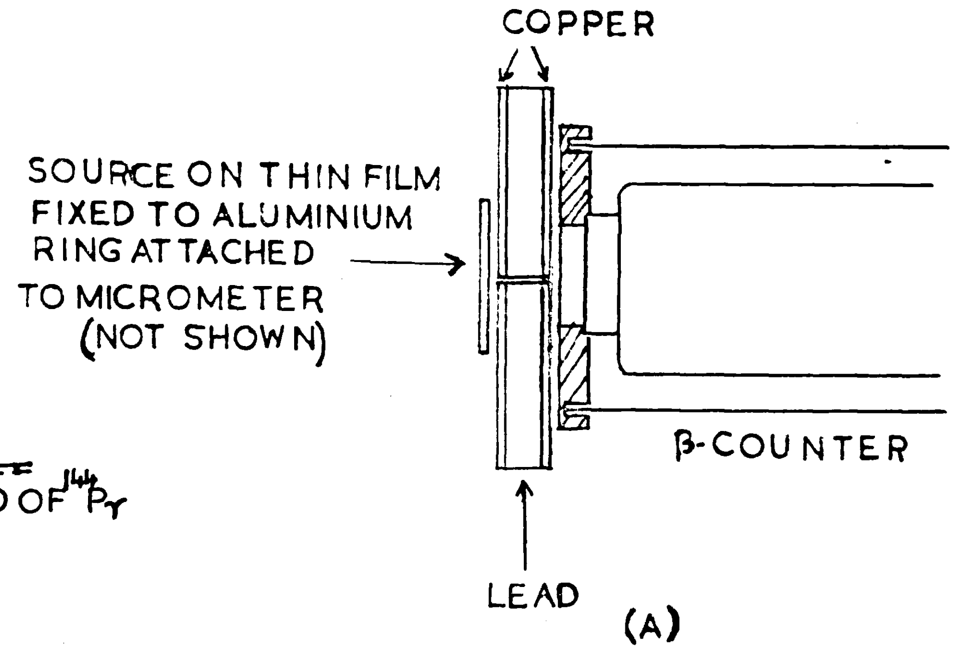

FIG.4·3 (A) ARRANGEMENT FOR UNIFORMITY TEST OF β SOURCE
(B) UNIFORMITY PLOT OF ^{144}Ce SOURCE

conducting film. The resolution of Th B - F line with 7 mm diameter of source deposit with the large spectrometer was 0.776% which was comparable to that obtained by ion collection from thoron on a 5 mm diameter metallic screw (0.869%). This revealed indirect evidence for the uniformity of the source deposit.

7. The ^{144}Ce - source

Cerium - 144 source was obtained from the Radiochemical centre at Amersham as a solution in HHcl. A few drops of the solution were evaporated by an infra red lamp. It was then dissolved in Dil. $^{N}/10$ HNO3. The solution was again dried under the infra red lamp and the nitrate was dissolved in a mixture of distilled water and alcohol. The solution was then sprayed on an aluminised thin film. The reason for dissolving the chloride salt in dil. HNO3 was because Hcl attacks aluminium. After dissolving in dil. $\frac{N}{10}$ HNO_3 it seems essential to get it dried again otherwise an increase in the proportion of water makes spraying difficult.

The distance of the capillary tip from the target was kept about 1 cm. The discharge current was fairly constant showing a stable spray.

(a) Uniformity test of ^{144}Ce - source

The uniformity of the cerium source deposit was tested by counting β-particles with a plastic scintillator. The counting arrangement is shown in Fig. 4.3. The β-rays were collimated through a 0.5 mm hole in ½" thick lead. To achieve a better collimation 1 mm thick copper plates

/having

collimating hole were fixed on both sides of the lead. The source ring was moved with a micrometer (not shown in Fig.). The flat top in Fig. 4.3 shows a uniform deposit throughout the region. The source diameter was approximately 7 mm.

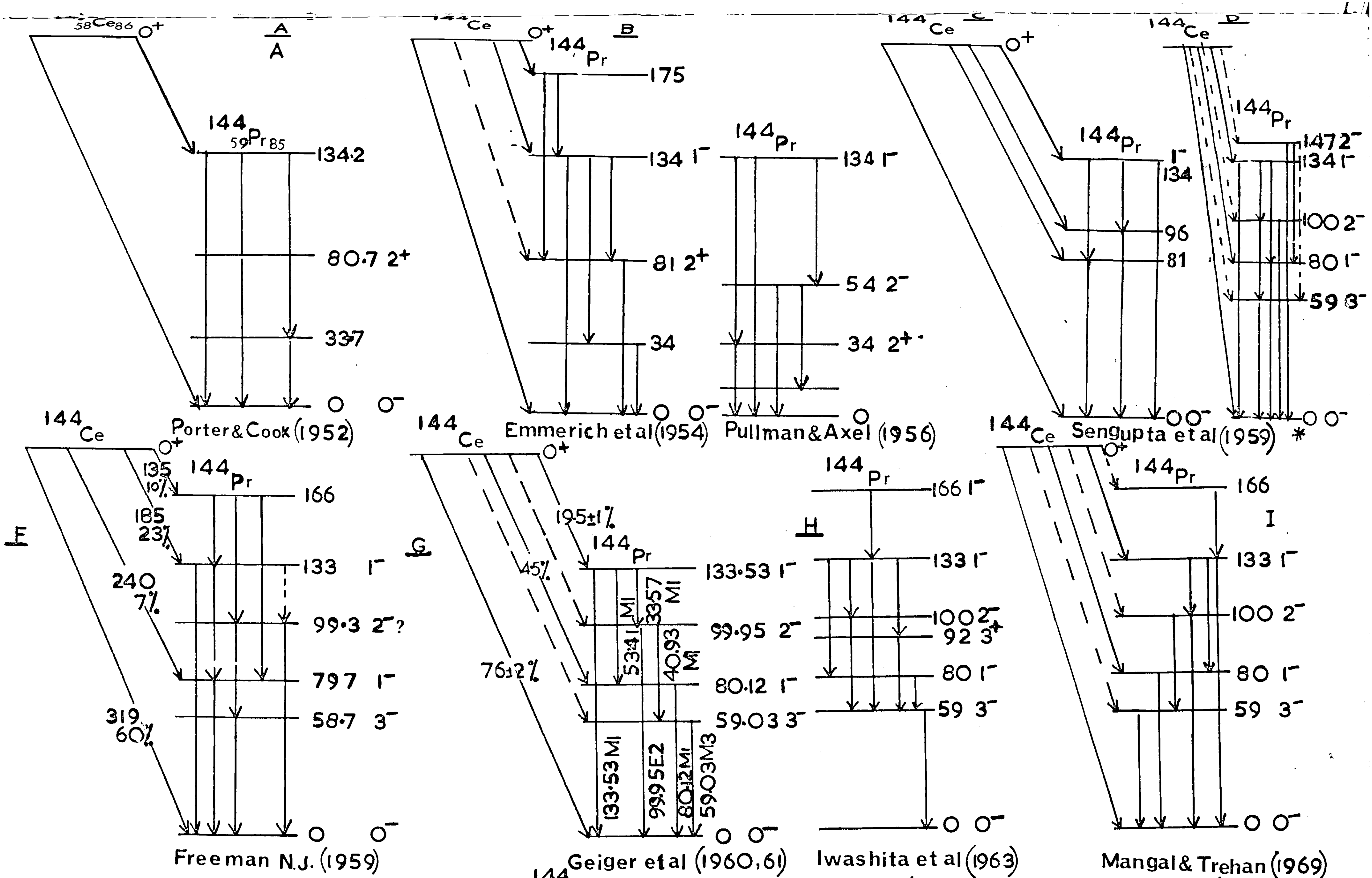

FIG. 5.1 DECAY SCHEMES OF ^{144}Ce BY DIFFERENT AUTHORS (ENERGIES ARE GIVEN IN keV)
* Forafontov et al (1962)

CHAPTER V

1. Decay scheme of ^{144}Ce

The ^{144}Ce nucleus is a fission product which has a half life of 285 days and decays by the emission of β^- rays and γ-rays to the ground state of ^{144}Pr which further decays to ^{144}Nd with a half life of 17.5 minutes. The odd-odd nucleus ^{144}Pr has been studied by various workers by means of the β- spectrum and conversion lines, $\beta^- - e^-$, $e^- - e^-$, γ-γ, $\beta - \gamma$ and $e^- - \gamma$ coincidence measurements. Energy levels in ^{144}Pr at 133 keV, 100 keV, 80 keV, and at 59 keV are well established but controversies still exist concerning the highest excited state in the ^{144}Pr nucleus. The decay schemes proposed by several workers are shown in Fig. 5.1.

Porter and Cook (1952), Pullman and Axel (1956), Hickock, Mickinley (1958), Sengupta et al (1959), Geiger and Graham (1960,61) and Fasching et al (1970) placed the upper excited state at 134 keV; Cork et al (1954) at 225 keV; Keller et al (1951), Emmerich, Auth and Kurabatov (1954) at 175; Forafontov et al at 145 keV and Freeman H.J. (1959), Iwashita et al (1963), Mangal and Trehan (1969) at 166 keV. In spite of the controversies over the upper excited level, these authors disagree over the existence of some of the low intensity γ-rays and ordering of the low intensity transitions.

(a) Existence of 166 keV level

Freeman (1959) through an extensive study of conversion lines, β^- spectra, β^- - γ and e^- - γ coincidence measurements proposed the decay scheme of ^{144}Ce with highest excited level at 166 keV. In his coincidence measurements he found the conversion line of 33.57 keV transition in coincidence with the 133.53 keV γ-ray. His conversion electron spectrum shows conversion lines assigned to 66 keV and 86 keV transitions and the Fermi-kurie analysis yields 135 keV β-feed to 166 keV level. The conversion lines spectra, e^- - γ and γ - γ coincidence measurements of Geiger and Graham (1960,61) show no evidence for the existence of an 166 keV level and assigned the highest excited level at 133.53 keV. However, they did not rule out the possibility of an additional weak conversion line of energy $\sim$ 34 keV feeding the 133.53 keV level. The conversion line studies of Geiger, Graham (1960,61) are more reliable as they were measured at momentum resolution of 0.1%. Iwashita et al (1959) in their γ - γ coincidence measurements found the presence of a weak peak at 66 keV in coincidence with the 100 keV γ-ray and thus confirmed the existence of a 166 keV level. Their γ - γ coincidence measurements show a weak γ-ray of 92 keV in coincidence with the 41 keV transition. They conclude that the 92 keV level is fed by the 41 keV transition from the 133 keV level and decays to the ground state. The presence of the 33 keV γ ray in cascade with the 53 keV γ-ray further suggests the existence of a 166 keV level. Their failure to observe the 86 keV γ-ray was due to the weakness of the transition.

/The

The $\gamma - \gamma$ coincidence, sum peak coincidence and γ-γ angular correlation measurements by Mangal and Trehan (1969) supported Freeman's decay scheme of ^{144}Ce and assigned the highest excited state in ^{144}Pr at 166 keV. Thus the possibility of the existence of two γ - rays of nearly 33 keV energy and hence the existence of the 166 keV level in ^{144}Pr is still to be solved.

The spin and parity of the ground state 0^- has been well settled, whereas those of the disputable levels, e.g. 166 keV, 92 keV and 146 keV are still to be confirmed. The spins and parities of 133.53 keV, 99.95 keV, 80.12 keV and 59.03 keV levelshave been measured by Geiger, Graham (1960,61), Burde, Rokavy and Engler (1962) and Iwashita et al (1963). The γ-γ angular correlation and $\gamma - \gamma$ coincidence measurements of Iwashita et al (1963) assigned a value of spin and parity 1^- to the 166 keV level. Attempts have been made by different authors to interpret the level spins and parities on the basis of different nuclear models. The failure of the single particle model in interpretation of the level spins and parities was that it assigned 1^- to the ground state of ^{144}Pr in contrast with the experimental value 0^-. The interpretation in terms of the unified model by Geiger and Graham (1960) has been proved more consistent with the experimental values. Burde et al (1962), and Iwashita et al (1963) have attempted to interpret the levels in terms of the shell model.

Till now all of these authors have used NaI (Tl) scintillators in the studies of γ-ray spectraand

/$\beta^- - \gamma$,

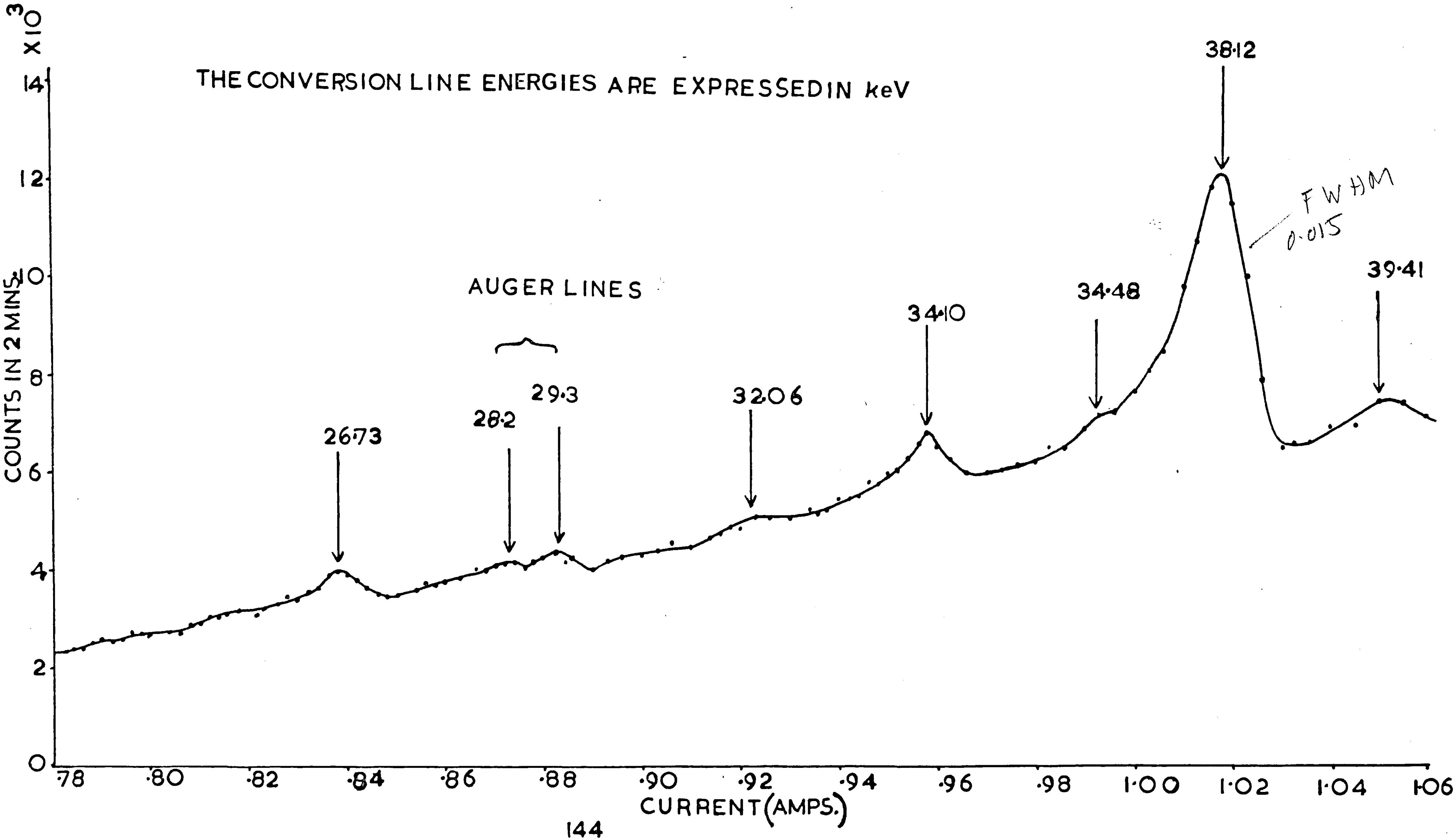

FIG.5·2 CONVERSION LINES OF ^{144}Ce MEASURED WITH THE LARGE SPECTROMETER

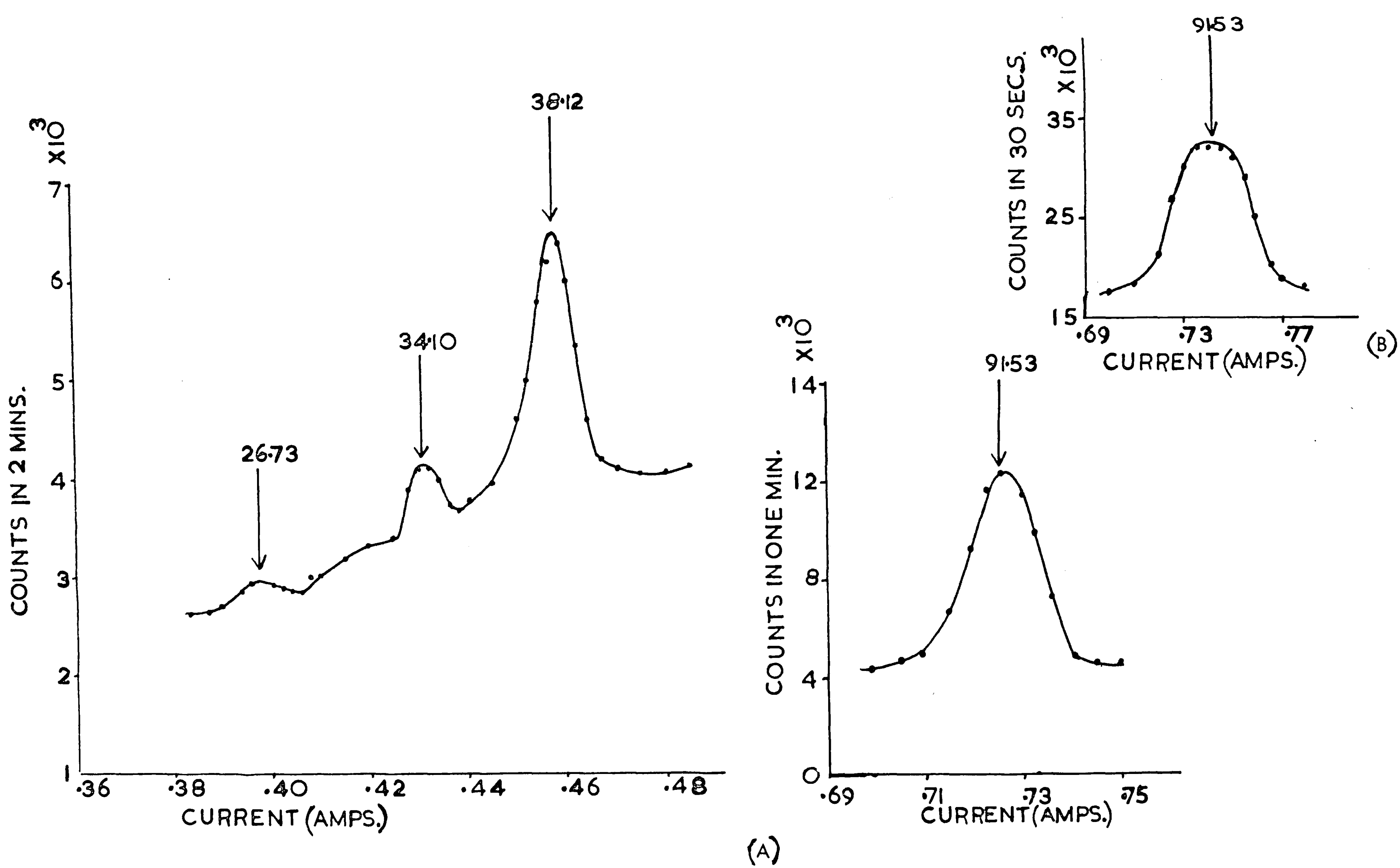

FIG. 5·3 CONVERSION LINES OF ^{144}Ce MEASURED WITH THE SMALL SPECTROMETER WITH SLIT OPENING (A) MIN. (B) WIDE. LINE ENERGIES ARE EXPRESSED IN keV.

β^- - γ, e^- - γ coincidence measurements of ^{144}Ce. NaI(Tl) scintillator has a high efficiency but a poor resolution and so the closely spaced low energy γ-rays in the decay of ^{144}Ce could not have been resolved by them. The interest lies especially in the K - X ray region where the 33.57 keV γ-ray is very close to the K X ray photopeak. None has attempted to study the decay scheme of ^{144}Ce with Ge(Li) detector and magnetic spectrometer.

In the present work an improved technique has been applied to study the present anomalies in the decay scheme of ^{144}Ce - especially the existence of the 166 keV level in ^{144}Pr. A 5 cc Ge (Li) detector and a Ge(Li) X-ray detector have been used in the studies of straight γ-ray spectra of ^{144}Pr. The ~~e~~ e^- - e^- coincidence measurements have been made by using a magnetic lens spectrometer in conjunction whth a Prolate spheroidal field β-ray spectrometer. They are described in this chapter. The e^- - γ coincidence measurements have been made by using the Ge(Li) X-ray detector with the large spectrometer (see ChapterVI).

2. <u>Conversion lines of ^{144}Ce</u>

Conversion lines of ^{144}Ce were measured with the large spectrometer with momentum resolution of 1.3% for 38.12 keV line (ig. 5.2). The source has been prepared by electro-spraying method. The conversion line spectrum below 38.12 keV measured with the small spectrometer is shown in Fig. 5.3A. The momentum resolution for 91.53 keV line was 2.3%. This spectrum was taken when the slit opening of the small spectrometer was minimum.

3. Arrangement for $e^- - e^-$ coincidence

(a) Introduction. The importance of coincidence counting technique lies in identification of weak lines which are not well revealed in single β or γ spectrum, in the studies of cascade nature of transitions and in measurement of lifetime. In the present work $e^- - e^-$ and $e^- - \gamma$ coincidence methods have been used in the study of the decay scheme of ^{144}Ce.

(b) Advantage of $e^- - e^-$ coincidence over $e^- - \gamma$ and $\gamma - \gamma$ coincidence

The $e^- - e^-$ coincidence technique has advantages over $e^- - \gamma$ and $\gamma - \gamma$ coincidence techniques. In the former, a high energy resolution can be arranged in both the channels without interference from the compton distribution, whereas in thelatter interference from compton electrons cannot be avoided. In a magnetic spectrometer, plastic scintillators are used which have considerably faster rise time than NaI (Tl) scintillators and Ge(Li) detectors. Therefore, a better time-resolution is achieved with magnetic spectrometers. In a magnetic spectrometer, the energy selection takes place before the particles reach the detector, therefore a stronger source can be used without overloading the counter unlike in a pulse height spectrometer. The main disadvantage with magnetic spectrometers is that they have less collecting powers than scintillation spectrometers and hence lower coincidence counting rates.

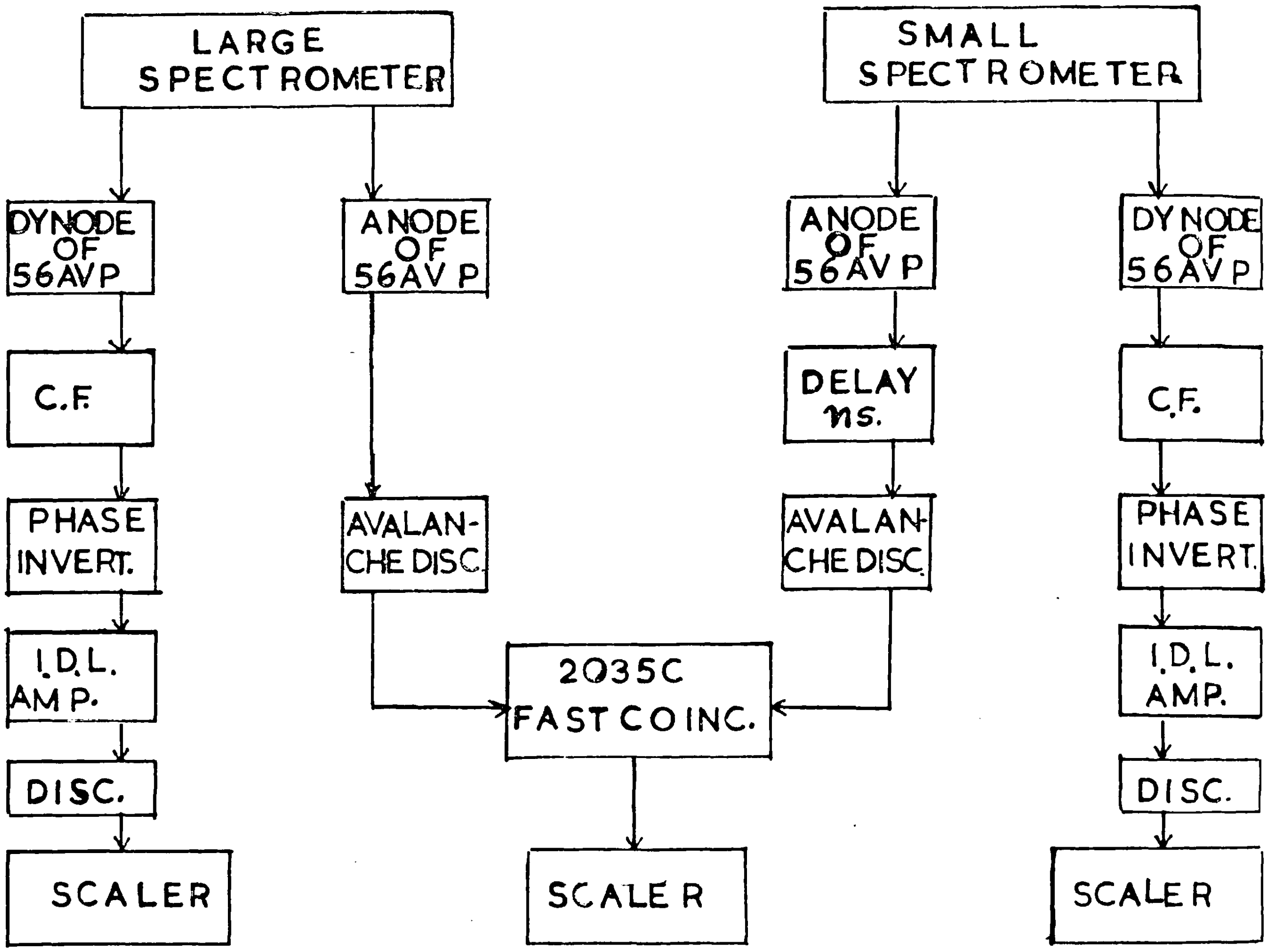

FIG.5·4 A BLOCK DIAGRAM OF e^{-}-e^{-} COINCIDENCE COUNTING.

(c) Experimental arrangement

In the present $e^- - e^-$ coincidence experiment the prolate spheroidal field β-ray spectrometer has been used with a magnetic lens (small spectrometer) spectrometer. As the energy selections in both the channels are achieved before the electrons arrive near the detector, hence it was sufficient to use only fast channels in $e^- - e^-$ coincidence measurements. This system was previously used by Michelson D. (1961), whereas French, S.(1966) used a fast slow coincidence system. Michelson used valve circuitry, E.M.I. photomultipliers and Ne 102 plastic scintillators, while French, S. (1966) improved the fast channel by using avalanche discriminators but retaining the existing detector and photolultiplier. In the present work the detecting systems of both the spectrometers have been modified (Chapter II), by using 56 A V P photomultipliers, NE 104 plastic scintillators, new light guides and avalanche discriminators. An equiangular spiral light guide has been used in the large spectrometer in order to improve the light collection efficiency. The timing signals are derived from the anode of the 56 A V P photomultiplier and are inverted by a transformer to trigger the avalanche discriminator circuit (Fig. 2.3A). The bias on the avalanche discriminator was kept above the detector noise level. No deterioration in rise time at the secondary of the transformer was observed. The coincidence circuit is shown in Fig. 5.4. The fast negative output pulses of avalanche discriminators gate the Harwell 2035C fast

/coincidence

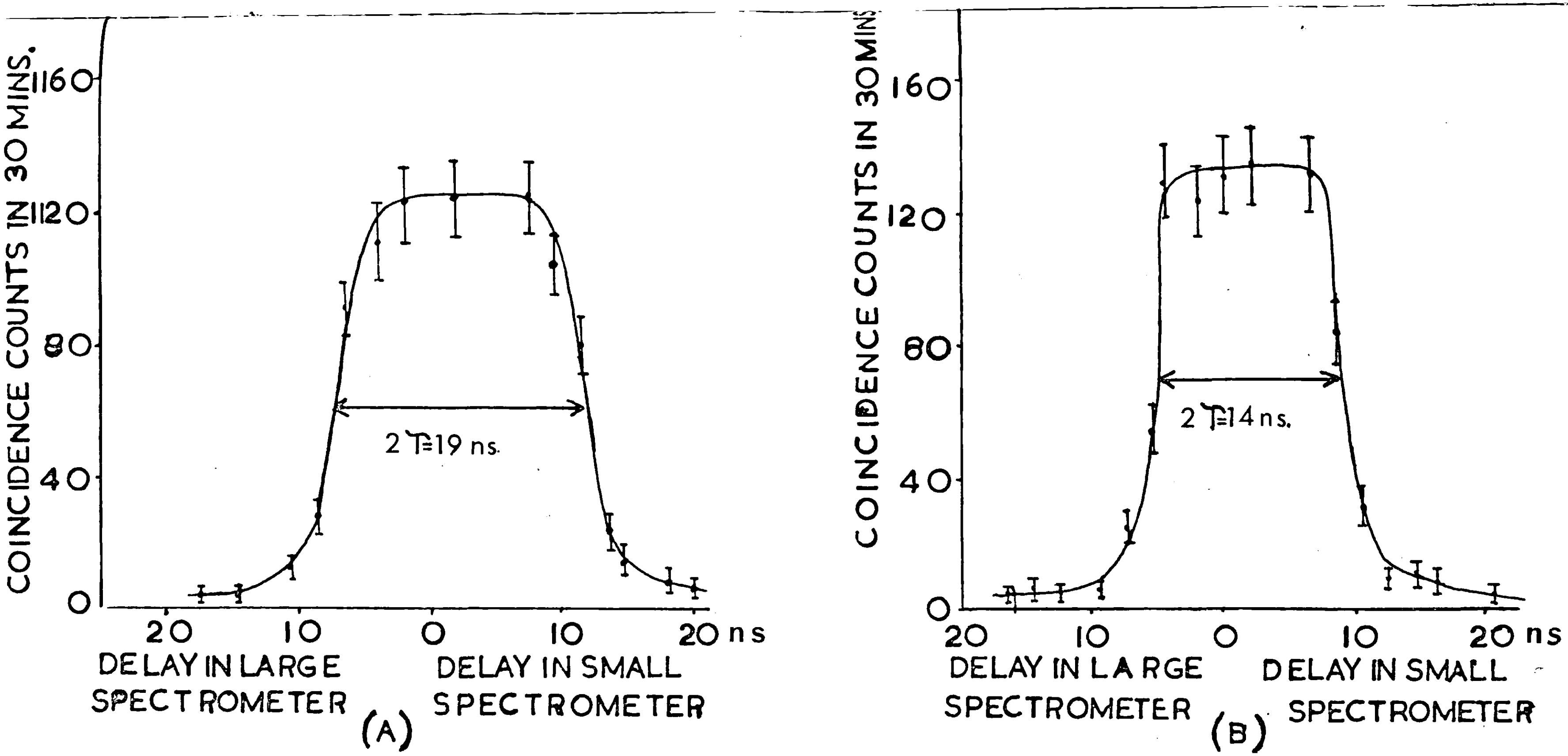

FIG.5·6 DELAY CURVES WHEN THE LARGE SPECTROMETER WAS FOCUSSED ON THE CONTINUOUS SPECTRUM NEAR 41 keV & SMALL SPECTROMETER ON THE 91·53 keV CONVERSION LINE OF ^{144}Ce.

(A) CLIPPING CABLES 3′
COMIXER BIAS 200

(B) CLIPPING CABLES 3′
COMIXER BIAS 300

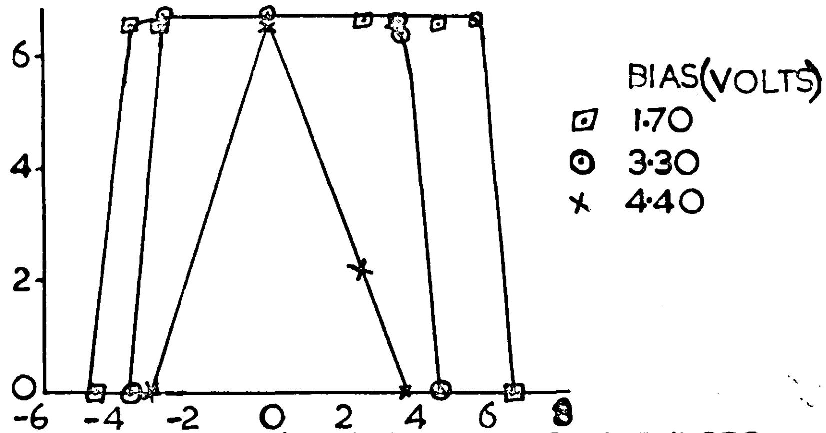

FIG.5·5 DELAY CURVES WITH THE ARTIFICIAL PULSES ON DIFFERENT BIAS SETTINGS.

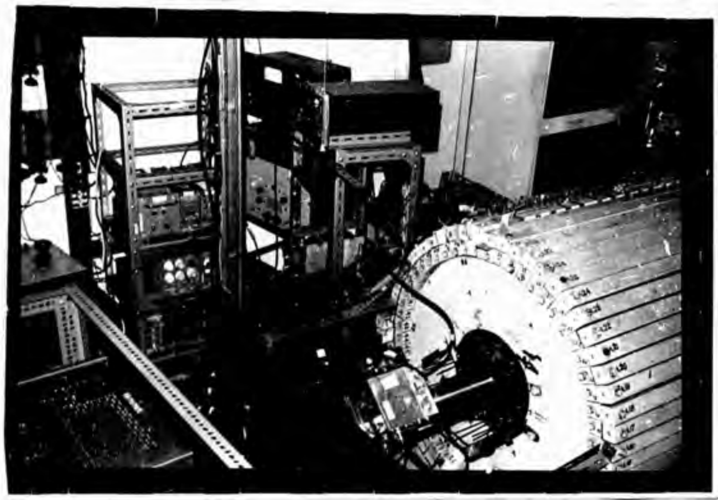

FIG. 5·6 (C) VIEW OF THE LARGE SPECTEROMETER AND ASSOCIATED ELECTRONICS

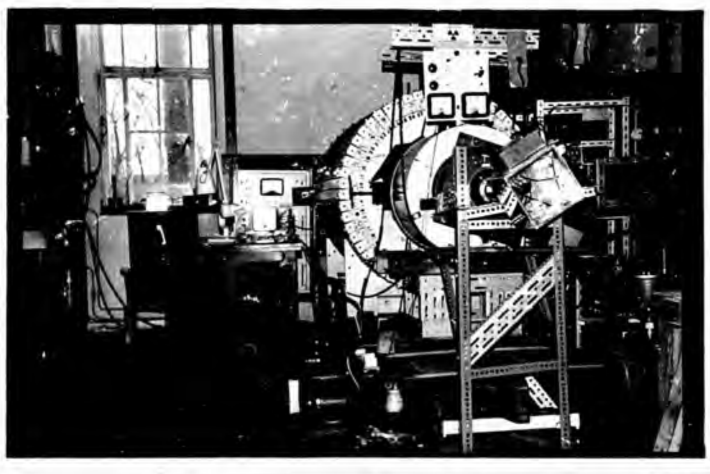

FIG. 5·6 (D) THE SPECTROMETERS ARRANGED FOR e^{-}-e^{-} COINCIDENCE EXPERIMENT coincidence unit. The coincidence pulses are counted with a fast Harwell 2019B scaler. The single pulses in the slow line were counted to check the position of the conversion line. However, the fast channels were also used after every reading to check the counting rate in a particular channel, simply by switching the other off. The coincidence circuit was first tested by splitting the avalanche discriminator output pulse into two and then feeding them into the fast coincidence unit. Delay curves on different conixer bias settings are shown in Fig. 5.5.

4. $e^- - e^-$ coincidence measurements with ^{144}Ce

The $e^- - e^-$ coincidence measurements of the γ-rays in cascade and also of those which are not in cascade in ^{144}Pr are described below

(a) Delay curves

The E. H. T. on the photomultiplier of the large spectrometer was kept at 2.2 kV while that on the small spectrometer was 2.32 kV. The 133.53 keV level has average short mean life time of the order of 6.6 ps. and therefore a prompt curve is expected between the 91.53 keV line (K133.53) and the continuous β-ray. A delay curve was plotted focusing the small spectrometer on the top of 91.53 keV conversion line and the large spectrometer on the continuous β-rays near the 41 keV region. The region near 41 keV was selected as it was free from conversion line and also it was near the 26.73 keV line. The purpose of the delay curve was to investigate the difference in transit time in both the spectrometers of the electron-energies to be investigated in

/coincidence

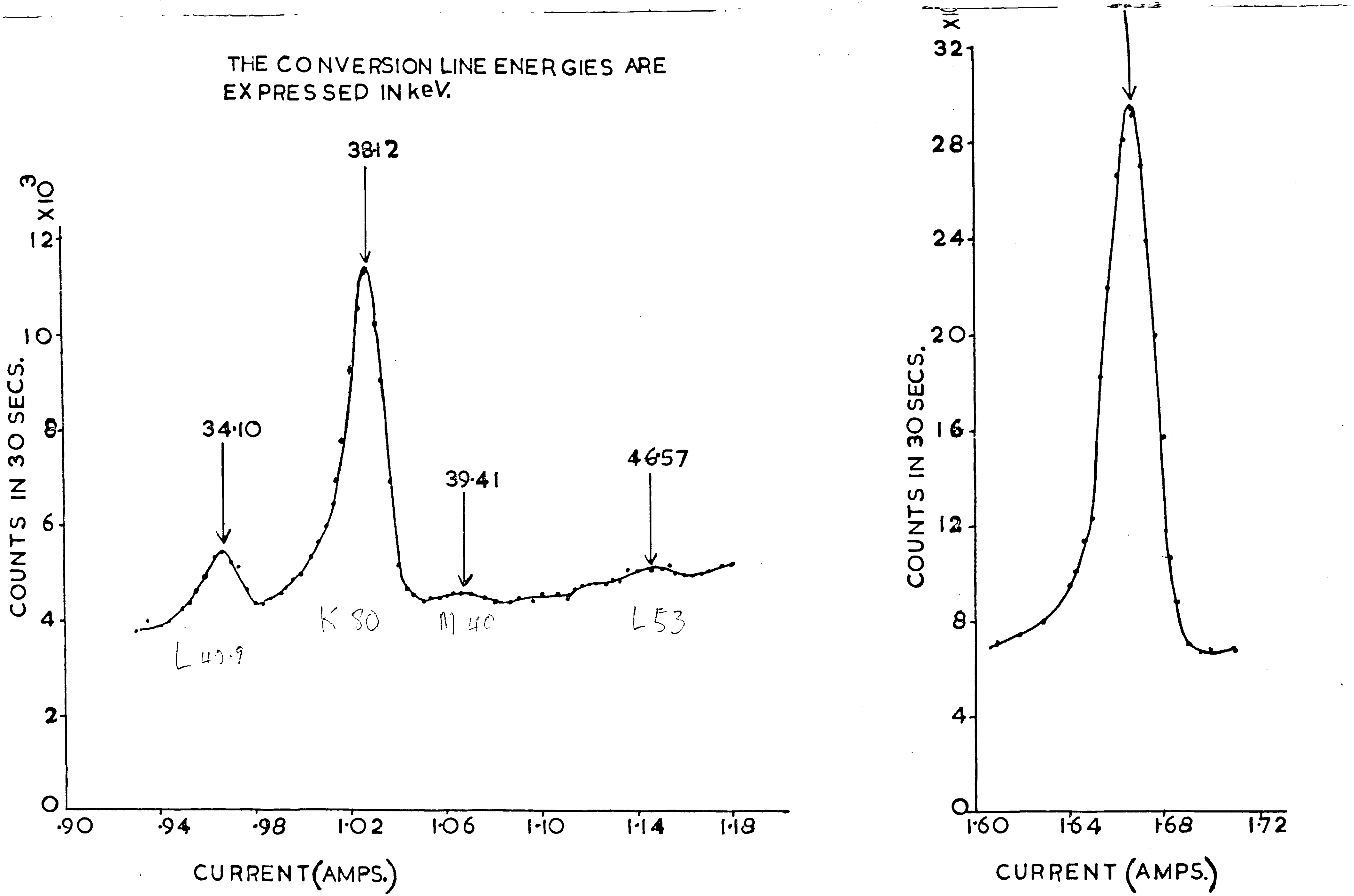

FIG. 5·7 CONVERSION LINES OF ^{144}Ce MEASURED WITH THE LARGE SPECTROMETER

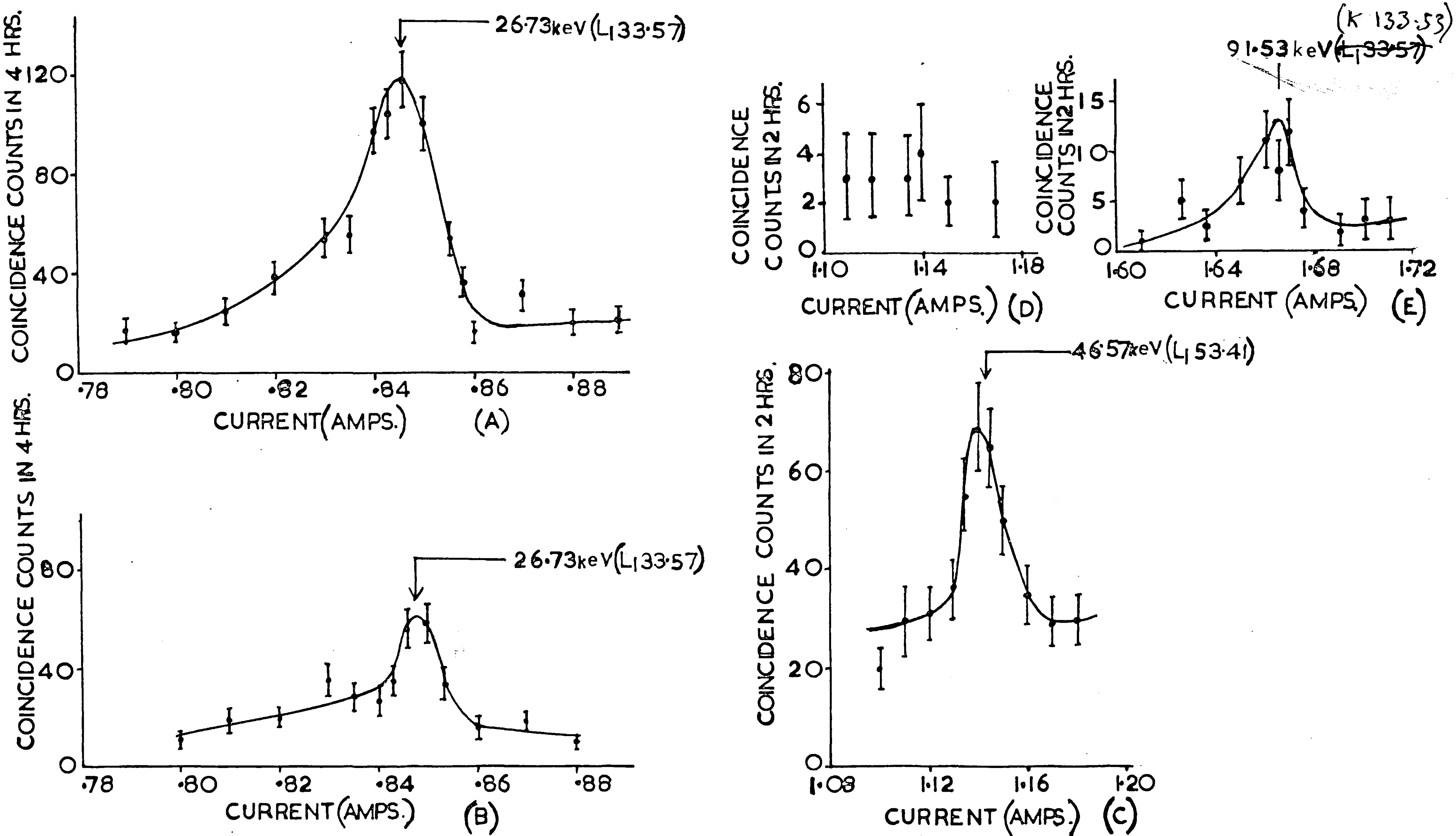

FIG. 5·8 COINCIDENCES WITH (A) 34·10 keV(L1 40·93) (B) CONTINUUM BELOW 34·10 keV(L1 40·93) (C) 38·12 keV(K 80·12) (D) CONTINUUM ABOVE 38·12 keV(K 80·12) (E) 38·12 keV(K 80·12) coincidence measurements. A 3' clipping cable on both channels of the fast coincidence unit gave rise to a resolving time of 14 ns. (Fig. 5.6). The change in transit time between 41 keV and 26.7 keV energy comes to $\sim$ 3 ns which is conveniently low in comparison to the resolving time. The delay curves for two co-mixer bias settings are shown in Fig. 56 A,B . The chance coincidence rate was calculated by introducing a big delay in either line which was found equal to 3×10^{-3} c/sec as calculated from the relation $N_c = 2\tau N_1 N_2$.

(b) L_1 53.41 - K80 12 coincidence

The small spectrometer was gated on the peak of the 38.12 keV (K 80.12) line and current in the large spectrometer was scanned. The 46.57 keV line (L1 53.41) is hardly visible in the single β-ray spectrum (Fig. 5.7), whereas in the coincidence spectrum (Fig. 5.8C) a big enhancement in the relative height of the 46.57 keV line is observed. Fig. 5.8D shows the coincidence spectrum when the small spectrometer was grated on the high energy side of the 38.12 keV line. An enhancement in the height of the 46.57 keV line in the coincidence spectrum shows that the 38.12 keV line is in coincidence with the 46.57 keV line.

(c) K 133.53 - K 80.12 coincidence

The 91.53 keV line appears in the coincidence spectrum Fig. 5.8E when the small spectrometer was gated on the top of the 38.12 keV line. No enhancement in the relative height of the 91.53 keV line is found. The appearance of the peak is because of the coincidence of the 91.53 keV line with

/the

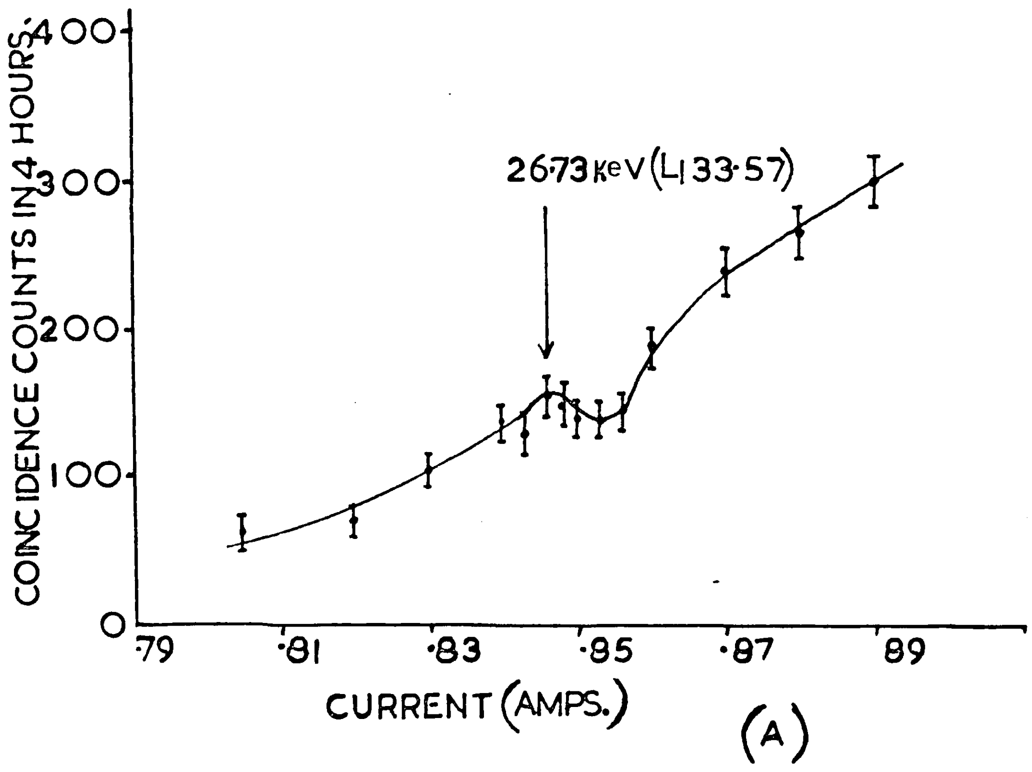

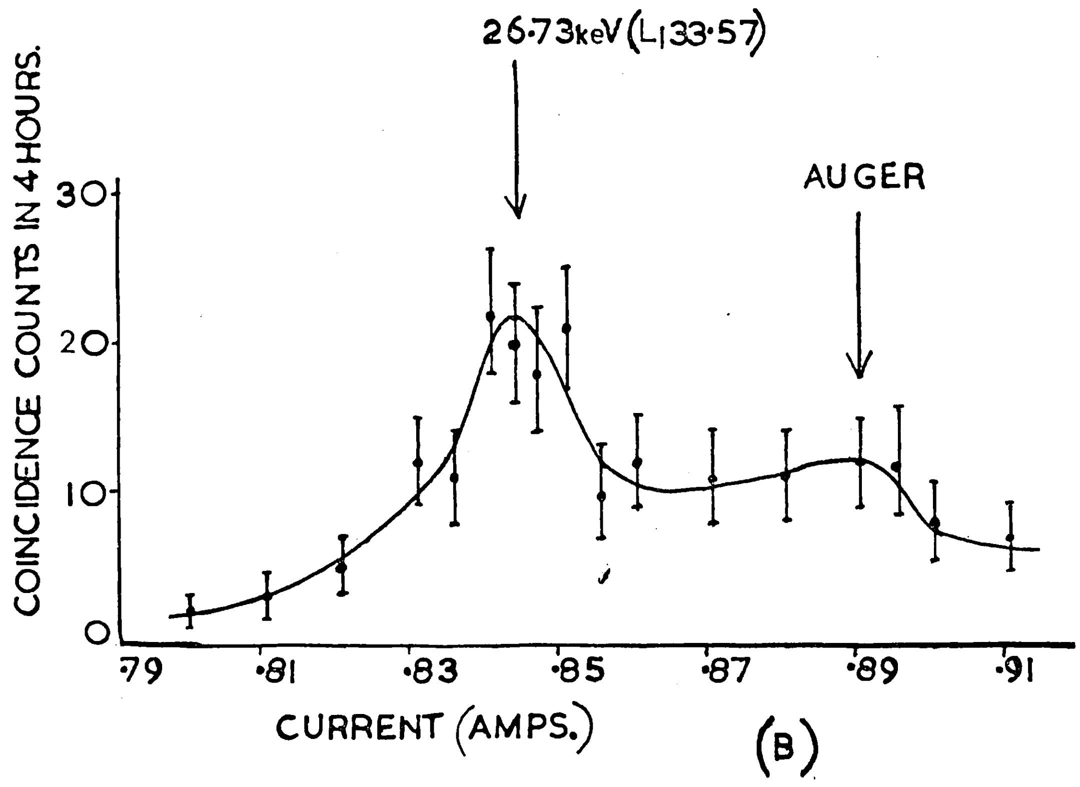

FIG. 5·9 (A) COINCIDENCES WITH THE 91·53 keV (K 133·53) CONVERSION LINE
(B) COINCIDENCES WITH CONTINUUM ABOVE 91·53 keV (K 133·53)

the continuous β-rays. The conclusion is that the K 133.53 is not in coincidence with the K 80.12 line.

(d) L_1 40.91 - L_1 33.57 coincidence

Fig. 5.8A shows the coincidence spectrum of the 26.73 keV ($L_1$33.57) line when the small spectrometer was gated on the peak of the 34.12 keV (L_1 40.91) line. The ratio of the height of the line to the continuum in the coincidence spectrum is 5:1 whereas in the single spectrum it is 1:3. The big enhancement in the relative height of 26.73 keV line in coincidence spectrum suggests that the 34.12 keV line is in coincidence with the 26.73 keV line. Fig. 5.8 shows the 26.73 keV line in coincidence with the continuous β-rays when the small spectrometer was gated on the low energy side of the 34.12 keV ($L_1$40.91) line. The reason for not gating on the high energy side of the 34.12 keV line was to exclude the contribution of the rising part of the 38.12 keV (K 80.12) line. The big enhancement in the intensity of the 26.73 keV line in the coincidence spectrum suggests a strong γ-ray having a large conversion coefficient.

(e) K133.53 - L1 33.57 coincidence

To verify the existence of a 166 keV level attempts have been made to see the coincidences between 91.53 keV (K 133.53) and 26.73 keV (L1 33.57) conversion lines. Because if 166 keV level were present it will decay to 133.53 keV level with the emission of ~ 33.57 keV γ-ray and hence a coincidence between their conversion electrons would be detected. Such experiments were attempted by

/Michelson, D.

Michelson, D. (1961) and French, S. (1966), but their results failed to find any evidence of a 166 keV level. With improved detecting systems in both the spectrometers, the same experiment was tried by gating the small spectrometer first on the peak of the 91.53 keV line and then on the high energy side of the 91.53 keV line and scanning the current in the large spectrometer. The two coincidence spectra of the 26.7 keV line (L_1 33.57) are shown in ~~the~~ Fig. 5.9. On comparing the coincidence spectrum of the 26.7 keV line Fig. 5.9A with that of the single spectrum Fig. 5.2 no such enhancement in the relative height of the 26.73 keV line is observed. The difference in the height of the lines in Fig. 5.9(A) and (B) is 17 whereas the standard deviation in Fig. 5.9A is $\pm$ 10. This difference of 17 counts is comparable to the statistical fluctuation. The rise in the coincidence spectrum above = 0.85 Amps can be caused by the fact that some of the unresolved Auger electrons are in coincidence with the 91.53 keV (K133.53) conversion line. From this particular measurement it is difficult to set the lower limit for a 166 keV to 133.53 keV transition.

CHAPTER VI

e⁻ - γ coincidence measurements of ^{144}Ce

1. Introduction

The e^- - γ coincidence measurements of ^{144}Ce have been made by Freeman (1959), Geiger et al (1961) and Forafontov (1962) using a magnetic spectrometer and NaI(Tl) scintillator. Because of the poor resolution of NaI(Tl) scintillator, many γ ray lines in the decay of ^{144}Ce could not have been resolved. The region of interest lies where the 33.57 keV γ-ray is masked by the K-X ray photopeaks. In the present work an improved technique of e^- - γ coincidence using a Ge(Li) X-ray detector in conjunction with the large spectrometer has been applied in the studies of the decay scheme of ^{144}Ce.

2. Experimental arrangements

(a) The Ge(Li) X-ray detector

The HE, GO x 25-3A Ge(Li) X-ray detector is mainly useful for the studies of low energy γ-rays. The detector has a thin Be-window and the F.W.H.M. at the 14 keV as claimed by the manufacturer is 290 ev.

The following are the specifications:-

Area	25 mm^2
Depth	3 mm
Operational voltage	- 500V
Leakage current	10 PA
Window z	Gold surface barrier
Window	0.008"Be

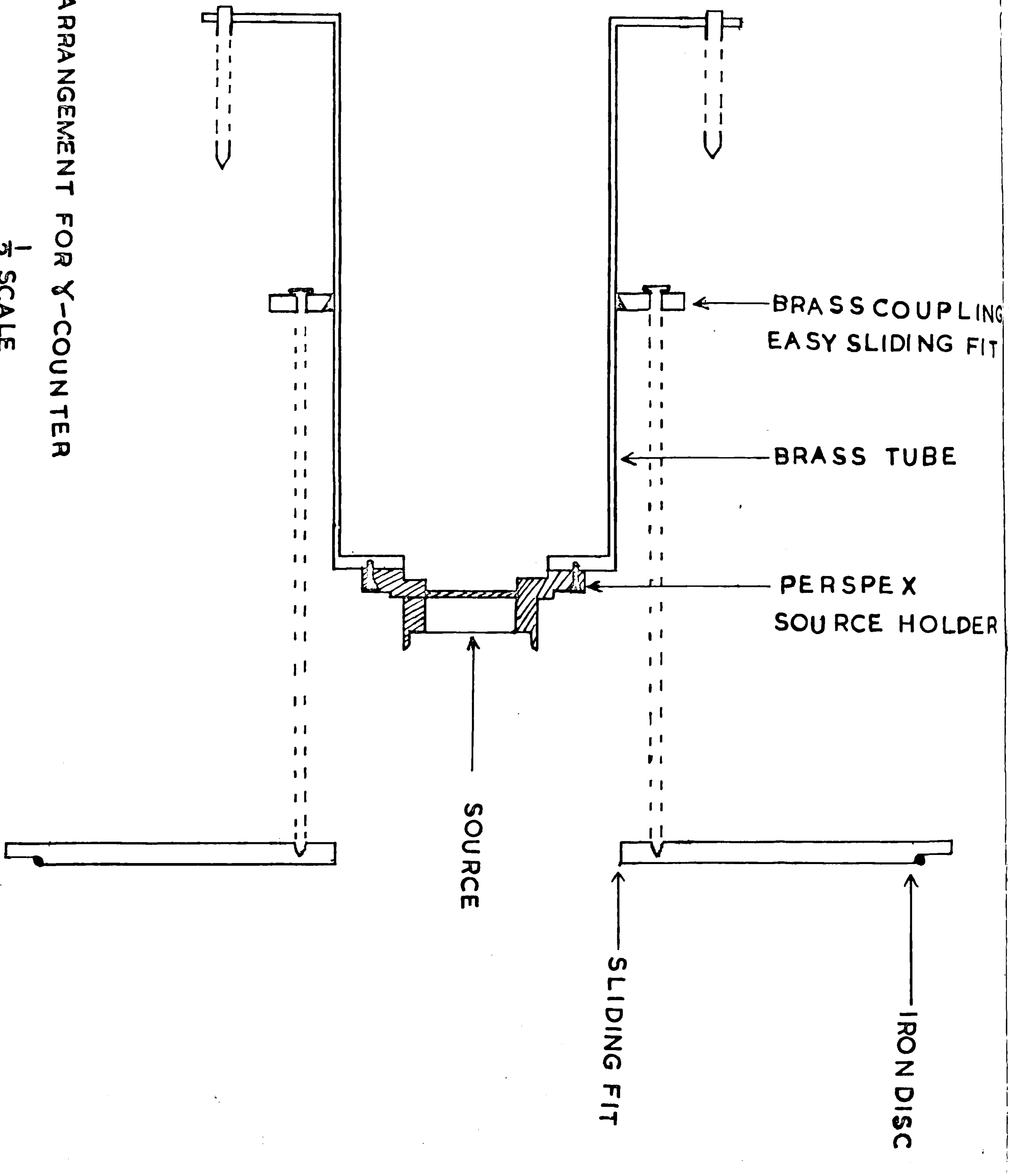

FIG. 6.1 ARRANGEMENT FOR γ-COUNTER
$\frac{1}{2}$ SCALE

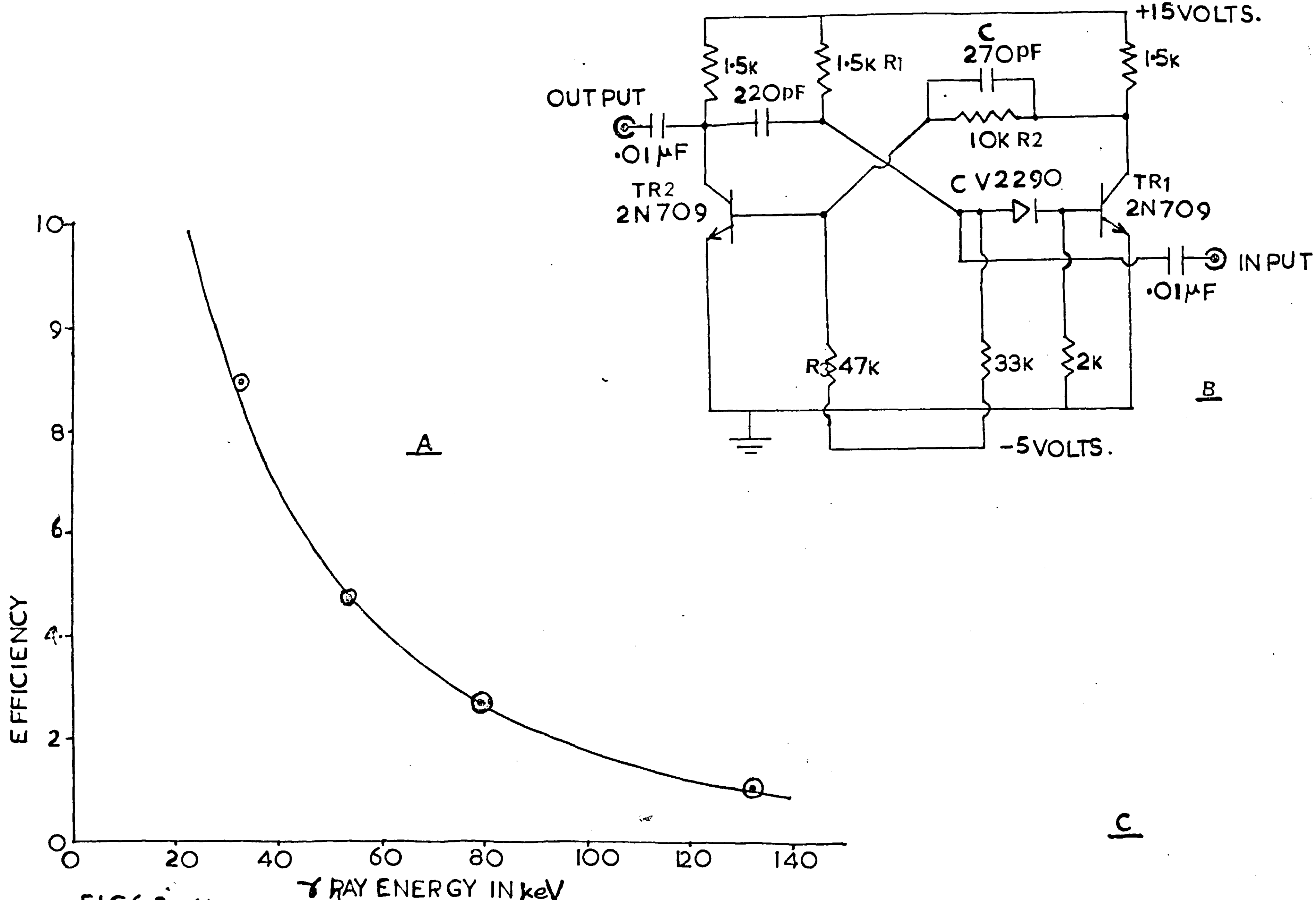

FIG.6·2 (A) EFFICIECY CURVE OF THE X-RAY DETECTOR
(B) GATE PULSE GENERATOR (C) OUT PUT PULSE FROM THE GATE PULSE GENERATOR

(b) Modifications to beta-gamma source holder

An arrangement to hold the γ-counter is shown in Fig. 6.1. The perspex source holder and the iron disc were the same as used by Freeman (1960), but a brass tube of a larger length and diameter (8" x 4") was used so as to cover the whole length of the Ge(Li) detector's cold finger and if necessary, the NaI(Tl) counter with a 56 AVP photomultiplier. The perspex thickness at the centre was kept at 1/8". The outer surface of the perspex was made conducting with an aluminium coating whereas the inner surface was painted black with aquadag to make it light tight.

(c) Gate pulse generator

The basic circuit of the gate pulse generator is given by Towers T.D. (1965). The circuit is shown in Fig. 6.2B. The author wishes to thank Mr. R.H.Thomas for bringing this circuit to his attention. It is a monostable circuit having ultra fast switching transistors, 2N 709. Before the monostable is triggered by the negative pulse from the slow coincidence unit, the transistor TR_1 is biased on by the current through the base resistor R_1 and the forward biased diode D (CV2290) whereas TR_2 is biased off by the resistors R_2 and R_3 i.e. TR_1 is conducting and TR_2 is cut off. On an application of a negative trigger pulse from the output of the slow coincidence, the diode D is cut off and TR_1

/starts

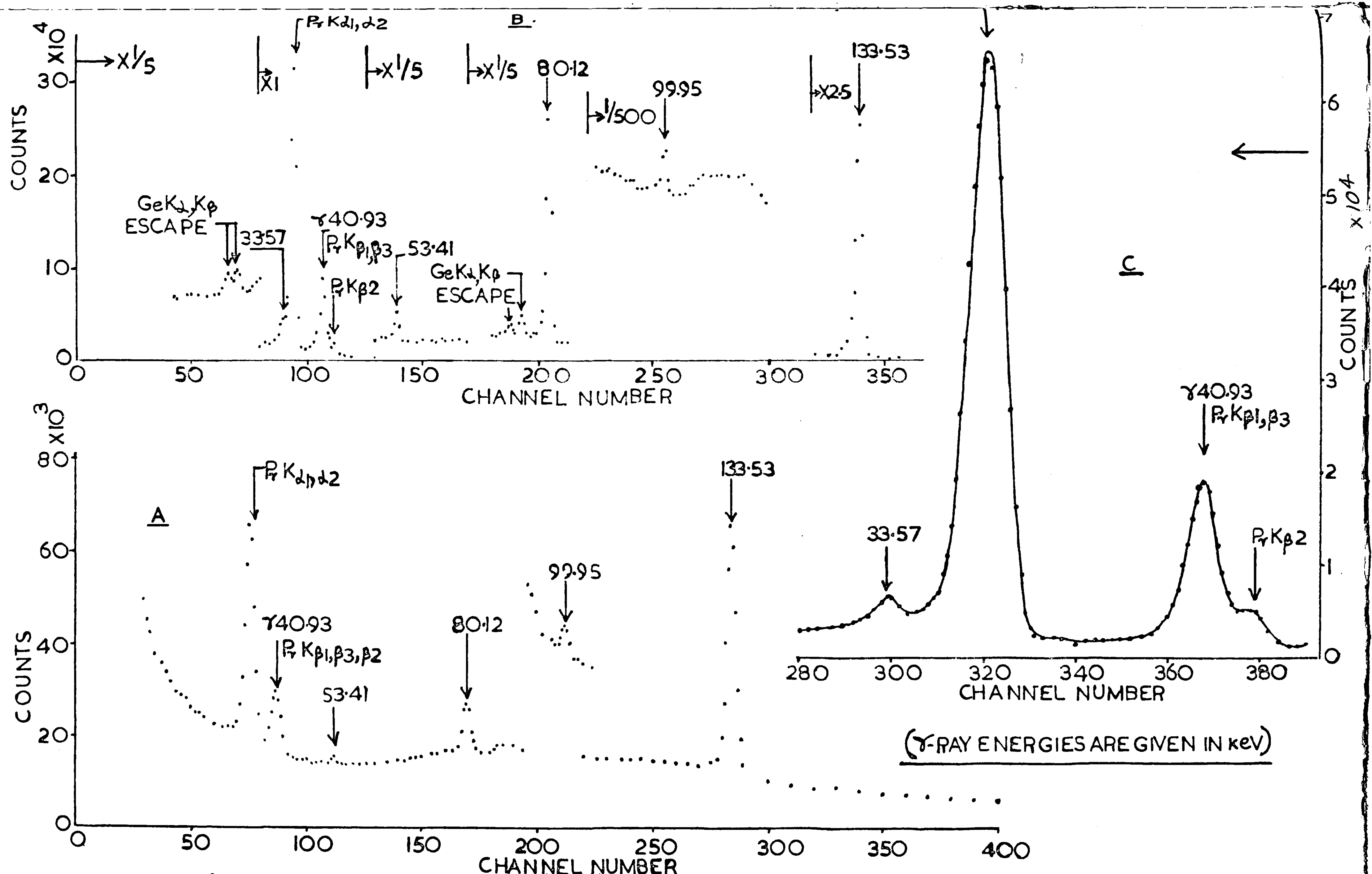

FIG.6·3 GAMMA RAY SPECTRUM OF $^{144}Ce \rightarrow ^{144}Pr$ MEASURED WITH THE (A) 5cc Ge(Li) DETECTOR (B) X-RAY DETECTOR, (C) X-RAY SPECTRUM ON THE EXPANDED CHANNELS.

starts switching off. The diode was used to protect the base emitter junction of TR_1 from exceeding its voltage rating. A regenerating action takes place through the cross-coupling resistor R_2 which drives the TR_2 on and the circuit flips into a semi stable state with TR_1 off and TR_2 on. The collector potential of TR_2 falls and a negative output pulse appears.on the collector. The capacitor C speeds up the transition between the stable and unstable states. An output pulse of the gate pulse generator is shown in Fig. 6.2 C.

(d) <u>The Harwell 2002A fast amplifier</u>

The Harwell 2002A unit is a distributed amplifier with a rise time of about 2.5 ns and a gain of 20dB. This amplifier was used in the Ge(Li) fast channel (Fig. 6.5). The fast output pulse of the Ortec 261 time pick off control is amplified by the distributed amplifier to about -5 Volt, which was suitable to operate the fast coincidence unit.

3. <u>The γ-ray spectra of ^{144}Ce</u>

Fig. 6.3A shows the γ-ray spectrum of ^{144}Ce below 133.53 keV measured with the 5 cc Ge(Li) detector. The 53.41 keV, 80.12 keV, 99.95 keV and 133.53 keV γ-rays are well separated. The F.W.H.M. for ^{241}Am 59.53 γ-ray photopeak was 2.1%. Due to a poor resolution, the 33.57 keV γ-ray has not been resolved from the Kα

/X-rays.

X-rays. The spectrum shows a single peak for Pr $K\alpha_1$, $K\alpha_2$ X-rays and γ33.57 and also for the γ40.93, Pr $K\beta_1$, $K\beta_3$, $K\beta_2$ X-rays. The hump on the higher energy side of the 80.12 keV photopeak is due to the compton background of the 133.53 keV photopeak.

Fig. 6.3B shows the γ-ray spectrum of $^{144}Ce \rightarrow {}^{144}Pr$ observed with the X-ray detector. The F.W.H.M. for the 14.35 keV line of 57 C_o was 500 ev. The γ 33.57 has been resolved from the $K\alpha$ X-ray (Fig. 6.3c). It shows a single photopeak for the $K\alpha_1$,$K\alpha_2$ and also for γ40.93 and $K\beta_1$, $K\beta_3$ X-rays. The two peaks below 33.53 keV and 80.12 keV are interpreted as the Ge escape peaks.

4. Efficiency of the X-ray detector

The relative efficiency of the X-ray detector for various γ-radiations was calculated in the manner suggested by Lieshout et al (1965). The relative efficiency can be expressed by the relation

$$\frac{A_1}{A_2} = \frac{I_1}{I_2} \, \frac{\varepsilon_1}{\varepsilon_2} \qquad (6.1)$$

where I_1 , I_2 are the accurately known intensities of the γ-radiations from a standard source, A_1, A_2 are the full photopeak areas measured experimentally and ε_1, ε_2 are the efficiencies of the detector for the two radiations.
The efficiency calibration of the X-ray detector was carried out with the Geiger (1960,61) values of γ-ray intensity of ^{144}Ce. Keeping ε_1 = 1 for the 133.53 keV, ε_2 for different γ-ray energies of ^{144}Ce was calculated.

/The

(A)

Fig. 6.4 (A). A detailed diagram showing the X-ray detector operating in conjunction with the large spectrometer.

(B) X-ray detector and the large spectrometer associated with electronics arranged for $e^{-} - \gamma$ coincidence measurements.

Continued

C

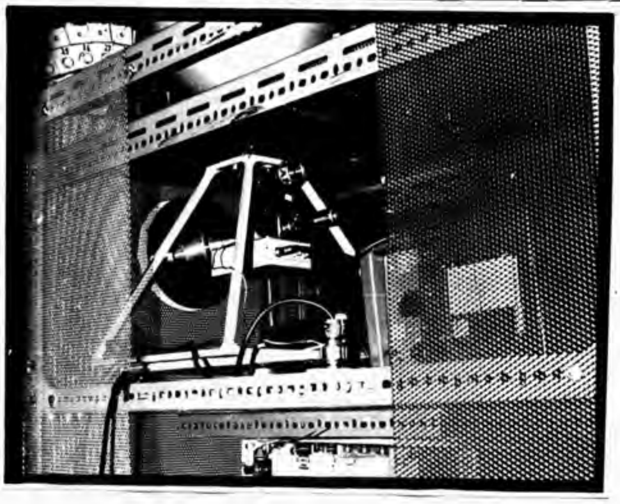

D

(E)

Fig.6.4 (C) Another view of the X-ray detector operating in conjunction with the large spectrometer.

(D) and (E) photographs showing the detector , preamplifier and electronics in a metallic cage.

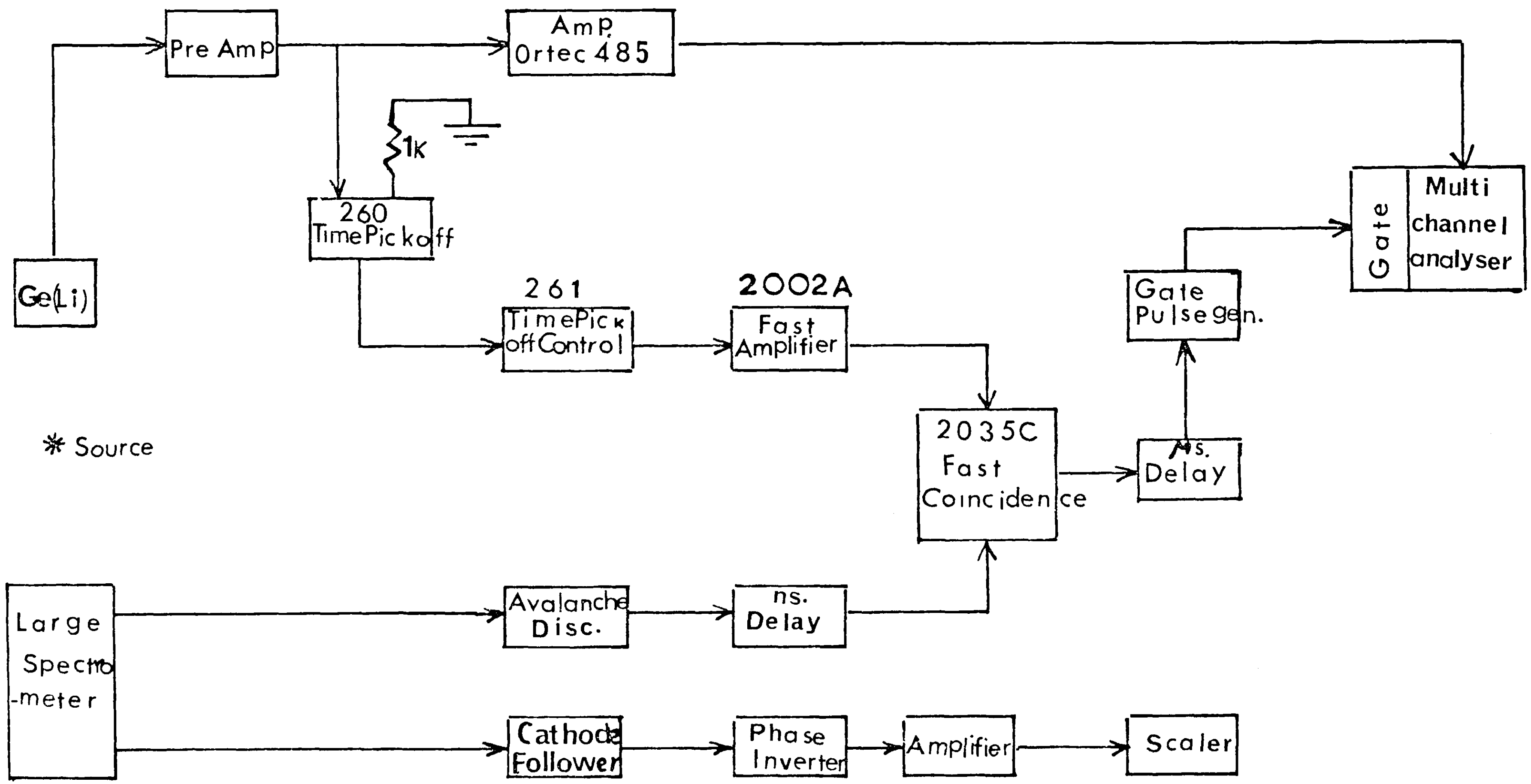

FIG. 6.5 $e^- - \gamma$ COINCIDENCE USING Ge(Li) & MAGNETIC SPECTROMETER WITH e^- GATE

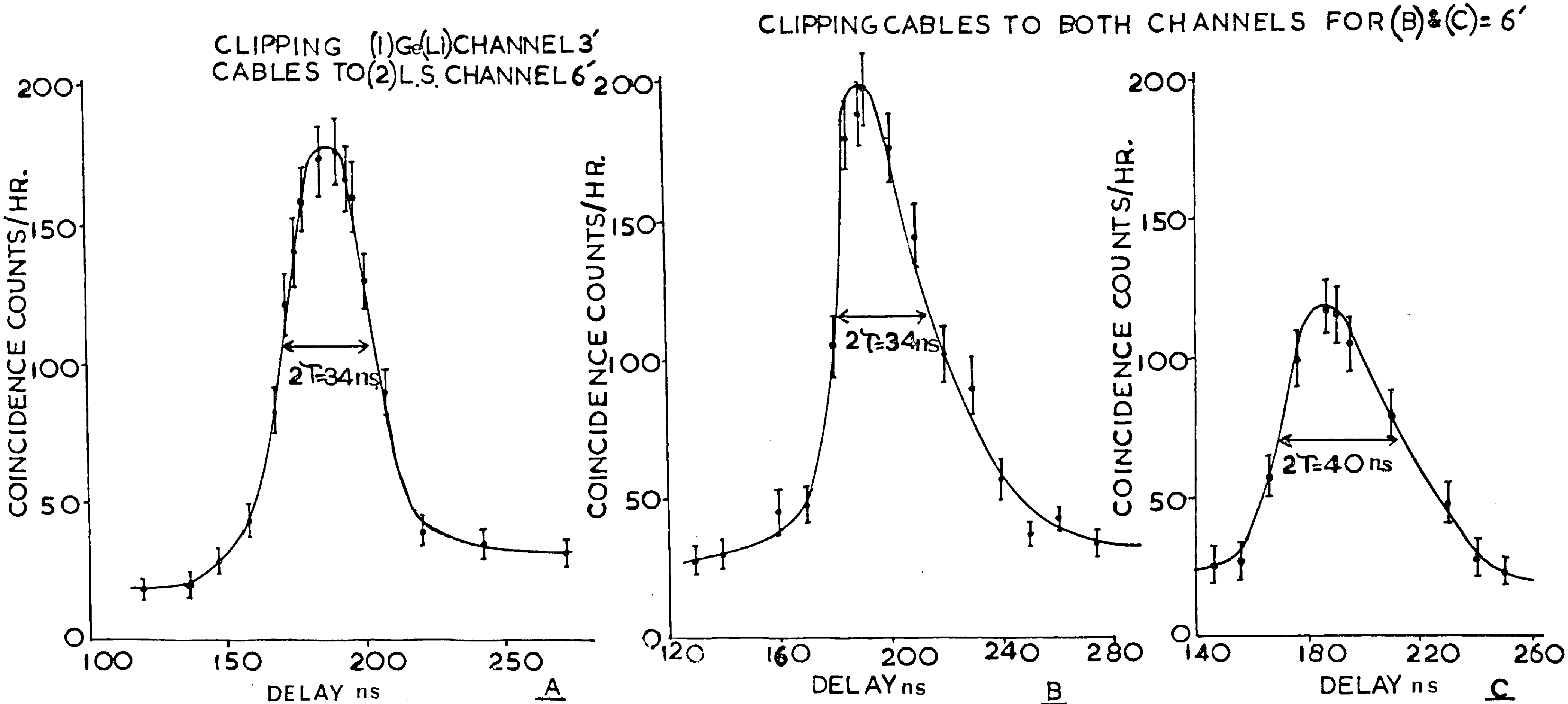

FIG. 6·6 DELAY CURVES (A) & (B) K133·53-γ (C) K80·12-γ.
(DELAY INTRODUCED IN LARGE SPECTROMETER LINE ONLY)

the efficiency curve is shown in Fig.6.2A.

5. The e^- - γ coincidence arrangements

Photographs of the Ge(Li) X-ray detector in conjunction with the large spectrometer are shown in Figs. 6.4, A,B,C. Fig. 6.5 shows the schematic diagram of the e^- - γ coincidence system with an e^- - gate. Nano-second delays are provided in the fast channel to adjust the time difference between the two fast pulses. The fast coincidence output pulse drives the gate pulse generator which produces a long (1.5 μS) pulse of nearly -12 volt (Fig. 6.20) necessary to open the gate of the Intertechnique multichannel analyser. Micro-second delays were used in the fast coincidence output line in order to match the arrival of the energy signal from the X-ray detector to the multichannel analyser. A drift of about two channels was found over a week in the system, which might be caused by a temperature change. In order to avoid the spurious counts the detector preamplifier and the associated electronics were surrounded by the metallic grids".

(a) Delay curves

Delay curves were plotted by gating the large spectrometer on the peak of the 91.53 keV (K133.53) conversion line and keeping the discriminator setting on the 261 time pick off control unit down to 20 keV. The delay curves with different lengths of clipping cables for ~~for~~ different electron energies are shown in Fig.6.6. The time resolution for the K133.53 - γ prompt curve was 34 ns, but for the K80.12-γ it was 40 nS.

An increase in the resolving

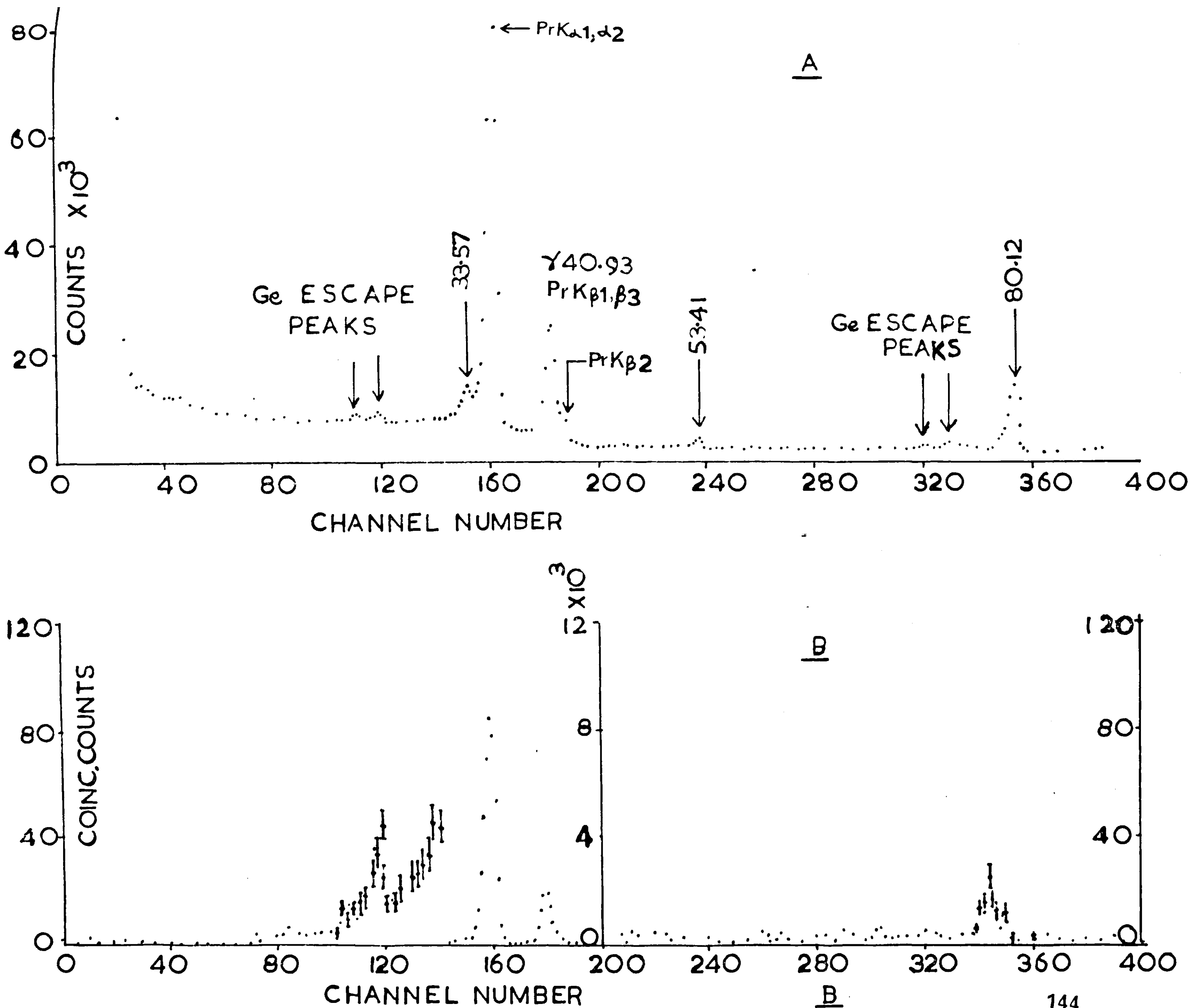

Designation	Energy in keV
Kα2	35·5502
Kα1	36·0263
Kβ3	40·6529
Kβ1	40·7482
Kβ2	41·7730

^{144}PrK X-RAYS

FIG. 6·7 THE GAMMA RAY SPECTRUM RESULTING FROM THE DECAY OF ^{144}Ce MEASURED WITH Ge(Li) X-RAY DETECTOR
(A) SINGLES (B) COINCIDENCES WITH 91·53 keV (K 1,33·53) CONVERSION LINE. (γ ray energies are given in keV)

resolving time was due to the lowering in pulse height of the K 80.12 keV conversion line. Lengths of the clipping cables used in both the fast channels were 6 feet. The maximum chance coincidence rate for the K133.53-γ and K80.12-γ coincidence was 2.1×10^{-3} and 1.1×10^{-3} counts/sec., respectively.

(b) K133.53 - γ coincidence

In order to verify the existence of a 166 keV level, the large spectrometer was focused on the top of the 91.53 keV (K133.53) conversion line and the coincidence γ-ray spectrum below 80 keV was scanned over the multichannel analyser. The coincidence spectrum is shown in Fig. 6.7. The coincidence peaks of Pr - K X-rays are due to the K133.53 K-X-rays which are emitted after the K conversion electron has escaped. The peak in the coincidence spectrum at ≃ 27 keV is interpreted as the Ge Kα escape peak coincident with the K133.53 conversion line. This finding has been confirmed in K80.12 - γ coincidence measurements (Fig. 6.8). The small peaks of the 80.12 ke V and 133.53 keV γ-rays are due to coincidence with the continuous β-rays. The coincidence spectrum does not show a γ-ray of 33.57 keV in coincidence with the K133.53 line.

(c) K80.12 - γ coincidence

Freeman (1959), Iwashita et al (1962) and Mangal et al (1969) reported a weak transition of ~ 86 keV resulting from a 166 keV to the 80.12 keV level. Thus if a 86 keV transition

/exists

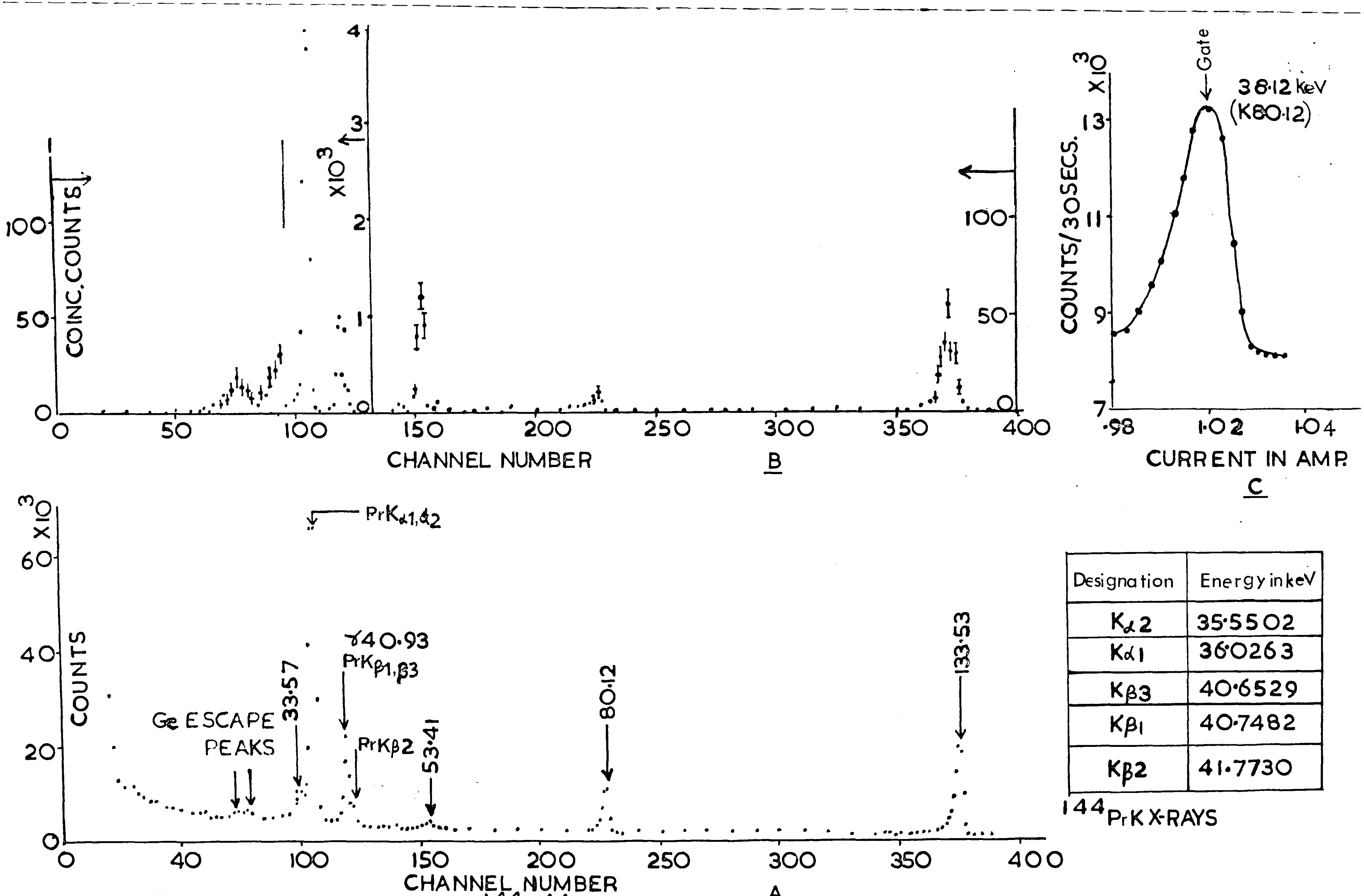

Designation	Energy in keV
$K_{\alpha 2}$	35·5502
$K_{\alpha 1}$	36·0263
$K_{\beta 3}$	40·6529
$K_{\beta 1}$	40·7482
$K_{\beta 2}$	41·7730

^{144}Pr K X-RAYS

FIG. 6·8 (A) SINGLE γ-RAY SPECTRUM OF $^{144}Ce \rightarrow ^{144}Pr$ MEASURED WITH Ge(Li) X-RAY DETECTOR (Gamma ray energies are given in keV)
(B) COINCIDENCES WITH K80·12 (C) 38·12 keV CONVERSION LINE MEASURED WITH THE LARGE SPECTROMETER.

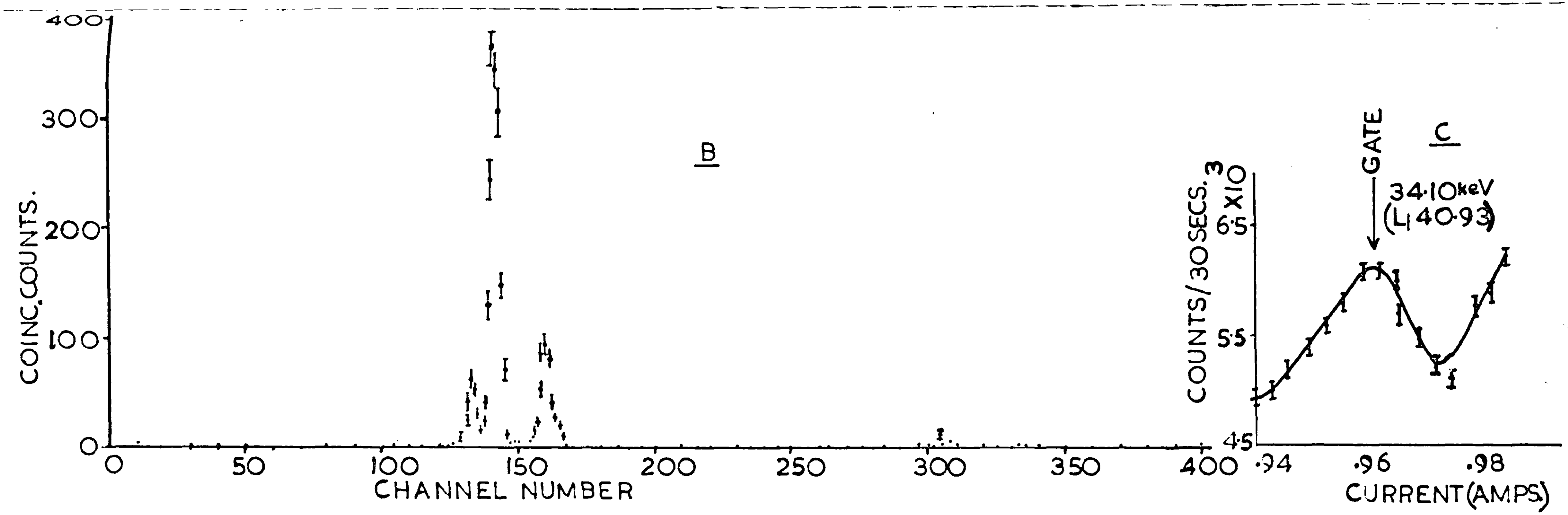

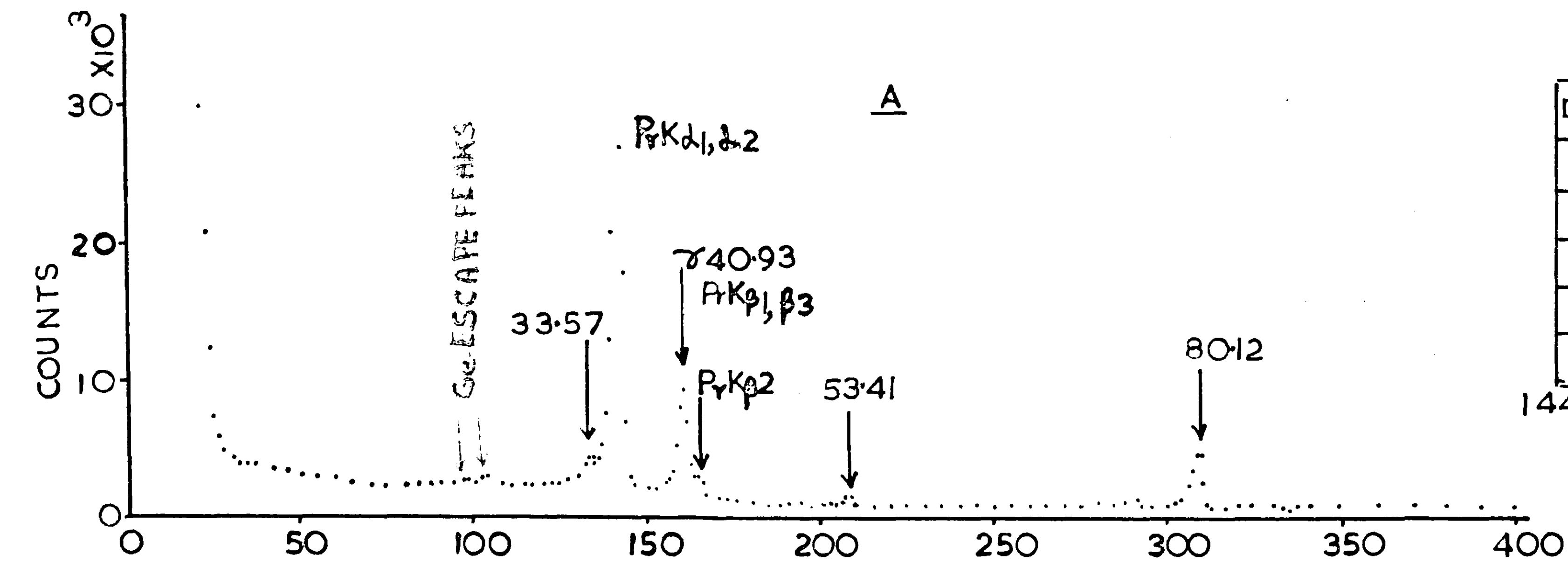

Designation	Energy in keV
Kα2	35.5502
Kα1	36.0263
Kβ3	40.6529
Kβ1	40.7482
Kβ2	41.7730

^{144}Pr K X RAYS

FIG 6.9 GAMMA RAY SPECTRUM OF $^{144}Ce \rightarrow {}^{144}Pr$ MEASURED WITH THE Ge(Li) X RAY DETECTOR (A) SINGLES (B) COINCIDENCES WITH L1 40.93 (C) THE 34.10 keV CONVERSION LINE MEASURED WITH THE LARGE SPECTROMETER exists it should appear in the K80.12 - γ coincidence spectrum. Fig. 6.8 shows the coincidence spectrum when the large spectrometer was focused on the peak of the 38.12 keV (K80.12) conversion line. The K-X-ray peaks in the coincidence spectrum are due to K80.12 fluorescent K- X-rays. A big enhancement in the relative height of the 53.13 keV photopeak shows that the K80.12 keV conversion line is in coincidence with the 53.13 keV transition. The small peak at $\sim$ 27 keV is the Ge Kα escape peak in coincidence with the K80.12 line. The spectrum does not show a coincident peak of 86 keV. No peak at 95 keV appears which is in contradiction with the findings of Keller & Cork (1951).

(d) <u>L140.93 - γ coincidence</u>

Iwashita et al (1962) found a transition of a 92 keV in coincidence with the 40.93 keV γ-ray while Freeman (1959) found a 66 keV transition originating from a 166 keV to 100 keV level. The $L_1$40.93 - γ coincidence measurements were carried out to test the existence of a 92 keV and a 66 keV transition. The e^- gate was set on the peak of the 34.10 keV (L140.93) conversion line (Fig.6.9C). The coincidence spectrum is shown in Figs. 6.9B and 6.10B. The relative height of the 33.57 keV photopeak in the single spectrum is 1:3.5 whereas in the coincidence spectrum it is 6:1. Such a big enhancement in the relative height of the 33.57 keV photopeak shows that the 34.10 keV ($L_1$40.93) conversion line is in coincidence with the 33.57 keV γ-ray. However, they do not show any

/coincidence

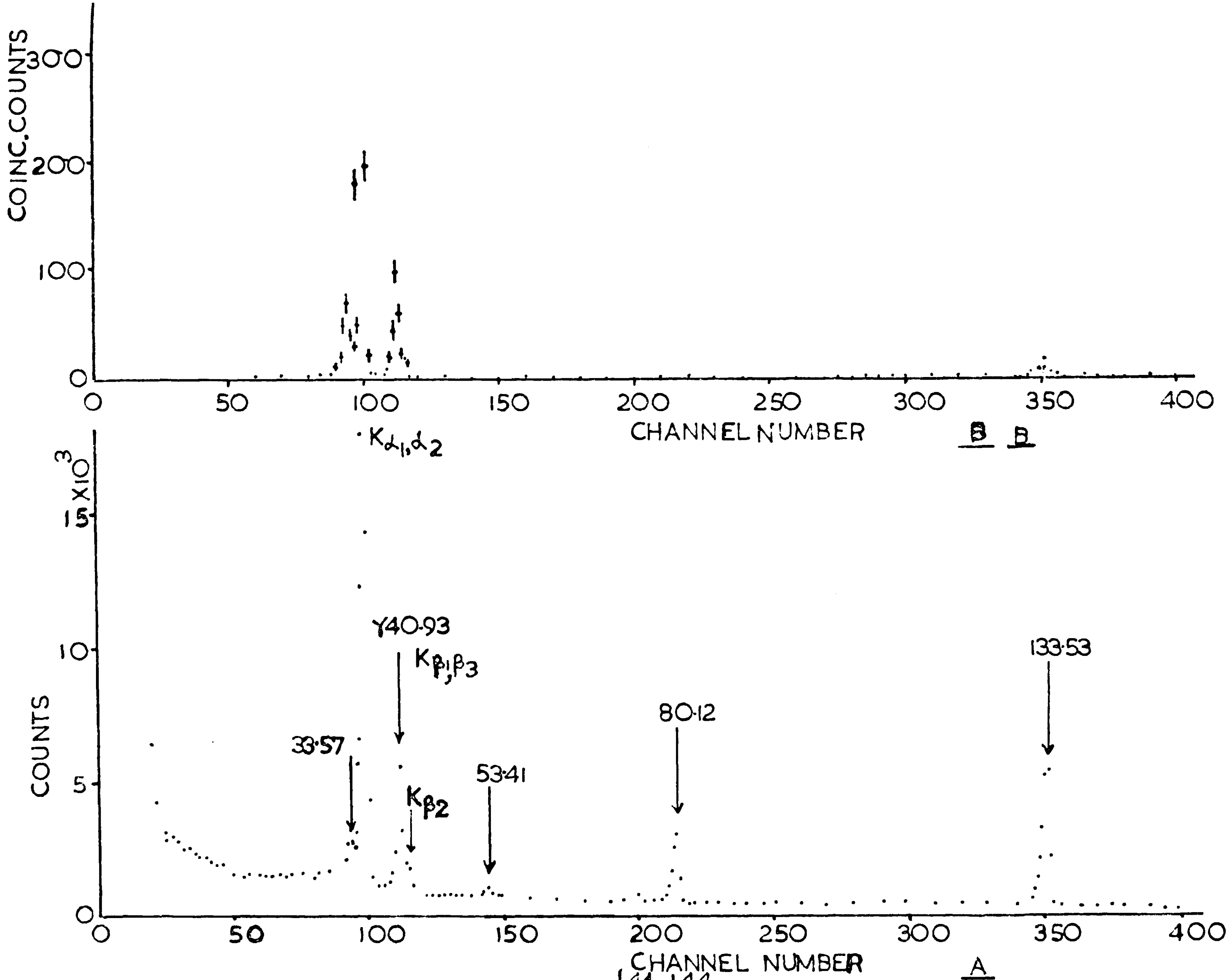

FIG. 6·10 GAMMA RAY SPECTRUM OF $^{144}Ce \rightarrow {}^{144}Pr$ MEASURED WITH THE X-RAY DETECTOR
(A) SINGLES (B) COINCIDENCES WITH L_1 40·93. (γ RAY ENERGIES ARE GIVEN IN keV)

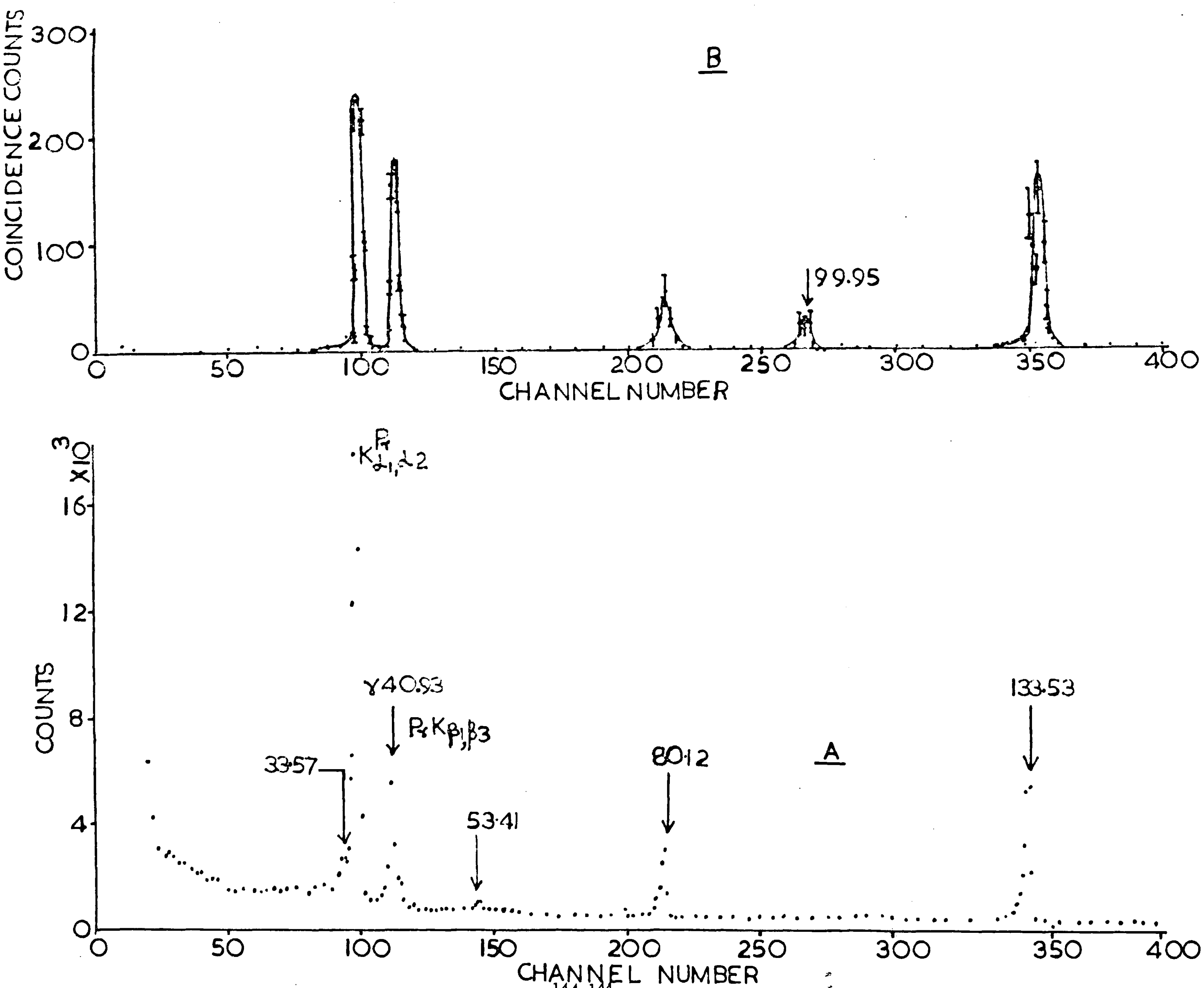

FIG. 6.11 γ-RAY SPECTRUM OF $^{144}Ce \rightarrow ^{144}Pr$ MEASURED WITH THE X RAY DETECTOR
(A) SINGLES (B) L_1 33.57–γ COINCIDENCES (γ RAY ENERGIES ARE GIVEN IN keV)

coincidence peak of either a 92 keV or a 66 keV, or the 133.53 keV transitions.

(e) $L_1 33.57 - \gamma$ coincidence

Fig. 6.11 shows the $L_1 33.57 - \gamma$ coincidence spectrum when the large spectrometer was focused on the peak of the 26.73 keV ($L_1 33.57$) conversion line. An enhancement in the relative heights of the coincident 40.93 keV and 99.95 keV photopeaks shows that they are in coincidence with the $L_1 33.57$ conversion line. The 99.95 keV γ-ray because of its weak intensity is hardly seen in the single γ-ray specurum (6.11). The 59.07 keV has a long life time (> 3 secs) hence no coincidences could be observed. No enhancement in the relative height of the 133.53 keV photopeak was observed which suggests that the 133.53 keV transition is not in coincidence with the $L_1 33.57$ keV conversion line. The small peak at 133.53 keV is due to its coincidences with the β-ray continuum.

The X-ray peaks in the coincidence spectrum are due to the coincidences of the fluorescent rays with the continuous β-rays.

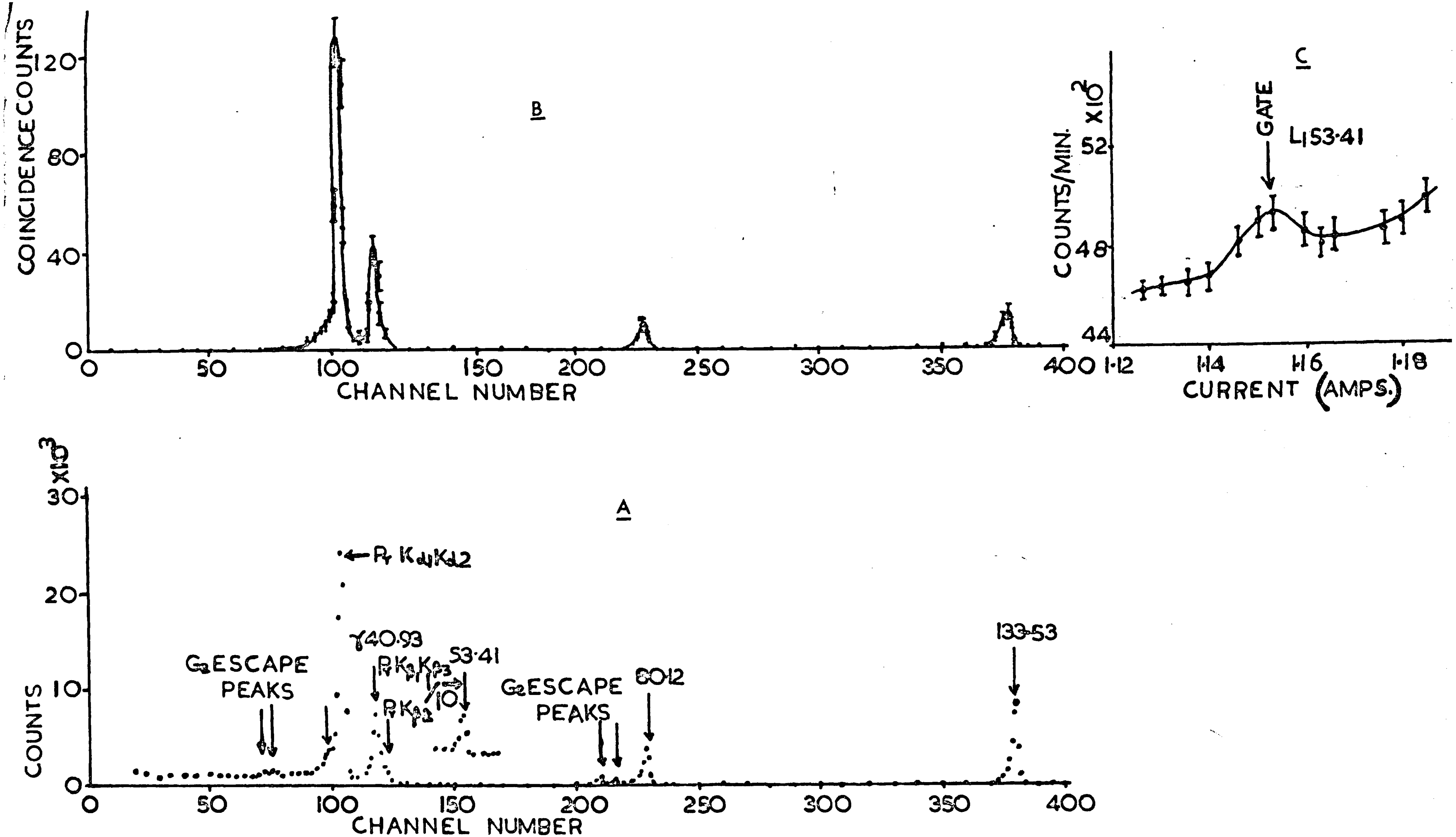

FIG. 6·12 γ-RAY SPECTRUM OF $^{144}Ce \rightarrow {}^{144}Pr$ MEASURED WITH THE X-RAY DETECTOR (A) SINGLES (B) L1 53·41–γ COINCIDENCES (C) THE L1 53·41 CONVERSION LINE MEASURED WITH THE LARGE SPECTROMETER (γ RAY ENERGIES ARE GIVEN IN keV)

L_I 53.41 - γ coincidence

Fig. 6.12 B shows the coincidence spectrum when the large spectrometer was focused on the top of the L_I 53.41 conversion line. The ratio of the height of the γ 80.12 and γ 133.53 photopeaks above the background in the single spectrum (fig. 6.12A) is 0.48 and in the coincidence spectrum it is 0.8 which shows that the γ 80.12 is in coincidence with the L_I 53.41 line. The appearance of the γ 133.53 photopeak in Fig. 6.12B is due to its coincidences with the β-ray continuum. The coincidence peaks of Ir k X-ray are due to the fluorescent K-rays of the K 80.12 conversion line. The spectrum does not show coincidences with γ 33.57.

6. Discussion

(a) 175 keV level

From the K80.12 - γ coincidence measurements, no peak at 95 keV is found which is in contradiction with the findings of Keller and Cork (1951). The $L_1$40.93 - γ coincidence does not show coincidences with the 133.53 keV γ-ray which is against the findings of Forafontov et al (1959).

(b) 166 keV level

Freeman (1959), Iwashita et al (1963) and Mangal et al (1969) placed the upper excited level in ^{144}Pr at 166 keV. The decay schemes of Freeman and Iwashita et al yield two weak transitions of 86.5 and 66 keV. The K133.53 - e^- (Fig.5.9), K133.53 - γ (Fig.6.7) and $L_1$33.57 - γ (Fig.611) coincidence measurements do not support a 33.57 keV quanta in coincidence with the 133.53 keV transition. Assuming the Geiger et al value of the intensity of 33.57 *, the upper limit of intensity of such transition is placed at ~ 0.016% per disintegration.

The K80.12 - γ coincidence (Fig.6.4) shows no evidence for a 86.5 keV transition. Taking the Geiger et al value of the intensity of γ 53.41 *, the upper limit of a 86.5 keV transition per disintegration is fixed at 0.22%. The hump on the high energy side of the 80.12 keV γ-ray in the singles γ-ray spectrum measured with the 5 cc Ge(Li) detector (Fig.6.3) is interpreted as the compton peak of the 133.53 keV γ-ray. A 66 keV peak does not appear in the L_1 40.93 - γ coincidence measurements (Fig.6.3A), and its intensity would be 0.015 times the intensity of γ 33.57.* Our present spectrum puts an upper limit on such a transition at 0.018% per disintegration.

6 10B & 9B

X

* The intensities shown in Table 6.1 were taken as standard values.

Table 6.1

E_γ keV	Gamma rays per 100 disintegrations
33.57	0.23
40.93	0.35
53.41	0.13
59.03	0.001
80.12	1.6
99.95	0.04
133.53	10.8

Energies and relative intensities of gamma rays emitted in the decay of ^{144}Ce (Geiger et al., 1960, 61).

(c) Escape peak at 27 keV

The coincident peak at 27 keV which appeared in the K133.53 - γ and K 80.12 - γ coincidence spectra can be interpreted in two ways: (1) Either it is due to a transition from a higher state of 160 keV to 133.53 keV level or (2) it is a Ge escape peak. If it were a γ-ray from a 160 to 133.53 keV level, then coincidences of 27 keV will be detected in the L_1 40.93 - γ , L133.57 - γ and L_1 53.41 - γ coincidence measurements also. Our results do not show any such coincidences, therefore, the possibility of a 27 keV transition is unlikely. The peak is due to Ge K_α, k_β escape in coincidence with the K133.53 and K 80.12 conversion lines.

The two Ge Kα, Kβ escape peaks are shown at the channels 111 and 119 in Fig. 6.7A and at 73 and 77 in Fig. 6.8A respectively. The single spectrum was run in each case for about 2 hours whereas the coincidence spectrum took more than a week and hence the drift of about 2 channels occurred which caused the coincidence escape peaks to merge into a single broad peak at channel 118 in Fig.6.7B and at channel 76 in Fig. 6.8B.

(d) 92 keV level

Iwashita et al found a 92 keV transition in coincidence with the γ 40.93. Our L_1 40.93-γ coincidence spectra (Fig.6.9, 6.10) do not show a 92 keV peak.

(e) 96 keV level

We do not find any evidence for a 96 keV level in opposition to the findings of Sengupta et al (1969).

(f) Support for the uppermost level at 133.53 keV

The $L_1$40.93 - e^- (Figs. 5.8 A,B), K80.12 - e^-

/(Figs.

(Figs. 5.8 C,D), $L_1$40.93 - γ (Fig. 6.9, 6.10), $L_1$33.57 - γ (Fig. 6.11) and $L_1$53.41 - γ coincidence measurements give a strong evidence for the 133.53 keV as the uppermost excited level of ^{144}Pr and that the 33.57 keV γ-ray arises solely due to the transition from the 133.53 keV to 99.95 keV level. Thus the possibility of two γ-rays of 34 keV is unlikely.

Conclusion

From our present results we do not find any evidence for a 175 keV, 136, keV, 96 keV or a 92 keV level. Hence we keep the uppermost excited level of ^{144}Pr at 133.53 keV supporting the decay scheme of ^{144}Ce by Geiger et al (1960,61) shown in Fig. 5.1~~8~~ G.

CHAPTER VII

1. Multipole radiation

Electromagnetic radiations are emitted when excited states of nuclei decay to lower states. They can be classified according to angular momentum L in units of $\hbar$ carried off by each quantum. For each value of angular momentum L there are two possible classes of radiations (i) Electric 2^L (E) pole and (ii) magnetic 2^L (ML) pole. These two radiations differ with respect to parity.

The transition probabilities per unit time for electrical and magnetic radiations are given as

$$T_E^{(L)} = \frac{4.4\,(L+1)}{L\,[(2L+1)!!]^2}\left(\frac{3}{L+3}\right)^2\left(\frac{E_\gamma}{197}\right)^{2L+1}\times(R)^{2L} \qquad (7.1)$$

$$T_M^{(L)} = \frac{1.9\,(L+1)}{L\,[(2L+1)!!]^2}\left(\frac{3}{L+3}\right)^2\left(\frac{E_\gamma}{197}\right)^{2L+1}\times(R)^{2L-2} \qquad (7.2)$$

where E_γ is in MeV and R is in Fermi.

The above expressions were based on the assumptions that the nucleus is spherical and that the γ-radiation is caused by the transition of a single proton from one nuclear state to another and that the proton moves independently within the nucleus. The equations 7.1 and 7.2 show that the emission probability of multipole quanta L decreases rapidly with increase of L and increases with increase in γ-ray energy E_γ. Also the electric transitions are faster than the magnetic transitions.

2. Selection rules for γ-radiation

Table 7.1

Type of radiation	Notation	ΔI change in angular momentum quantum No.	Parity change Δπ
Electric dipole	E_1	± 1	Yes (-1)
Magnetic dipole	M_1	± 1	No (+1)
Electric quadrupole	E_2	± 2	No (+1)
Magnetic quadrupole	M_2	± 2	Yes (-1)
Electric Octupole	E_3	± 3	Yes (-1)
Magnetic Octupole	M_3	± 3	No (+1)
Electric 2^L-pole	E_L	$\pm L$	$(-1)^L$
Magnetic 2^L-pole	M_L	$\pm L$	$-(-1)^L$

3. Semiconductor detectors

(a) Introduction

Mackay (1949) was the first to use semiconductor as a particle detector in nuclear physics. The solid state detector has an advantage over the gas counter, as the electron-hole pairs produced in a solid state detector is large, it has a smaller fractional statistical fluctuation and has a high energy resolution. The average energy required per ion produced in a gaseous ionization is 30 eV whereas in a solid state detector for an electron-hole pair it is 3.55eV.

(b) Interaction of γ-radiations with semiconductor detectors

Gamma rays lose their energies in semiconductor by exciting the electron to the conduction band. The excited electron is free to move in the whole of the crystal lattice. A vacancy known as a hole is created in the outer shell which moves from atom to atom throughout the lattice. The total number of electron-hole pairs thus produced yields the measure of the γ-ray energy absorbed in the semiconductor detector. The interaction of γ-rays with semiconductor takes place mainly by three mechanisms (i) photoelectric process (ii) compton scattering and (iii) pair production.

(c) Lithium drifted Germanium detector

An ideal counter is that having a very low density of free electrons or holes at room temperature so that current noise should be a minimum, a long carrier drift length to make the charge collection efficient and a high atomic number to give a good stopping power and a high photoelectric interaction with γ-rays. A single crystal with all these properties is difficult to obtain. In most cases Ge and Si crystals are used as counters. Even the commercially available pure Ge has high impurity concentration which are electrically active and produce large number of electron-hole pairs. The electron-hole pairs give rise to a noise signal which overwhelms the signal produced by a γ-ray. These impurities are made inactive by drifting lithium ions into the bulk of the Ge-crystals under a strong electric field under carefully controlled conditions. Each impurity

/becomes

becomes fully ionized and they collectively make no contributions to the free carrier concentrations, thus producing a region of high resistivity.

(d) Comparison between Si (Li), Ge(Li) detectors and NaI(Tl) Scintillator

The Ge(Li) detector has an advantage over NaI(Tl) scintillator as it has a faster rise time ($\sim$ 20 to 40 ns) whereas NaI(Tl) scintillator has a rise time equal to 250 ns. Therefore a Ge(Li) detector has superior time resolution to that of NaI(Tl) scintillator. Silicon detectors have the advantage that they can be operated at room temperature while the Ge(Li) detectors are always operated at the liquid nitrogen temperature. Germanium has a considerably higher atomic number than silicon, has photoelectric cross-section nearly 40 times that of silicon, and finally a greater stopping power for γ-ray absorption. The mean energy per electron-hole pair for Germanium is lower (2.84ev) than that of silicon (3.23eV). Thus the Germanium detector has a better statisticcs and a faster rise time than the silicon detector.

(e) Leakage current in semiconductor

The leakage currents arise from the detector surface and from the detector volume. An imperfection captures a bound electron from the lattice producing a free hole. If such carrier generation process produces electron-hole pairs in the depletion layer - they are rapidly swept apart by the electric field. This is a space-charge generated leakage current which is under normal conditions

/less

less than 10^{-5} Ampere cm^{-3}.

(f) Irradiation effects

A deterioration in the properties of the semi-conductor appears when it is exposed to radiations for a long time. A continuous bombardment of radiation produces lattice defects and imperfections in the detector. These imperfections serve as trapping centres which cause an increase in resistivity, lowering in carrier life-time, increase in rise time of the pulse and deterioration in resolution.

4. Preamplifier noise

The high resolution obtainable from the semiconductor detectors is limited by the preamplifier noise which is a function of the total input capacitance to the preamplifier noise. Leakage current, bias and feedback resistor thermal noise, F E T noise are the examples of the preamplifier noise sources. The noise contribution due to F E T is a minimum in the temperature region of 110 - 130K. Hence the F E T's are always kept as close to the detector as possible for cooling and to reduce the stray capacity. The noise contribution to the F.W.H.M. of the preamplifier N E 5287A to Ge(Li) detectors having capacity 0 to 5 pF is nearly 1.1 keV for double integration and single differentiation.

5. Pile-up effects

The overlapping of a sequence of pulses produces stair-case effects called Pile-up effects. It can occur at all

/stages

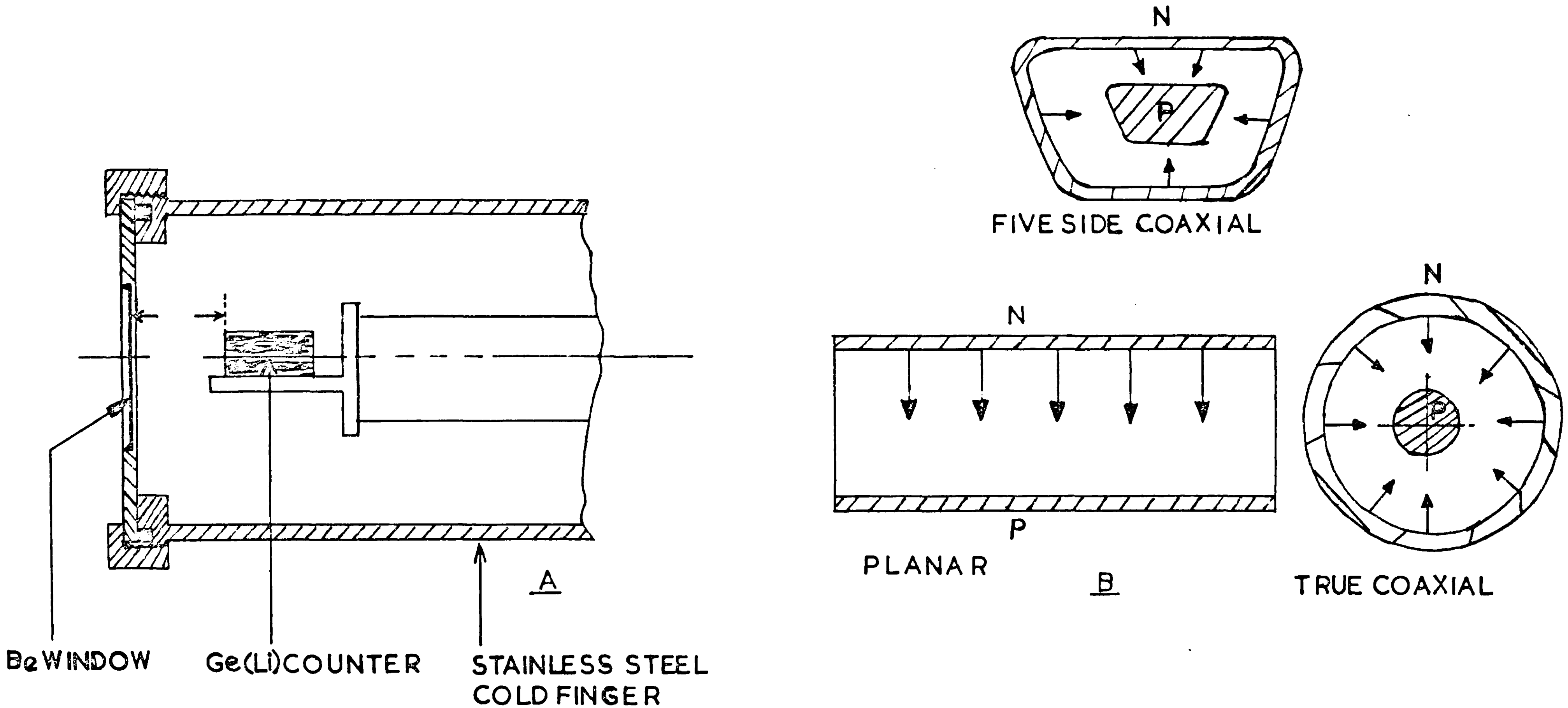

FIG. 7·1 (A) Ge(Li) COUNTER FIXED IN A CRYOSTAT
(B) DETECTOR CONFIGURATIONS

stages both in the preamplifier and amplifier and is one of the causes for spectral broadening. In the main amplifier pile-up occurs on the primary pulse and on the undershoot. Those pulses which fall on the undershoots of earlier ones will appear to have lower amplitudes. The statistical fluctuations in the magnitude of the base line depression result in dispersion in the measured pulse heights. A further dispersion in pulse height is caused by the non-linearity of the amplifier over the range of base line variation. The latter effect is reduced to a small value with a single differentiation and the long duration overshoot is eliminated with double differentiation.

(6) The 5 cc Ge(Li) detector

A 5 cc N.E. Ge(Li) detector has been used in γ-γ coincidence measurements. The sectional diagram of the detector mounting is shown in fig. 7.1A. The detector is housed in a chamber with a thin beryllium window and is cooled at liquid nitrogen temperature. The detector is provided with a NE 5287 A preamplifier the first stage of which with F.E.T. is also cooled.

The Be - having low atomic number, will not absorb the low energy γ-rays and hence is suitable for the study of low energy γ-radiations. The following are the specifications of the 5 cc Ge(Li) detector:-

Detector No. GDP 578

Optimum operating voltage	500 v + ive
Leakage current	1×10^{-9} ampere

/sensitive

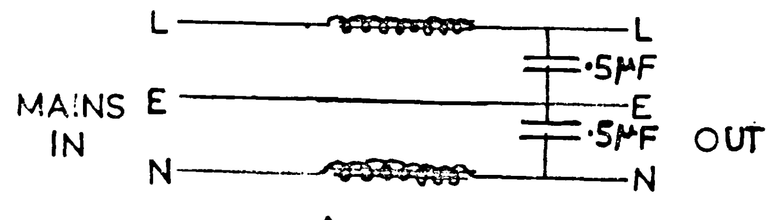

A

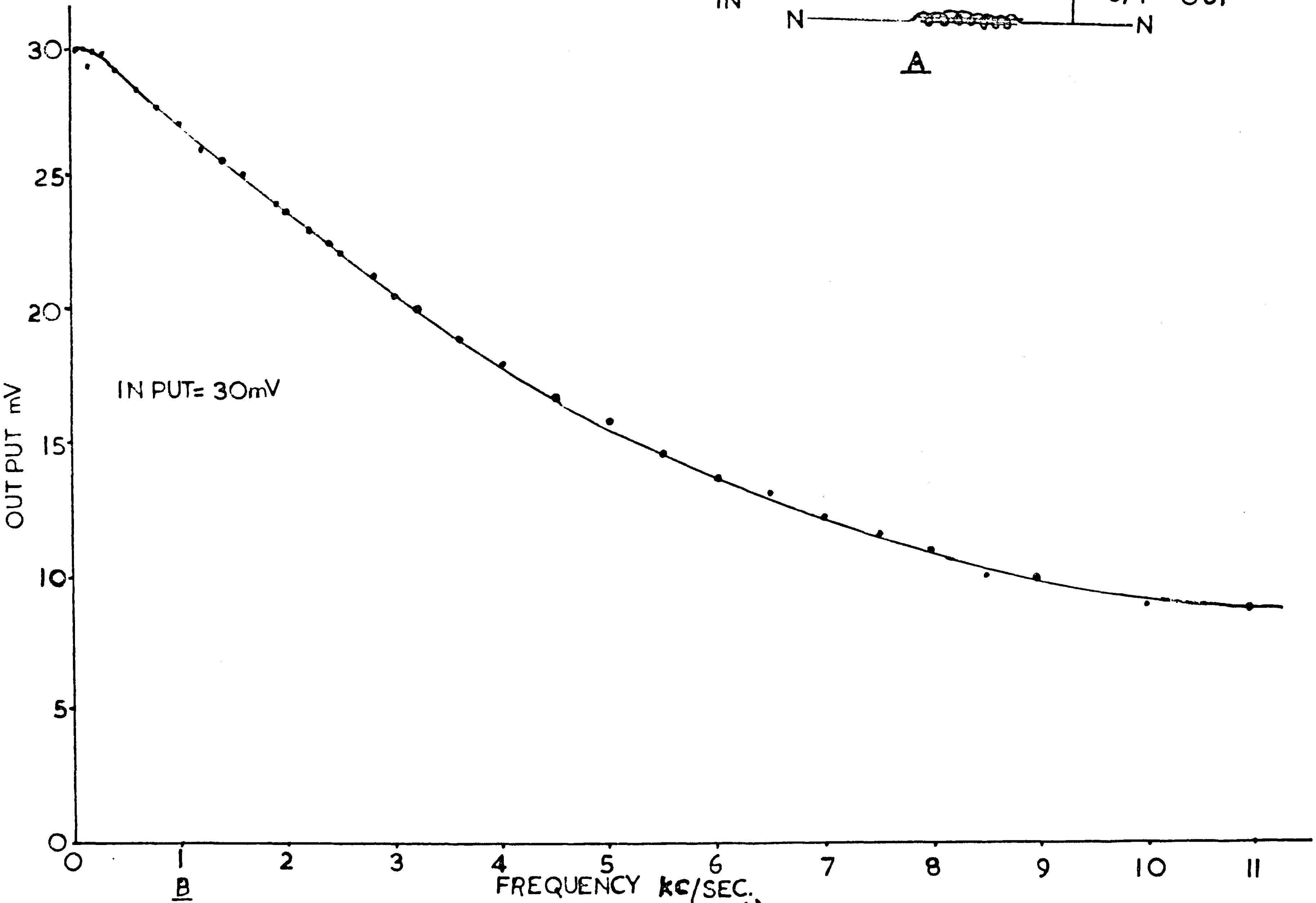

B

FIG.7·2 (A) MAINS FILTER C.E.R.N. DESIGN (B) FREQUENCY RESPONSE OF THE MAINS FILTER

sensitive volume	5 cc
configuration	Planar
capacitance	5 pF
window	Be

(a) Cryostat: The cold finger is made of stainless steel which is filled with liquid nitrogen via a Union Carbide drip-feed Dewar. The detector is mounted at the end of the cryostat. The cold finger and the detector are encapsulated by an aluminium outer casing. The interspace between the detector and the casing is evacuated by an ion pump down to a pressure of abour 10^{-6} Torr.

7. Performance of 5 cc Ge(Li) detector

(a) Avoidance of mains pick up

Mains pick up caused spurious counts at the beginning with the 5 cc Ge(Li) detector. The use of a special type of mains filter (shown in Fig. 7.2A) proved most useful in getting rid of pick ups. The characteristics of the mains filter are shown in Fig. 7.2B.

A further precaution against spurious pick up has been taken by placing the detector and associated electronics in a metallic wire grid cage in γ-ray spectroscopy and in $e^- - \gamma$ coincidence measurements.

(b) Resolution

The resolution of a Ge(Li) detector depends mainly on three factors (i) preamplifier noise (ii) detector noise (iii) statistical effects of production of electron-hole pairs. If A represents the detector theoretical resolution assuming gaussian statistical variation, D

/the

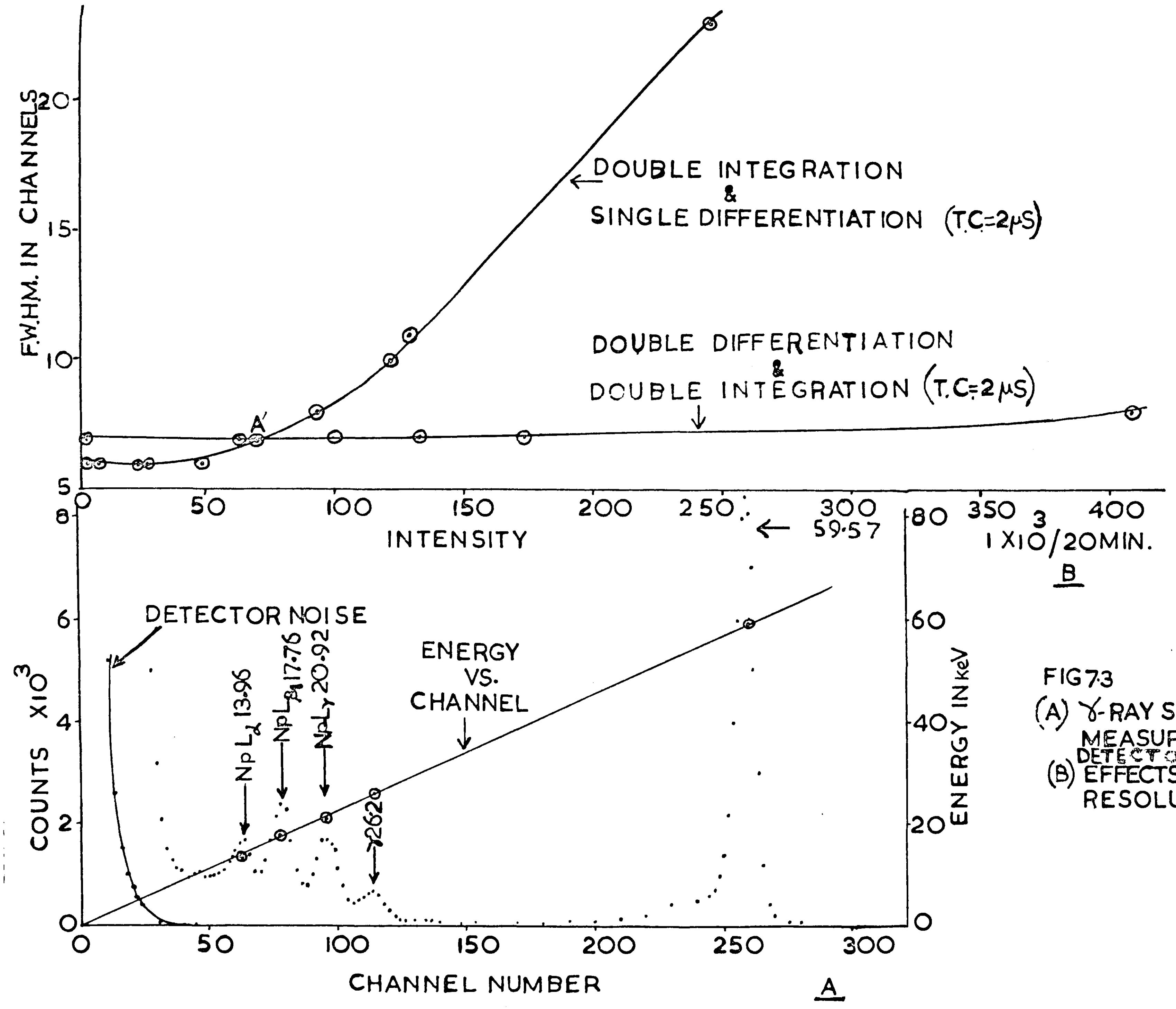

FIG 7.3
(A) γ-RAY SPECTRUM OF ^{241}Am MEASURED WITH THE 5cc Ge(Li) DETECTOR
(B) EFFECTS OF COUNTS RATE ON RESOLUTION

the noise contribution from detector leakage current and C the noise contribution from detector bias. Then the resolution F W H M is given as

$$F\,W\,H\,M\ \ Ge(Li) = \left[A^2 + B^2 + C^2 + (\text{Preamplifier noise})^2\right]^{\frac{1}{2}}$$

where $A = 4.1\sqrt{E}$, $B = 2.35 \times 2.98\ Ne$

$C = 2.35 \times 2.98\ Ne^1$, $Ne = \sqrt{\frac{1\ t}{4e}}\ \epsilon^2$

$Ne^1 = \sqrt{\frac{KT}{2R}}$, ϵ is base of Naperian logrithms.

t = pulse shaping time constant, e = electron charge K is Boltzman constant and T is absolute temperature.

The ^{241}Am isotope has γ-ray and x-ray lines in the low energy region, the most intense one is the 59.57 keV γ-ray. These lines could be used to check the calibration and resolution of the Ge(Li) detector in the low energy region. The γ-ray spectrum of ^{241}Am measured with the 5 cc Ge(Li) detector is shown in Fig. 7.3A. The energy calibration line passes straight through the origin which shows the response of the detector to be linear. At low energies the statistical fluctuations contribution to the line width is smaller than the preamplifier noise but at higher energies the contribution due to the statistical fluctuation in the production of electron-hole pairs is predominant. The contribution to the line width due to statistical fluctuation can be estimated by subtracting in quadrature the line width of the pulser from that of the γ-ray peak.

(c) Stability test of the detector

In order to test the stability of the detector and the electronic system, the detector was run continuously

/for

for 24 hours and γ-ray counts of ^{241}Am was stored in the 400 channel Intertechnique multichannel analyser. A gain drift of 0.3% was found with the 59.57 keV γ-ray photopeak.

(d) Effects of counting rate on resolution and peak position of γ-ray

High counting rate generates pulse pile-up which causes dispersion in the pulse height spectrum. The effect of the counting rate on the resolution of a Ge(Li) detector has been studied by placing ^{137}Cs β sources of different strengths at the same distance from the detector. Intensity of the 661 keV photopeak has been calculated by summing up the number of counts in each channel above the base line. Measurements were done for amplifier settings having (i) double integration and single differentiation (ii) single differention and double integration keeping time constants 2μs in each case. The F.W.H.M. vs. intensity of photo-peaks in each case has been plotted and shown in Fig. 7.3B. With double integration and double differentiation the pile-up effects get reduced considerably and the F.W.H.M. remains fairly constant over a considerable range of counting rate. With double integration and single differ-entiation an improvement in resolution appears which remains constant up to the point A′ (seeFig. 7.3B) and then it increases with the increase in counting rate. With double integration and single differentiation, no deterioration in F.W.H.M. value appears up to the total counting rate of 1778 counts per second, which is very low for coincidence

/measurements.

measurements. The Canberra biased amplifier 1462 is designed to get rid of the pile-up effects and it can be used at fairly high counting rate. In present γ-γ coincidence experiment neither this biased amplifier nor post-amplifier base restorer was available hence the distance of the source from the detector and time constants were adjusted to get a better resolution. The Edinburgh amplifier NE 5259 and the biased amplifier NE 5261A were found too much sensitive to counting rate and therefore a weak source and a long distance from the detector were essential to get rid of pile-up effects.

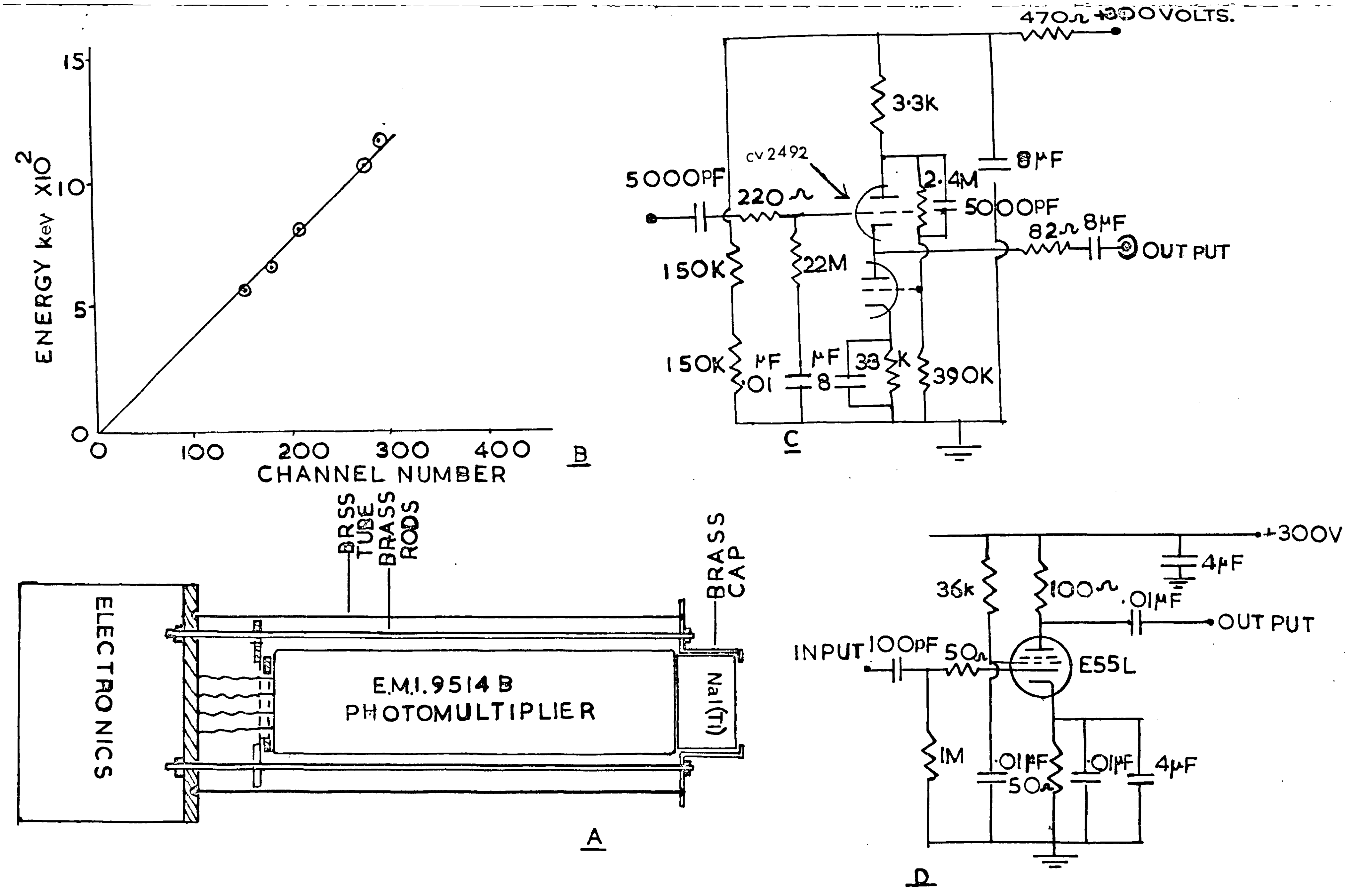

FIG. 7·4 (A) γ – COUNTER. (B) LINEARITY RESPONSE OF γ COUNTER (C) WHITE CATHODE FOLLOWER (D) E55L LIMITER

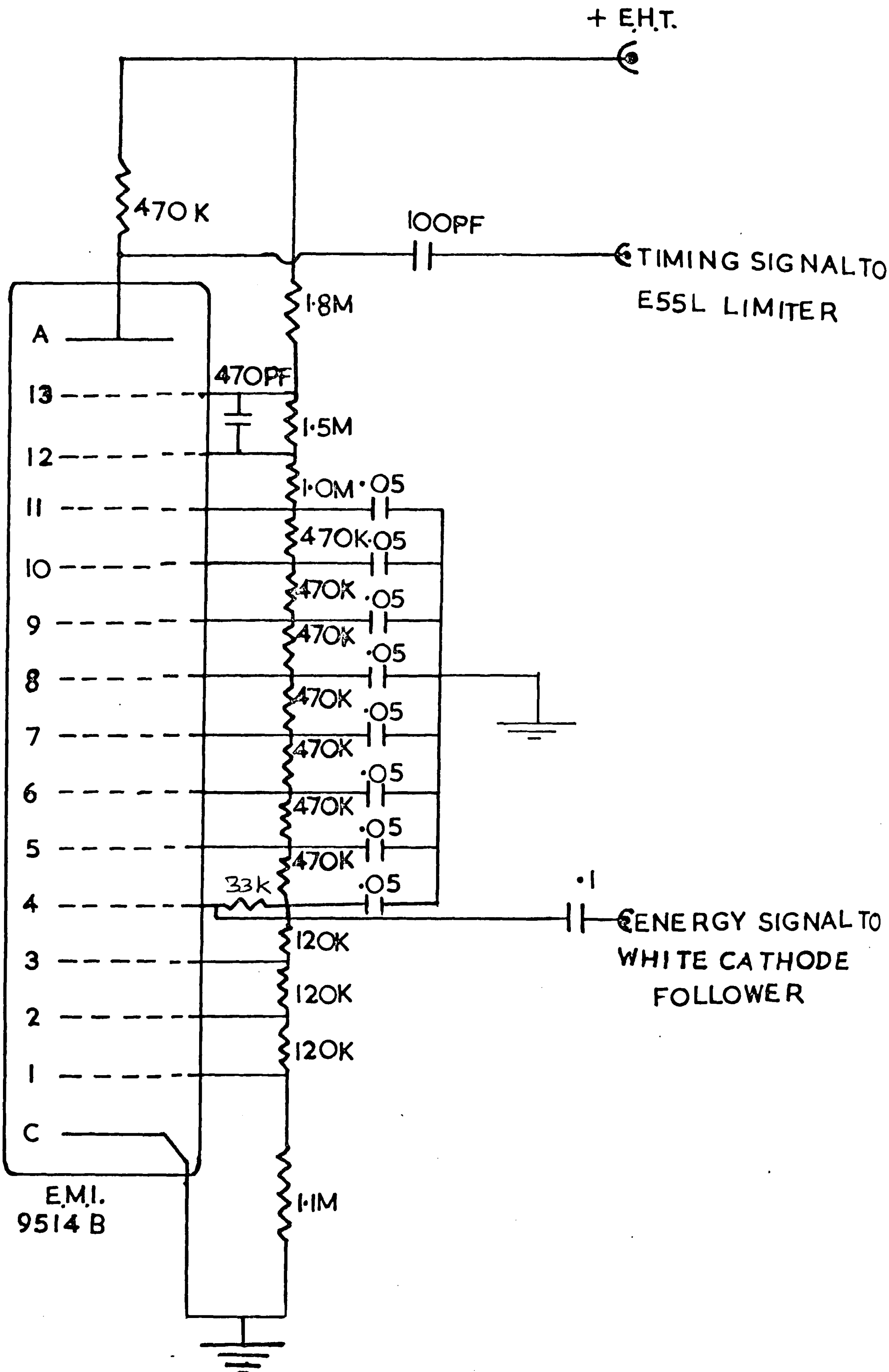

FIG.7·5 PHOTOMULTIPLIER CIRCUIT FOR γ-COUNTER

8. White cathode follower

(a) The circuit diagram of the white cathode follower shown in Fig. 7.4C is based on the design of Nuclear Enterprise preamplifier model NE 5202A. It is a double cathode follower which is used to achieve an overall amplification nearer to unity. A full description of the circuit appears in Section 4 of the "N.E.Instruction manual for integrated and demountable assemblies".
(b) E55L limiter - see Appendix I

9. The NaI (Tl) Counter

The NaI(Tl) Harshaw crystal ($1\frac{1}{2}$" x 1") mounted on E M I 9514 B photomultiplier is shown in Fig. 7.4A. An energy resolution of 8.2% for the $^{137}C_s$ 661 keV γ-ray has been achieved. Fig. 7.4B shows the pulse height linearity response of the counter.

(a) Photomultiplier circuit

The potential divider circuit for E M I 9514B photomultiplier of the γ-ray counter is shown in Fig. 7.5.

The decoupling capacitors have been used to stabilise the dynode potentials. The timing signals from the anode feeds the E 55L limiter which produces a fast positive pulse of 5 volts (Fig.7.4D). The limiter output further triggers the avalanche discriminator producing a very fast narrow-negative pulse (Fig.2.4d). The energy signal is derived from the 4th dynode which eventually goes to the grid of the White Cathode follower. The connecting lead from the anode to the grid of E 55 L limiter was kept short.

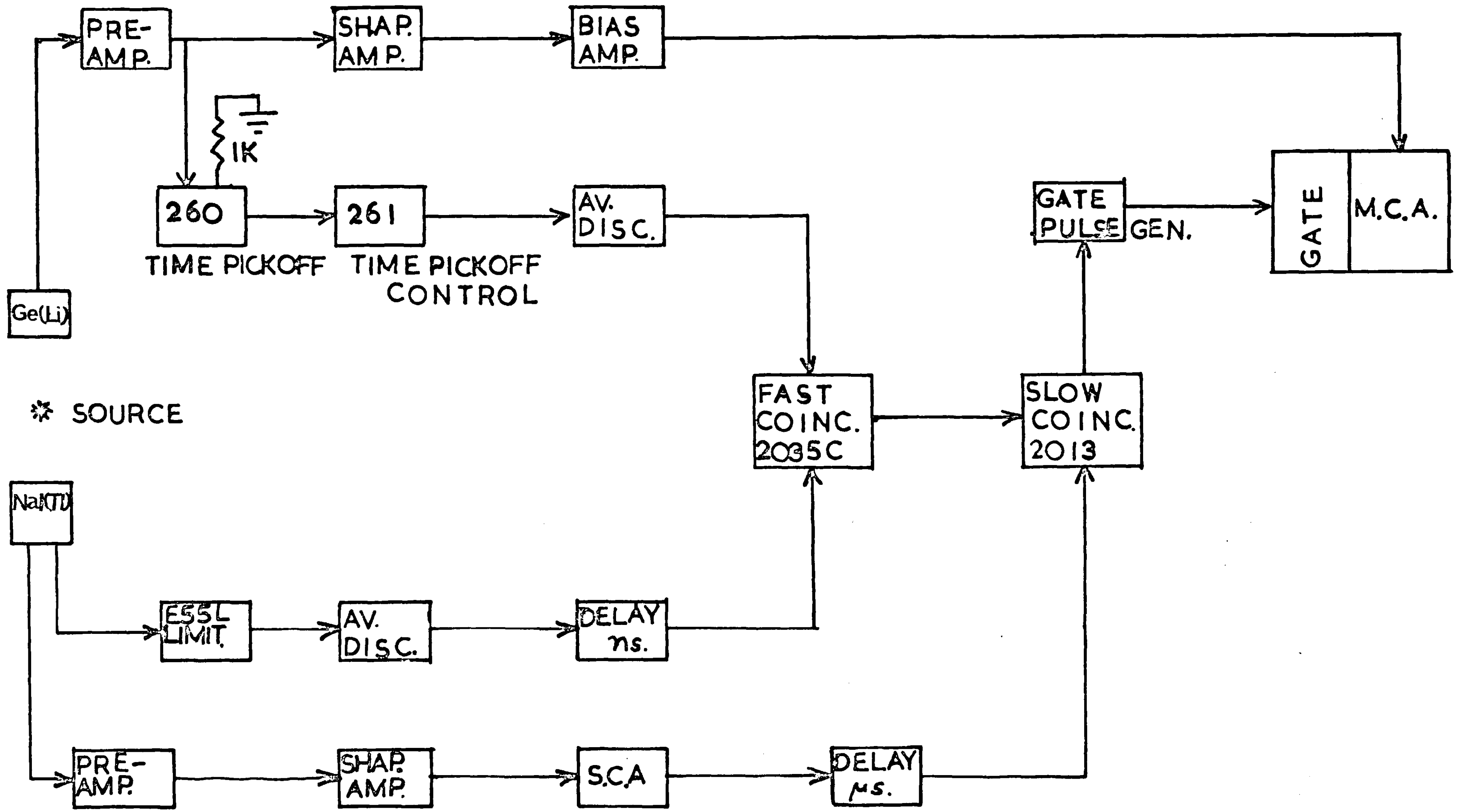

A

B

FIG. 7.6 (A) Ge(Li)/ NaI(Tl) γ-γ COINCIDENCE
(B) PHOTOGRAPH OF THE NaI(Tl) COUNTER & THE 5cc. Ge(Li) DETECTOR ARRANGED FOR γ-γ COINCIDENCE MEASUREMENTS.

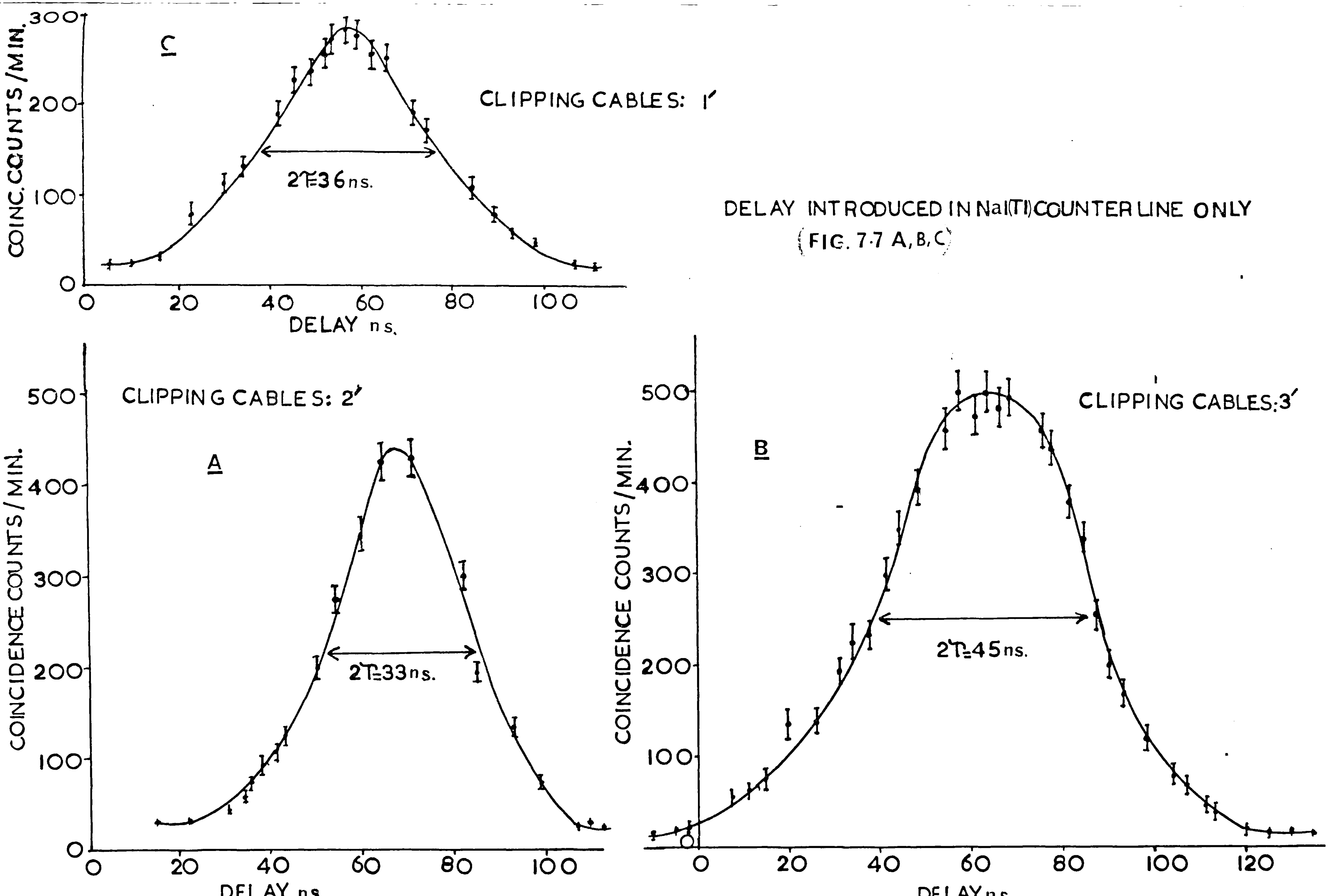

FIG. 7·7 DELAY CURVES WITH DIFFERENT LENGTHS OF CLIPPING CABLES

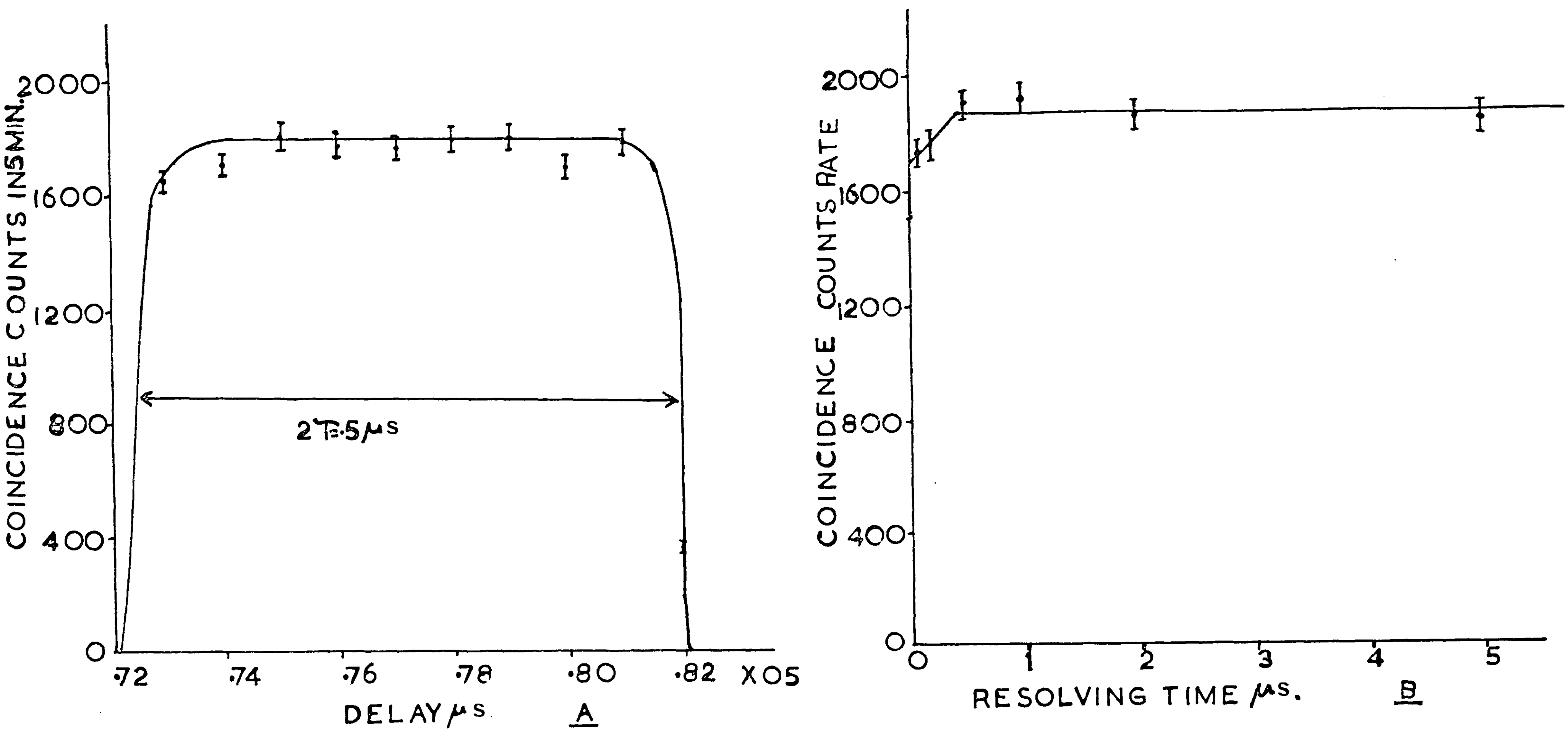

FIG. 7·8 (A) DELAY CURVE WITH SLOW COINCIDENCE
(B) RESOLVING TIME CURVE

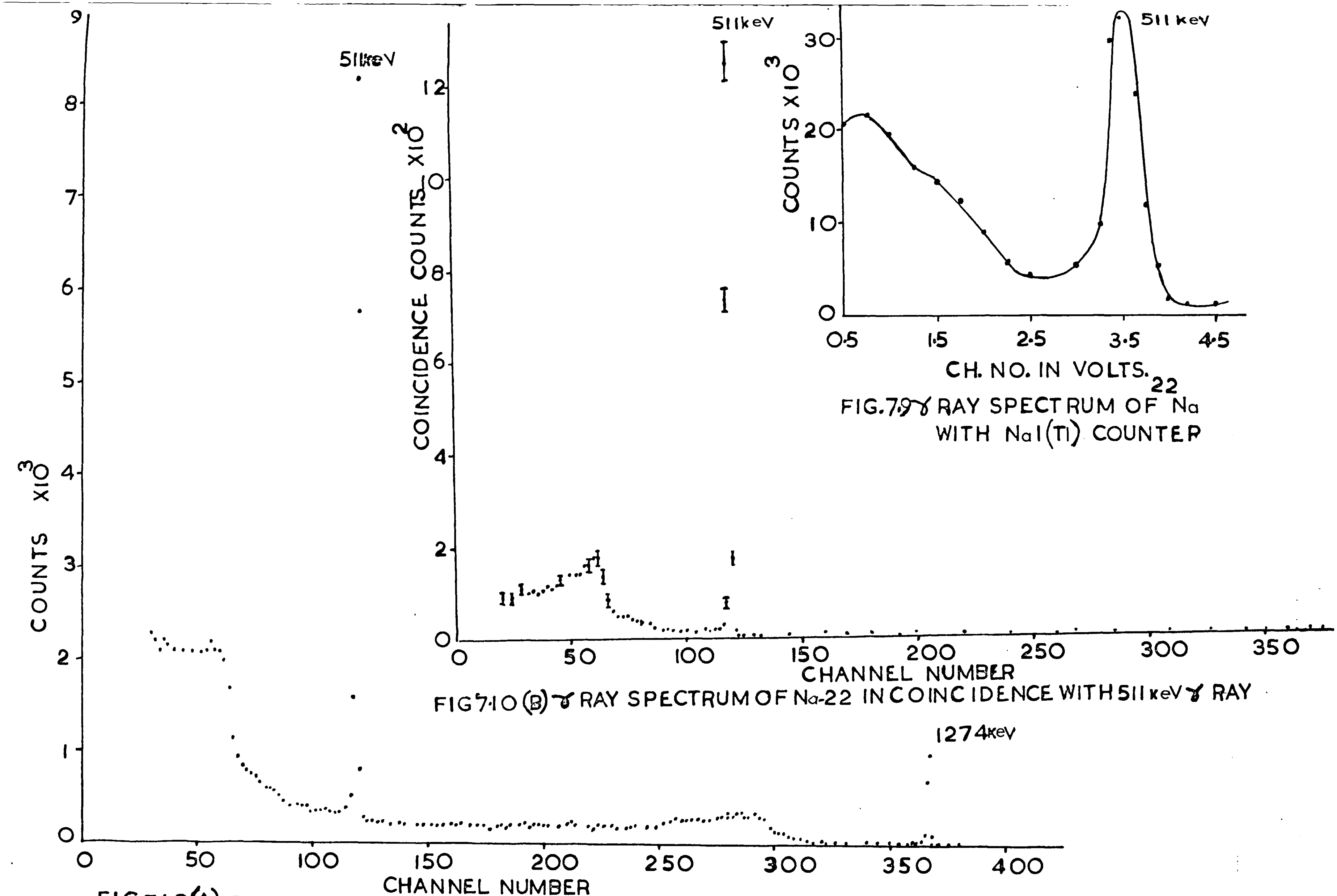

FIG. 7.9 γ RAY SPECTRUM OF ^{22}Na WITH NaI(Tl) COUNTER

FIG 7.10 (B) γ RAY SPECTRUM OF Na-22 IN COINCIDENCE WITH 511 keV γ RAY

FIG. 7.10 (A) GAMMA RAY SPECTRUM OF Na-22 WITH 5 c.c. Ge(Li) DETECTOR

10. γ - γ coincidence experiment

The Ge(Li)/NaI(Tl) Fast and Slow γ-γ coincidence arrangement is shown in Fig. 7.6A. This coincidence arrangement has been used in the studies of cascade nature of the 569 MeV γ-rays of ^{207}Bi.

(a) Delay curves

Delay curves for fast coincidence were plotted with a ^{22}Na γ-ray source, keeping different lengths of clipping cables (see Fig. 7.7). A 3' clipping cable was found suitable to give a time resolution of 45 ns. On making the length of both clipping cables smaller, the coincidence counts rate reduces though with some improvement in resolving time. Similar measurements were made with the slow coincidence unit to set the resolving time for maximum coincidence counts rate. The coincidence counts rate falls rapidly when the resolving time reduces below 0.5 μs. (Fig. 7.8B). The minimum permissible resolving time for the slow coincidence unit was 0.5 μs. The maximum chance coincidence rate was 0.4 c/sec (Fig. 7.7B).

(b) Coincidence spectrum of ^{22}Na.

The single γ-ray spectrum of ^{22}Na with NaI(Tl) scintillator has been shown in Fig. 7.9. The lower level of the S.C.A. was set at 2.5 Volt and the window opening at 2 Volt so as to cover the full photopeak area of the 511 keV γ-ray. The single γ-ray spectrum of ^{22}Na with the Ge(Li) detector is given in Fig. 7.10(A).

The coincidence spectrum between two annihilation quanta of 511 keV shows a satisfactory working of the

/coincidence

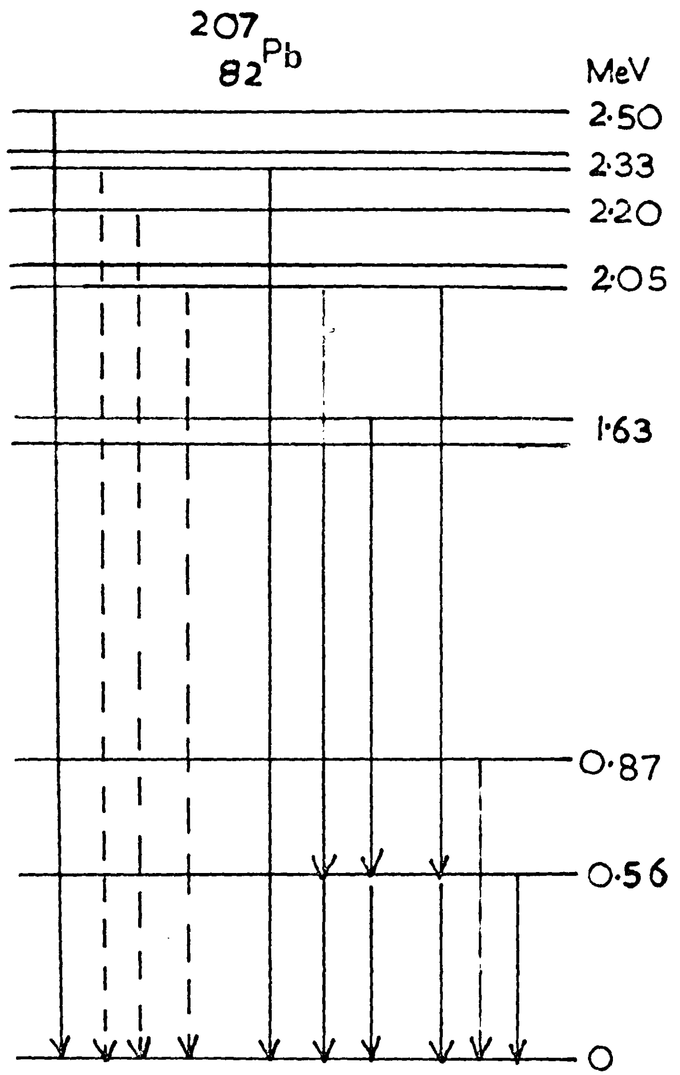

PRESCOT et al (1954)

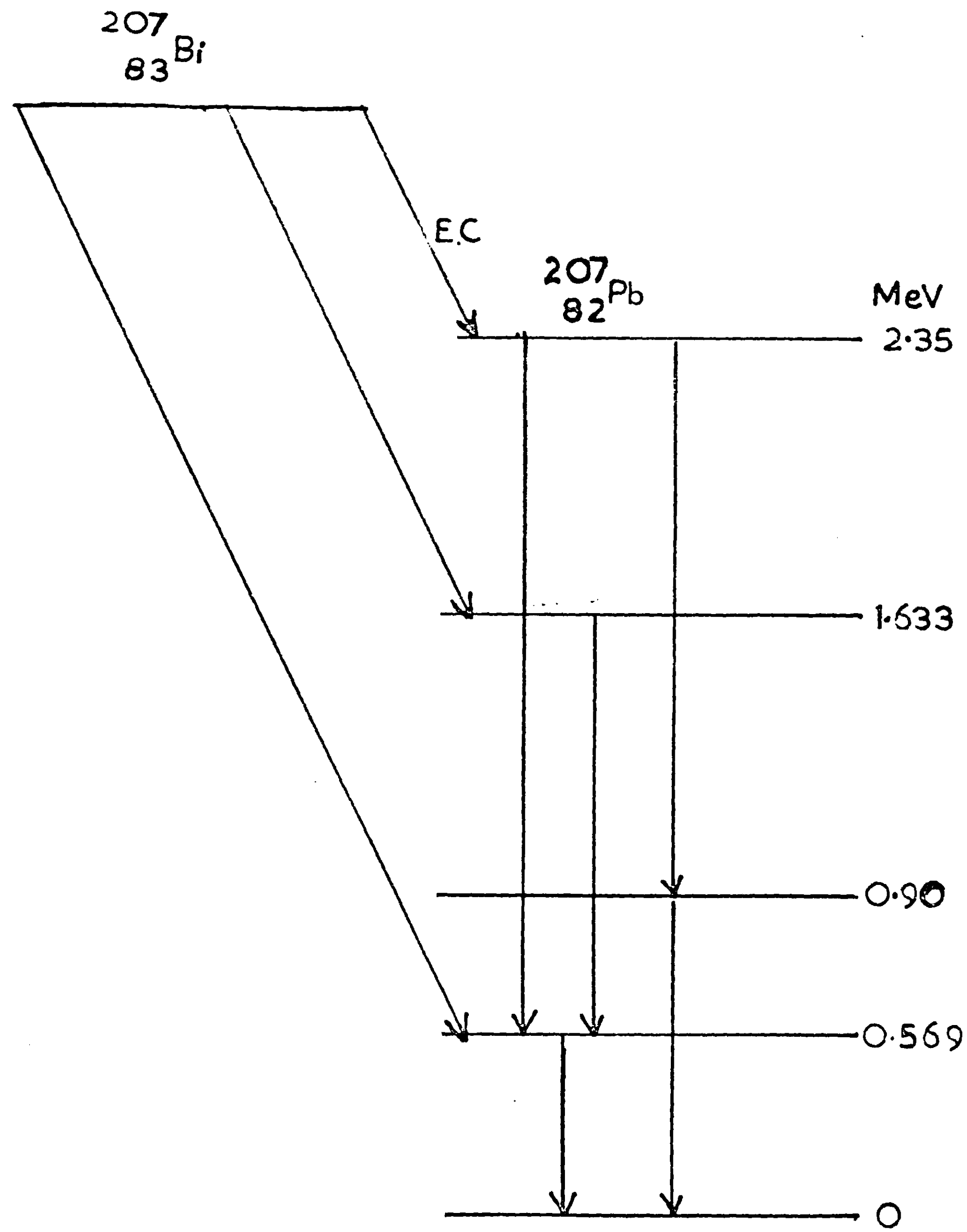

ALBURGER et al (1955)

FIG 7.11 THE DECAY SCHEME OF ^{207}Bi

coincidence system.

11. The Decay of ^{207}Bi

(a) Introduction

^{207}Bi isotope was discovered by Neuman and Pelman (1951) who found that the nuclide decays by electron capture to ^{207}Pb with a half life of about 28 years. The conversion electron spectrum of Neuman shows eight γ-rays above 2 MeV in the decay of ^{207}Bi., While Wapstra et al (1954) found the presence of two transitions of energies 0.56 and 1.06 MeV. The coincidence data of Prescott (1954) gave evidence of four γ-rays of energies 0.57, 1.07, 1.76 and 2.47 MeV and suggested the possibility of a 1.07 MeV doublet. The conversion electron spectra of Alburger et al (1955) gave a slight indication of a very weak line corresponding to a transition of about 0.9 MeV. Till now NaI (Tl) scintillators have been used by various workers in the γ-ray studies of ^{207}Bi.

The present Ge(Li)/NaI(Tl) γ-γ coincidence system was designed primarily to do coincidence measurements with ^{144}Ce source and at the beginning attempts were made to search for the existence of two γ-rays of equal energies 0.569 MeV in the decay of ^{207}Bi (Prescott 1954). Unfortunately the 5cc Ge(Li) detector failed during the experiment and hence γ - γ coincidence measurements with ^{144}Ce could not be performed and also those made with the ^{207}Bi remained incomplete. However, some of the important coincidence measurements taken with ^{207}Bi are presented in this chapter. The decay schemes of ^{207}Bi by Prescott

/et

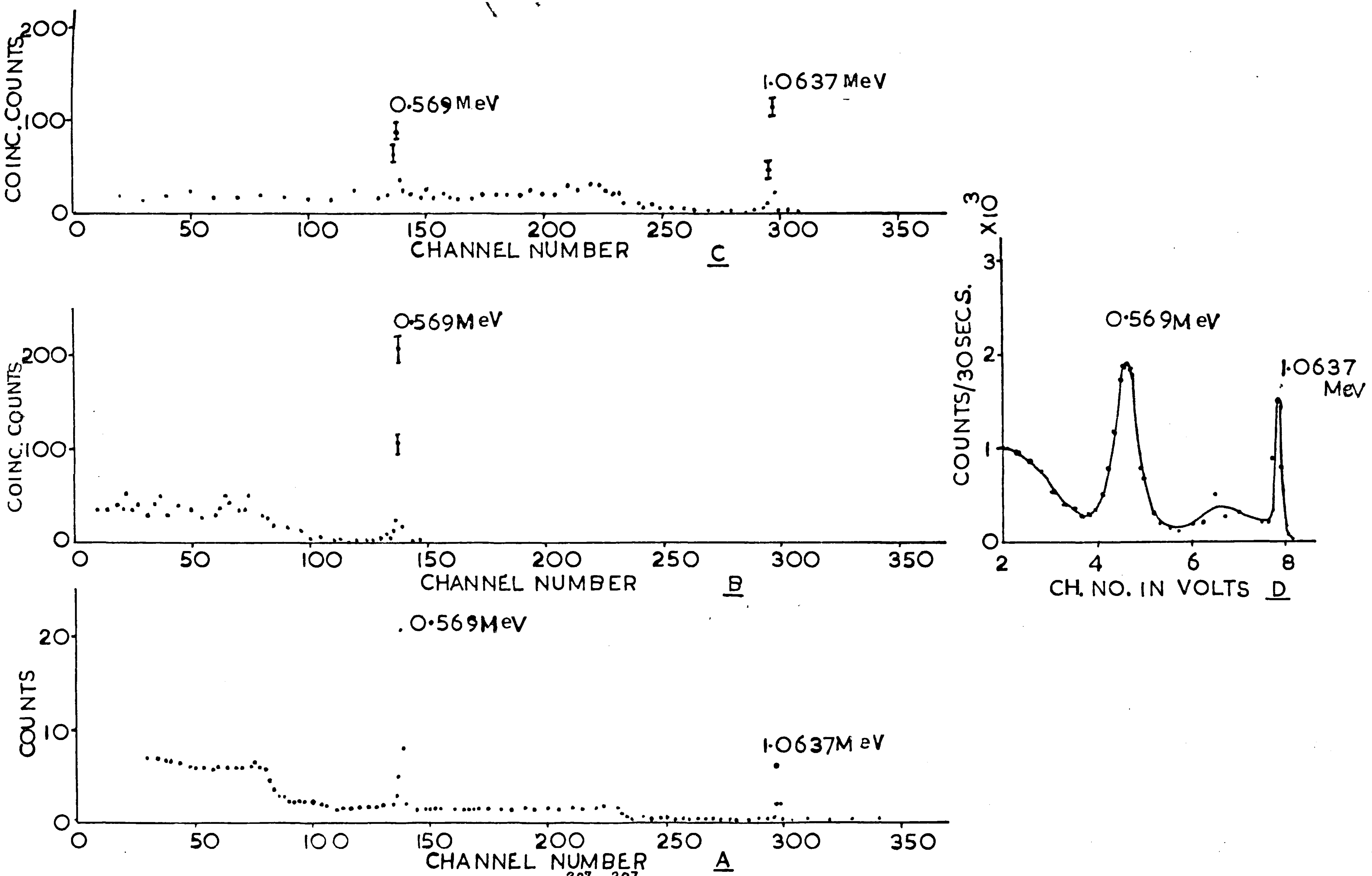

FIG. 7·12 GAMMA RAY SPECTRUM OF THE $^{207}Bi \rightarrow {}^{207}Pb$ DECAY
(A) SINGLE SPECTRUM WITH Ge(Li) DETECTOR (B) COINCIDENCES WITH 1·067 meV γ RAY
(C) COINCIDENCES WITH 0·569 meV γ RAY (D) SINGLE SPECTRUM WITH NaI(Tl) COUNTER

et al (1954) and Alburger et al (1955) are given in Fig. 7.11.

(b) γ 1.0637 - γ 0.569 coincidence

Single γ-ray spectra from the decay of ^{207}Bi below 1.0637 MeV measured with the NaI(Tl) scintillator and with the 5 cc Ge(Li) detector are shown in Fig. 7.12. Fig.7.12B shows the coincidence spectrum when the window of the single channel analyser was set on the NaI(Tl) spectrum which included the full 1.0637 γ-ray photopeak. The only peak to appear is the 0.569 MeV γ-ray which shows that the 1.0637 MeV γ-ray is in coincidence with the 0.569 MeV γ-ray.

Fig. 7.12C shows the coincidence spectrum when the channel window on the NaI(Tl) spectrum was set to include the full 0.569 MeV γ-ray photopeak. An enhancement in the photopeak height of the 1.0637 MeV γ-ray above the background indicates that the 0.569 MeV γ-ray is in coincidence with the 1.0637 MeV γ-ray.

The coincidences at 0.569 MeV in Fig.7.12C can be interpreted in two ways:-

(i) The coincidences are with the compton background of the 1.073 MeV γ-ray or (ii) they are with the compton background as well as with a second γ-ray of 0.569 MeV. If it were due to the compton background alone, the ratio of the area of the 1.067 MeV photopeak to its compton background under the 0.569 MeV photopeak will remain the same both in the single coincidence spectrum while in the presence of another γ-ray of 0.569 MeV, the ratio will get reduced in the latter cases. The ratios were calculated in both

/the

the single and coincidence spectrum. In the single spectrum the ratio was $\frac{1}{1.9}$, whereas in the coincidence spectrum it was $\frac{1}{1.88}$. Thus the results show that the coincidence peak of 0.569 MeV γ-ray is entirely due to the coincidences with the compton background of 1.067 MeV quanta and there are no two γ-rays of 0.569 MeV.

APPENDIX I

The Mullard E55L pentode valve has been used in the limiter circuit of the NaI (Tl) γ - counter. The valve has a long durability and can be operated at about 55 mA anode current. The circuit is based on the design by Abdarabbani, Rafat Batul (1968) with some adjustments. The output pulse amplitude was adjusted to a desired value by adjusting the cathode resistor. A 100Ω anode load resistor was used in order to match the transmission line. The anode current flowing through the valve was 50 mA which produces a fast standard output pulse of + 5 volt.

R E F E R E N C E S

Abdarabbani (Rafat Batul)	Ph.D. thesis (1968) University of London
Alburger and Sunyar	Phys.Rev.99 (1955) 695
Bellitini et al	Nucl.Inst. & Meth.27 (1964) 38
Bennee N.W.	Ph.D.Thesis, University of London (1968)
Bequerel	Comptes Rendus 122 (1896) 501
Brunix and Rudstam	Nucl.Inst. & Meth. 13 (1961) 131
Carswell & Milsted	J. Nucl.Energy 4 (1957) 51
Chadwick	Phys.Gens.16 (1914) 383 ch.1
Cork et al	Phys.Rev. 96 (1954) 12 95
Emerich et al	Phys.Rev. 94 (1954) 110
Evans, P.R.	Ph.D. Thesis, University of London (1958)
Evans et al	Proc.Phys.Soc.72 (1958) 949
Fashing et al	Phys.Rev. Vol C (1970) No.3 P 1126
For a fontov et al	J E T P (U.S.S.R) 36 (1959) 330
Forafontov et al	Nucl.Phys.35 (1962) 260
Freeman N.J.	Ph.D. thesis, University of Exeter (1958)
Freeman N.J.	Proc.Phys.Soc. 74 (1959) 449
French, S.	M.Sc. thesis (1966) University of London

Gerholm T.R. — Rev.Sc. Inst. 26 (1955) 1071

Geiger et al — Nucl.Physics 16 (1960) 1 - 26

Geiger et al — Nucl. Phys. 28 (1961) 387 - 406

Hickock et al — Phys.Rev.109 (1958) 113

Hyman et al — Nucl. Ins. & Meths. 35 (1964) 393.

Iwashita et al — J. Phys. Soc. Japan 18 Oct. (1963) 1358

Keller, Cork — Phys. Rev. 84 (1951) 1079

Lieshout et al — α, β, γ ray spectroscopy Ed. Siegbahn (1965) Vol.I p 529.

Mangal et al — J. Phys. Soc. Japan 27 No.1 (1969) July p 1

McKay — Elmore W.C. and M. Sands Electronics Ch.4. National Nuclear Energy Series. Div. V. Vol.1 (1949)

Michelson, D. — Ph.D. thesis, University of London (1961)

Michelson, D. — Private communication (1968)

Michelson & Richardson — Nucl. Inst. & Meths. 21 (1962) 355

Michelson & Richardson — Proc.Phys.Soc. 81 Part 3 No. 521 (1963) 553-70

Neuman et al — Phys.Rev. 81 (1951) 958

Pate & Yaffe	Can.J.Chem.33 (1955) 15-23
Porter and Cook	Phys.Rev. 87 (1952) 464
Prescott et al	Proc. Phys. Soc. 67A (1954) 540
Pullman, Axel	Phys. Rev. 102 (1956) 1366
Richardson, H.O.W.	Phil.Mag. 40 (1949) 233
Sengupta et al	Indian J. Phys. 33 (1959) 388
Tove et al	Rev. Sc. Inst. 27 (1956) 143
Towers T.D.	Elements of transistor pulse circuits (1965) 54
Von Bayer and Hahn	Physik 11 (1910) 488
Von Bayer Hahn & Meitner	Phys. Z.S. 12 (1911) 273, 378
Von Bayer, Hahn & Meitner	Phys. Z.S 13 (1912) 264
Wapstra	Ark Fysik 7 (1954)279
Wahab and Kane	Nucl.Inst. & Meth.15 (1962) 15
Yaffe	Ann. Rev. of Nucl. Sc. 12 (1962) 153-188

Total number of pages 129